Functional Investigation of Variants Identified in Patients with Retinal Dystrophy

using ciliopathies and stem cells as a model system

Hey, Amalie Brunbjerg

Publication date:
2020

Document Version
Publisher's PDF, also known as Version of record

Citation for published version (APA):
Hey, A. B. (2020). *Functional Investigation of Variants Identified in Patients with Retinal Dystrophy: using ciliopathies and stem cells as a model system*. Roskilde Universitet.

Functional Investigation of Variants Identified in Patients with Retinal Dystrophy

– using ciliopathies and stem cells as a model system

PhD Dissertation by

Amalie Brunbjerg Hey

June 2020

This dissertation has been submitted to:
The Doctoral School of Science and Environment, Roskilde University

Table of contents

Acknowledgements

I would like to thank my two supervisors, Jesper Troelsen and Lisbeth Birk Møller for their invaluable help and guidance throughout this project. I am grateful for the opportunity to work with two such experts in the field.

Also, my warmest thanks to my Colleagues at the Kennedy Center for everything, from help in the laboratory and creating an enjoyable working environment. Special thanks to Eva, Pia H., Pia S., Judy, Anne, Susanne, and Jette for their support and technical assistance.

Thanks to Poul Hyttel and Maria Pihl for their invaluable knowledge and guidance in the field of electron microscopy.

Thanks also to Søren Tvorup Christensen for sharing his vital experience in supervising projects and for his help making sure the exams for my student project groups went smoothly.

Lotte Bang Pedersen for donating hTERT-RPE1 cells and for fruitful discussions.

Thanks also to the Velux Foundation for their economical support.

Lastly, a thank you to my family and friends for supporting me through the process.

This project could not have been done without you!

Abstract

Retinal dystrophy is a leading cause of blindness in the western world. A large number of genes have been found associated with this disease and a specific gene panel has been designed in order to evaluate DNA samples from individuals with suspected retinal dystrophy. Through targeted next generation sequencing DNA is screened for genetic variants in this gene panel. Many patients receive their diagnosis this way. However, for some gene variants it is difficult to assess the pathogenicity. Through donation of a skin biopsy, fibroblast cells from an individual without a diagnosis, can be investigated through different cellular assays to help elucidate the cellular phenotype and ultimately provide a molecular genetic diagnosis. In this dissertation one such case is presented; a missense variant in the *RAB28* gene showed altered subcellular localization of the RAB28 protein in fibroblast cells from two individuals homozygous for the variant establishing this specific *RAB28* missense variant as likely pathogenic. An example which underlines the importance of functional assays in this type of work.

However, some genes are only expressed in certain tissues and therefore fibroblast cell may not always be the best system to investigate potential effects in specific differentiated cells and tissues. In these cases, it can be useful to generate induced pluripotent stem cells (iPSC) and differentiate these cells into the cell type of interest and subsequently apply functional assays. To set up the methods for this strategy, fibroblast cells from individuals suffering from Bardet-Biedl syndrome (BBS) were reprogrammed into iPSC using electroporation of the reprogramming factors OCT3/4, SOX2, KLF4, LIN28, L-Myc and a short hairpin RNA targeting P53.

Investigation of undifferentiated BBS fibroblast cells showed that these cells had disturbed Hedgehog signaling and that the length of the primary cilium may be disturbed as a consequence of the *BBS* gene variants.

As both *RAB28* and genes with *BBS* variants have important impact on retinal function and maintenance, iPSC generated from the BBS-fibroblast cells were differentiated into retinal pigment epithelial (RPE) cells and used as model system for the investigations in this dissertation.

RPE cells derived from the BBS-iPSC were generated and investigated (data from one experiment). A directed differentiation approach was chosen and mature RPE cells with pigmentation, tight junctions and phagocytic capability from control iPSC. Interestingly, RPE cells derived from the BBS-iPSC were not able to differentiate into mature RPE cells. The morphology of the BBS-RPE differed substantially from the control-RPE as BBS-RPE were larger and more elongated. The BBS-RPE cells did gain pigment in the first growth phase, but this was later lost. Electron microscopy revealed loose cellular junctions. This finding was confirmed in RNA expression studies where expression of genes associated with adherens junctions were increased compared to genes associated with tight junctions. The BBS-RPE also showed poor phagocytic capabilities and they had no expression of genes associated with mature RPE cells. The BBS-RPE had very long primary cilia compared to control cells, showed dysregulated Hedgehog (Hh) and Wnt signaling and signs of mitochondrial stress. To improve maturation, prolonged culture of control- and BBS-RPE with agonists and antagonists targeting Wnt and Hh signaling was tested. Control-RPE seemed to benefit from Wnt inhibition, but BBS-RPE showed no sign of improved RPE maturation. Even though these data are preliminary, this indicates that the BBS proteins are important for cilia and RPE cell function, differentiation and maturation.

This work shows that research in rare genetic variants is important for two reasons; first, it helped clarify pathogenicity of one gene variant, and second, basic research will provide more information that in the future may lead to development of treatments for persons with retinal dystrophy.

Abstract/resumé – dansk

Retinal dystrofi er en stor årsag til at mennesker bliver blinde i vesten. Mange gener er blevet korreleret med denne sygdom og et særligt gen-panel er blevet designet for at muliggøre evaluering af DNA prøver fra personer man tror har retinal dystrofi. Ved brug af targeteret next generation sekventering bliver DNA screenet for genvarianter i dette panel. Langt de fleste patienter får en diagnose på denne måde, men der er nogle genvarianter der er svære at vurdere effekten af. Ved at donere en hudbiopsi kan fibroblastceller dyrkes fra personer uden en diagnose og funktionelle studier af disse celler kan hjælpe med at undersøge hvilken fænotype cellerne har og forhåbentlig give en endelig diagnose. I denne afhandling præsenteres en sådan case: En missense variant i *RAB28* genet gav ændret lokalisering af RAB28 proteinet i fibroblastceller fra to personer der var homozygote for varianten. Dette muliggjorde klassificering af RAB28 varianten til mulig patogen. Dette er et godt eksempel der illustrerer vigtigheden af funktionelle studier i dette arbejde.

Nogle gener er kun udtrykt i specifikke vævstyper og derfor er fibroblastceller ikke altid det bedste cellesystem at undersøge. I sådanne sager kan det være nyttigt at lave inducerede pluripotente stamceller (iPSC) og differentiere dem til den celletype man vil undersøge og herefter lave funktionelle studier. For at udvikle og indføre denne metode i vores laboratorium er fibroblastceller fra personer med Bardet-Biedl syndrom (BBS) blevet lavet om til iPSC ved at elektroporere OCT3/4, SOX2, KLF4, LIN28, L-Myc og en short hairpin RNA mod P53 ind i cellerne.

Undersøgelser af udifferentierede BBS fibroblastceller viste at Hedgehog (Hh) signalering var forstyrret og at længden på det primære cilie var forskellig fra kontrol celler. BBS proteinerne er altså vigtige for både Hh signalering og for regulering af cilielængde.

Både *RAB28* og *BBS* generne er vigtige i forhold til funktionen af retina. Derfor blev iPSC lavet fra BBS fibroblastceller differentieret til (retinal pigmenterede epithelium) RPE celler og brugt som model system i denne afhandling.

BBS-iPSC blev differentieret til RPE celler og undersøgt. RPE differentiering blev udført som en dirigeret proces, med tilførsel af vækstfaktorer og små molekyler for at drive processen (data fra et forsøg er inkluderet). Celler fra en kontrol iPSC linje blev succesfuldt lavet til modne RPE celler. Disse celler var pigmenterede, havde tæt celle-celle kontakt via tight junctions og kunne udføre fagocytose. BBS-iPSC kunne ikke danne mode RPE celler, hvilket var meget overraskende. Morfologien af disse celler var markant anderledes end kontrol cellerne, da BBS-RPE cellerne var større og mere aflange. Disse celler udviklede pigmentering tidligt i forløbet, men dette forsvandt igen. Elektron mikroskopi viste at BBS-RPE cellerne havde løs celle-celle kontakt. Dette fund blev valideret på RNA niveau, ved øget ekspression af gener associeret med adherens junction i forhold til gener associeret med tight junctions. BBS-RPE cellerne havde meget lav fagocytose aktivitet og udtrykte heller ikke nogen gener associeret med modne RPE celler. Ydermere, så havde BBS-RPE cellerne lange primærcilier sammenligner med kontrol celler, de havde forstyrret Hh og Wnt signalering go viste tegn på mitokondrie stress. I et forsøg på at modne BBS-RPE cellerne, blev der tilføjet WNT og Hh pathway agonist og antagonist til cellemediet i et længere forløb til både kontrol-RPE celler og BBS-RPE celler. Dette medførte dog ikke modning i BBS-RPE cellerne. Kontrol-RPE cellerne havde derimod en lille fordel af Wnt inhibering i forhold til modning. Selvom data fra dette forsøg er preliminære, indikerer dette at primærciliet og BBS proteinerne er vigtige for RPE celle differentiering, modning og funktion.

Arbejdet i denne afhandling viser at forskning i sjældne genetiske varianter er vigtigt og aktuelt. Sammenkædning af DNA studier og cellestudier hjalp med at klassificere en ellers ukendt genvariant. I

nogle tilfælde kan sådanne studier virke som grundforskning, men disse resultater kan måske i fremtiden bruges til at udvikle nye behandlingsmetoder og strategier for mennesker der har retinal dystrofi.

Preface and Aim

This dissertation has been submitted to the doctoral school of science and environment at Roskilde University.

The work presented in this dissertation was carried out in the laboratory of Lisbeth Birk Møller at the department of clinical genetics at the Kennedy center; part of the Capital region Denmark hospital (University Hospital Rigshospitalet).

Supervisors:
Internal: Jesper Troelsen, Department of Science and Environment, Roskilde University,
External: Lisbeth Birk Møller, Department of Clinical Genetics, The Kennedy Center, Rigshospitalet.

The aim of this PhD project was:

- To conduct functional investigation of gene variants discovered in individuals suffering from retinal dystrophy.
- To create iPSC lines from individuals suffering from Bardet-Biedl syndrome.
- Differentiation of these iPSC into RPE cells.
- Compare phenotypes between fibroblast and iPSC-derived RPE cells from individuals suffering from BBS to gain proof of concept knowledge of these cell systems and gain new insights into the retinal phenotype of Bardet-Biedl syndrome.

Publications

The following papers are included in this dissertation:

- Research paper I:
  Generation of induced pluripotent stem cells, KCi001-A derived from a Bardet-Biedl syndrome patient compound heterozygous for the *BBS1* variants c.1169T>G/c.1135G>C – *Published* (Hey, Saltõkowa, *et al.*, 2018a).

- Research paper II:
  Generation of induced pluripotent stem cells, KCi002-A derived from a patient with Bardet-Biedl syndrome homozygous for the *BBS10* variant c.271insT – *Published* (Hey, Saltõkowa, *et al.*, 2018b).

- Research paper III:
  Generation and characterization of three isogenic induced pluripotent stem cell lines from a patient with Bardet-Biedl syndrome homozygous for the *BBS5* variant; c.214G>A, p.(Gly72Ser) – *Published* (Hey *et al.*, 2019).

- Manuscript I:
  A missense mutation in *RAB28* in a family with Cone-rod dystrophy and postaxial polydactyly prevents localization of RAB28 to the primary cilium – *Published* (Jespersgaard *et al.*, 2020).

- Draft I:
  BBS1, BBS5 and BBS10 patient cells show signaling defects and dysregulated ciliary length.

- Draft II:
  The BBS proteins are required for RPE cell maturation

The following paper was published during the PhD project:

- Comparison of two different culture conditions for derivation of early hiPSC (Hey, Saltõkova, *et al.*, 2018).

Abbreviations

ACMG	American College of Medical Genetics and genomics.
AMP	Adenosine monophosphate
APC	Adenomatous Polyposis Coli
BBS	Bardet-Biedl syndrome
BBSome	Bardet-Biedl protein complex
bFGF	basic Fibroblast Growth Factor
cAMP	cyclic Adenosine monophosphate
C. elegans	*Caenorhabditis elegans*
Cilium	Primary cilium
CK	Casein kinase
Dkk	Dickkopf-related protein 1
DNA	Deoxyribonucleic Acid
DHh	Desert Hedgehog
DVL	Disheveled
ECD	Extra Cellular Domain
FRZ	Frizzled
GLI(A, R)	Glioma-associated oncogene, Effectors of Hh signaling
GPCR	G protein-coupled receptor
GSK3β	Glycogen Syntase Kinase 3 beta
GTPase	Guanosine Triphosphate hydrolysing enzyme transforming GTP to Guanosine Di-phosphate
HGVS	Human Genome Variation Society
Hh signaling	Hedgehog signaling
IFT	Intra flagellar transport
IGF-1	Insulin-like Growth Factor-1
IHh	Indian Hedgehog
iPSC	induced pluripotent stem cell
LRP 5/6	Lipoprotein-receptor-related protein 5/6

OMIM	Online Mendelian Inheritance in Man, database
OSKM	Transcription factor combination (OCT3/4, Sox2, Klf4 and c-Myc)
PCR	Polymerase Chain Reaction
PEDF	Pigment-derived Epithelial-Derived Factor
PKA	Protein kinase A
PKD	Polycystic Kidney Disease
PTCH1	Patched1
Retinal	Retinaldehyde
RNA	Ribonucleic Acid
RPE cells	Retinal pigment epithelial cells
SHh	Sonic Hedgehog
STR	short tandem repeat
SMO	Smoothened
TZ	Transition zone
Ub	ubiquitinylated
VEGF	vascular endothelial growth factor
VUS	Variant of unknown significance
Wnt	Signaling pathway – blend of words Wingless and Int-1

1. Introduction

A leading cause of blindness in children and young people in the western world is hereditary retinal dystrophies. Retinal dystrophy is a heterogenous group of diseases that cause degeneration of cells in the retina such as photoreceptors and retinal pigment epithelium (RPE) cells. So far, over 150 genes have been linked to retinal dystrophies, and the list is growing. However not all individuals with a clinical retinal dystrophy diagnosis have a complete molecular genetic diagnosis. This PhD project is part of a large project that aim to give more people a molecular genetic diagnosis by applying targeted screening for gene variants using a specially designed retinal dystrophy gene panel and next generation sequencing. A large fraction of the investigated cases have received a final molecular genetic diagnosis but in the remaining cases, the screening resulted in the discovery of several new gene variants with uncertain pathogenicity.

Functional studies of patient cells can help elucidate pathogenicity and disease mechanisms of genetic variants that are difficult to classify. As a tool to setup functional analysis of cells from individuals having variants in genes associated with retinal dystrophy, cells from individuals with Bardet-Biedl syndrome variants in *BBS1*, *BBS5* and *BBS10* as well as a variant the *RAB28* gene, have been applied. The cells with variants in Bardet-Biedl syndrome genes have a plethora of signaling defects, which make them ideal for evaluation of applied cellular assays.

In the following sections an introduction to key aspects in retinal dystrophy, variant analysis, the ciliopathy Bardet-Biedl syndrome plus affected signaling pathways, stem cell generation, retinal differentiation and the role of RAB28 in cilia will be given.

1.1. Retinal dystrophy

Retinal dystrophy is a collective name for a heterogenous group of diseases affecting 1:4000 that causes visual impairment or loss of vision. The retina has an inner and an outer layer of neurons. The outer layer consists of the RPE cells and the photoreceptor cells whereas the inner layer is composed of horizontal cells, bipolar cells, ganglion cells and amacrine cells. The cell types mainly affected in the retina are the photoreceptors and the RPE cells (Willoughby *et al.*, 2010; Nash *et al.*, 2015). The photoreceptor cells are responsible for transducing light signals to the brain, who will then translate this information into a picture. This process happens through a coordinated pathway involving both photoreceptor cells and RPE cells. Photoreceptor cells use the protein retinal localized in the discs in the outer segment (see Figure 1) for light sensation but they are dependent on the RPE cells for recycling of this protein to maintain their function (see below) (Kevany and Palczewski, 2010).

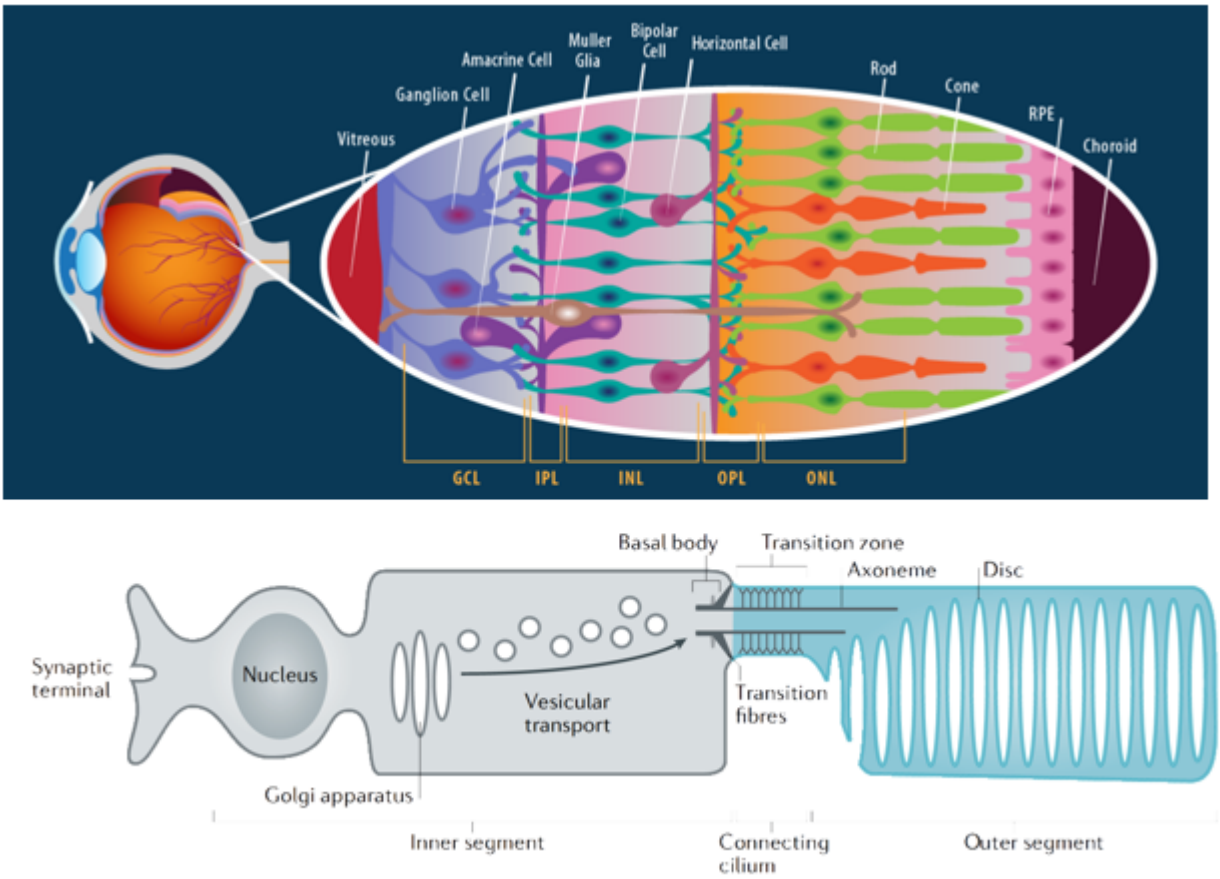

Figure 1 Schematic overview of the eye and the photoreceptor cells. The retina is located at the back of the eye and consists of many different cell types. Below is a schematic presentation of a photoreceptor cell showing the inner segment, where protein synthesis takes place and the highly organized outer segment where the discs are formed. The two compartments are connected by a modified primary cilium. Modified from https://discovery.lifemapsc.com/library/images/the-cellular-structure-of-the-retina and (Nachury and Mick, 2019).

Vision is affected differently depending on the type of retinal dystrophy. The rod photoreceptor cells are responsible for sight in low-light conditions, and malfunction of these cells lead to night blindness. Cone photoreceptor cells are responsible for high acuity vision and color perception. Loss of cone photoreceptors cells is more severe. It can start as loss of peripheral or central vision and develop into complete blindness. Either rods or cones can be affected separately or both cell types can be affected. Some retinal dystrophies first affect rods, causing night blindness, and later develop into full blindness also involving the degeneration of the cone photoreceptor cells. For cone-rod dystrophies this could present as developing night blindness that progress into loss of central vision or complete blindness (Nash *et al.*, 2015). See Figure 2 for examples on three types of vision loss.

Figure 2 Overview of three different types of vision loss. Modified from https://www.fightingblindness.org/diseases/bardet-biedl-syndrome-bbs.

Retinal dystrophies have been studied in affected individuals as well as in animal models, giving us some answers to the underlaying pathologies of this group of diseases however more cell studies are needed to elucidate the exact cellular mechanisms that are disturbed (Kostic and Arsenijevic, 2016; Van Cruchten *et al.*, 2017).

1.2. Gene Variant Evaluation

A DNA sample from a person with retinal dystrophy is investigated for genomic variations using next generation sequencing of a gene panel consisting of genes known to cause retinal dystrophy to find a variant that underly the disease. Depending on the difficulty in finding the variant, exome sequencing of the non-coding DNA as well as whole genome sequencing can be applied. Then the pathogenicity of the variant needs to be determined. Variants that cause a change on protein level, such as frameshift, deletion or nonsense variants, are relatively easy to classify as they will often lead to loss of protein function or proteasomal degradation of the protein. If the variant causes a silent, missense, or in-frame deletion/insertion change in the DNA, the pathogenicity evaluation is much more difficult.

A set of guidelines, the ACMG (The American College of Medical Genetics and Genomics) standards and guidelines, have been developed to make evaluation and classification of new sequence variants easier and to make sure the same methods are applied in the process. The guidelines set up five categories for classifying variants: (1) pathogenic, (2) likely pathogenic, (3) uncertain significance (VUS), (4) likely benign, (5) benign, and stress the importance of using the standard nomenclature developed by Human Genome Variant Society (HGVS) (Richards *et al.*, 2015). When evaluating the variant, it is necessary to search the literature and databases for information. Several databases exist, and the guidelines state the importance of using databases that are up to date, that literature is of high quality and that the HGVS nomenclature is used. Lastly, it is useful to do *in-silico* analysis of the variant using programs that can predict the effects of the variant on; nucleotide/amino acid level, primary and alternative transcripts, non-coding sequences and protein level (structure and/or function). Due to the complexity of the data analysis and interpretation, it is also highly recommended that an expert in molecular genetics or genetic pathology interpret the variant data. Furthermore, it is important to keep the guidelines updated (Mathe *et al.*, 2006; Tavtigian *et al.*, 2006; Adzhubei *et al.*, 2010; Schwarz *et al.*, 2010; Richards *et al.*, 2015; Vaser *et al.*, 2016; Karczewski *et al.*, 2017; Rentzsch *et al.*, 2019).

The ACMG guidelines provide a good foundation to make sure variant analysis is performed in a comparable and harmonized manner. Even though we continue to learn more and develop methods that are more sensitive, there is still many variants that are classified VUS. This may be due to the increased availability of sequencing in the clinic and the increased detection of VUS. This is both frustrating to the investigated individual and bad in terms of finding suitable treatment options. A strategy to gain more

knowledge is to apply functional assays on material, such as fibroblast cells obtained through a skin biopsy, from the individual in question. From that, it is possible to evaluate the cellular effects of the variant in question. If the patient has several variants, then analysis of results has to be done with caution as it is difficult to conclude which effects are from the observed variants and which might be caused by other variants or just from genetic variation in general. Additional studies using knock down of the gene where the variant is located can help ascertain that the variant is the cause indeed.

Some variants affect genes that function in certain tissues, and in these cases the use of stem cell-derived models is of special interest as it is possible to generate the specific cell type affected. Stem cells can be generated from the affected individuals own cells (Takahashi *et al.*, 2007), further underlining the benefit of recommending these individuals with retinal dystrophy to donate cells for functional assays. The creation of a biobank with cell samples from individuals with retinal dystrophy would be very beneficial in evaluation of cases that are unsolved, as methods for investigating cellular effects continue to be developed and refined.

In this dissertation, one example of the integration of cellular studies in variant analysis is presented that help classify a novel variant in the *RAB28* gene as likely pathogenic (See Manuscript 1). In this case, subcellular localization studies of patient fibroblast cells showed a connection of the variant to RAB28 protein localization in the primary cilium.

1.3. Primary Cilia

The primary cilium (cilium) is present in a single copy on most quiescent cell types in vertebrates as a membrane protrusion sensing the environment of the cell. Cilia are composed of a ring containing 9 microtubule doublet pairs forming a tube called the axoneme emanating from the basal body, which is a modified mother centriole of the centrosome of the cell (Sorokin, 1962, 1968) (See Figure 3). This gives the cilium a characteristic “9+0” axonemal structure. Motile cilia are similar but have a central pair of microtubules as well as motor proteins to generate locomotion, giving this axoneme a “9+2” structure (Satir and Christensen, 2007; Heydeck *et al.*, 2018). The basal body is important in cilia biogenesis, as it contains important structures, e.g. transition fibers, that aid in vesicle docking and docking of the basal body at the plasma membrane of the cell (Sorokin, 1962, 1968). Cilia biogenesis happens after cell division, during quiescence, when the centrioles are not needed to form the mitotic spindle (Tucker, Pardee and Fujiwara, 1979). The two centrioles are reorganized, and tubulin subunits are added to the mother centriole to form the axoneme. As cilia do not synthesize proteins, active transport is required for cilia biogenesis, axoneme elongation and cilia homeostasis (Sung and Leroux, 2013; Lechtreck, 2015; Taschner and Lorentzen, 2016; Morthorst, Christensen and Pedersen, 2018) and depending on cell type, axoneme elongation can begin before the basal body has docked at the plasma membrane (Sorokin, 1962, 1968). Ciliary length is determined by a dynamic addition and removal of tubulin subunits at the tip of the cilium, regulated by *proteins and kinases*. This causes the ciliary length to be an equilibrium of the speed of tubulin addition and removal – also known as dynamic instability (Avasthi and Marshall, 2012; Broekhuis, Leong and Jansen, 2013).

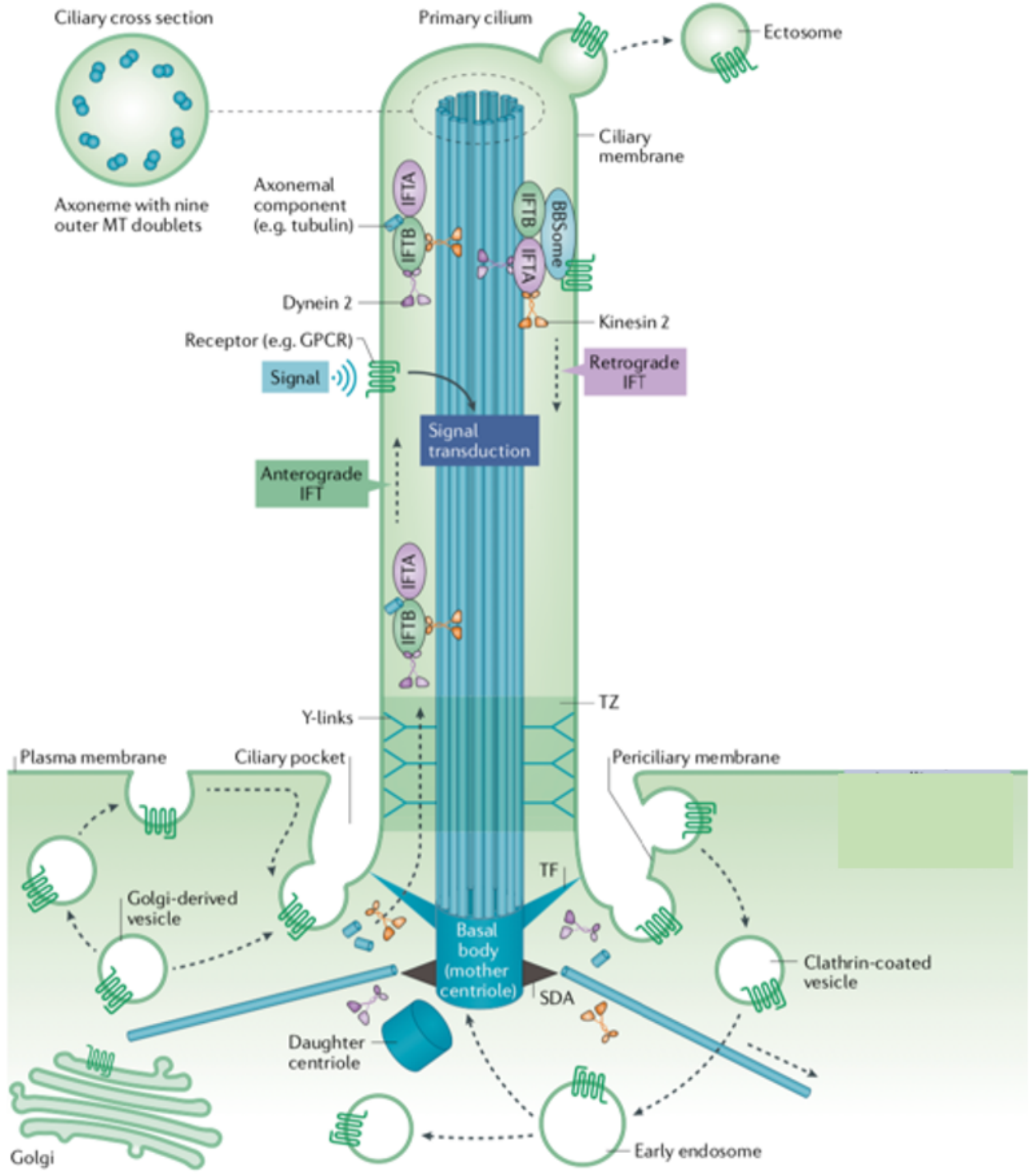

Figure 3 Structure of the primary cilium. Modified from (Anvarian *et al.*, 2019)*. The primary cilium projects from the basal body and consists of a ring of 9 microtubule doublets. The ciliary membrane is continuous with the plasma membrane of the cell but structures at the transition zone (TZ) and base of the cilium such as Y-links and transition fibers help form a selective barrier that requires active transport to cross. The transport machinery in cilia is termed intra flagellar transport (IFT). Complexes consisting of the motor proteins dynein 2 and kinesin 2, IFTA and IFTB complexes, the BBSome are assembled into IFT trains that can carry cargo, such as tubulin or signaling receptors, in anterograde or retrograde directions. The ciliary pocket and periciliary membrane are areas where vesicular transport take place. Delivery of signaling receptors from the Golgi network is mediated through vesicular transport to the plasma membrane or the ciliary pocket from where the IFT machinery will take over. During receptor removal from the cilium, IFT trains will deliver the receptor at the periciliary membrane where it can be phagocytosed onto a clathrin-coated vesicle and be degraded by the endo-lysosomal system or recycled. Alternatively, receptors can exit the cilium at the tip through ectocytosis.*

The membrane of the cilium is continuous with the cell membrane, but the composition is quite different. The region at the base of the cilium, the area between the basal body and the ciliary axoneme is called the transition zone (TZ). The TZ contain Y-links that, together with the transition fibers, help form a selective barrier that requires active transport of most proteins to be able to enter and exit the cilium (Garcia-Gonzalo and Reiter, 2017) (see Figure 3). This together with the ciliary transport system, intra flagellar transport (IFT), and vesicular transport allows the ciliary membrane to differ from that of the cell and be enriched with signaling receptors making this organelle an ideal signaling hub.

IFT trains travel along the microtubules in the ciliary axoneme carrying cargo to the tip (anterograde direction) or to the base (retrograde direction) (Lechtreck, 2015; Taschner and Lorentzen, 2016) (see Figure 3). This is an important process for both maintenance and biogenesis of the cilium, as this organelle is unable to synthesize proteins (Sung and Leroux, 2013; Lechtreck, 2015; Taschner and Lorentzen, 2016; Morthorst, Christensen and Pedersen, 2018). IFT function through complexes consisting of IFTA (Mukhopadhyay *et al.*, 2010; Liem *et al.*, 2012; Fu *et al.*, 2016; Badgandi *et al.*, 2017; Hirano *et al.*, 2017) and IFTB, which is further composed of two subcomplexes; IFTB1 (the core complex consisting of IFT88, -81, -74, -70, -56, -27, -25 and -22) and IFTB2 (the peripheral complex consisting of IFT172, -80, -57, -54, -38, -20) (Lucker *et al.*, 2005, 2010; Taschner *et al.*, 2011, 2014, 2016; Taschner and Lorentzen, 2016; Prevo, Scholey and Peterman, 2017) in combination with the motor proteins heterotrimeric kinesin 2, carrying the complex in the anterograde direction towards the ciliary tip, and cytoplasmic dynein 2 carrying cargo in the retrograde direction to the ciliary base (Kinesin; (Walther, 1994; Kozminski, Beech and Rosenbaum, 1995; Vashishtha, Walther and Hall, 1996)) (Dynein; (Pazour, Wilkerson and Witman, 1998; Pazour, Dickert and Witman, 1999; Porter *et al.*, 1999)). It was initially thought that IFTA and IFTB only participated in transport in one direction, but we now know that they participate in both anterograde and retrograde IFT (Pedersen *et al.*, 2005; Mukhopadhyay *et al.*, 2010; Behal *et al.*, 2012; Keady *et al.*, 2012; Liem *et al.*, 2012; Bhogaraju *et al.*, 2013; Eguether *et al.*, 2014; Mourão, Christensen and Lorentzen, 2016; Eguether, Cordelieres and Pazour, 2018). For instance, four proteins of the IFTB complex assist in different IFT directions; the anterograde transport of tubulin during ciliogenesis is promoted by IFT81 and IFT74 (Bhogaraju *et al.*, 2013) whereas IFT25 and IFT27 work in ciliary export of Hedgehog signaling components (Keady *et al.*, 2012; Eguether *et al.*, 2014; Mourão, Christensen and Lorentzen, 2016; Eguether, Cordelieres and Pazour, 2018) (see section below for more information about this signaling pathway). IFTA also has a secondary role, as it has been found to interact with TUBBY protein TULP3 to promote transport of G protein-coupled receptors (GPCRS) into cilia (Mukhopadhyay *et al.*, 2010; Badgandi *et al.*, 2017; Hirano *et al.*, 2017). The IFT complexes also interact with the BBSome – a protein complex consisting of 8 BBS proteins functioning as an adaptor between the IFT complex and cargo (Ou *et al.*, 2005; Nachury *et al.*, 2007; Lechtreck *et al.*, 2009; Jin *et al.*, 2010; Seo *et al.*, 2011). It was initially thought that the BBSome served as a coat promoting transport of signaling receptors into the cilium but now it has been proposed to mainly function in the regulation of signaling protein export from the cilium (Lechtreck *et al.*, 2009, 2013; Jin *et al.*, 2010; Nachury, 2018). Although we have come far in identifying the mechanisms for ciliary transport, import and export, this system is complex, and we have still have much to learn. Another way of ciliary exit is through ectocytosis. This is a process where cargo accumulates at the tip of the cilium, causing the membrane to bulge out and eventually burst free as a small membrane enclosed vesicle (Wood *et al.*, 2013; Cao *et al.*, 2015; Nager *et al.*, 2017).

One way to induce the formation of primary cilia is by reducing the amount of fetal bovine serum in the used growth medium. This will promote the cells to exit the cell cycle, go into growth arrest and form the cilium.

Furthermore, the serum may contain growth factors that can inhibit ciliogenesis, so formation of the cilium may be promoted through the absence of these as well. This method is easy and widely used, as it does not grossly affect cellular survival (Santos and Reiter, 2008).

The first evidence of IFT being involved in disease was found in experiments with *C. reinhardtii* where a variant in the *IFT88* gene, which is part of the IFTB1 complex, caused loss of cilia and polycystic kidney disease (PKD) (Moyer *et al.*, 1994; Pazour *et al.*, 2000). Since then, several diseases have been linked to ciliary function and collectively these diseases are called ciliopathies. Photoreceptor cells have a specialized primary cilium that connects the inner and outer segment of the cell (See above) Ciliary disruption in photoreceptor cells can lead to their degeneration and development of retinal dystrophy (Datta *et al.*, 2015). PKD and retinal dystrophy is also symptoms observed in the ciliopathy Bardet-Biedl syndrome.

1.4. Bardet-Biedl Syndrome

Bardet-Biedl syndrome (BBS) is a heterogenous multi-organ autosomal recessive disorder characterized by variants in one of 23 BBS genes that are all connected to ciliary function (see below). Estimated prevalence range from 1:59 000 to 1:160 000 in Europe classifying BBS as a rare disease (Hjortshøj *et al.*, 2010; Forsythe and Beales, 2013; Shamseldin *et al.*, 2020).

The first case of BBS was reported by Laurence and Moon in 1866, and separately by ophthalmologists Bardet and Biedl in the 1920's (Bardet, 1995; Biedl, 1995; LAURENCE and MOON, 1995). The patients had a broad spectrum of symptoms; retinal dystrophy, polydactyly, obesity, learning difficulties and genital anomalies and were first divided into two; Laurence Moon syndrome and Bardet-Biedl syndrome (BBS). As several of the symptoms overlap between the two syndromes, today patients are diagnosed with BBS. The first clue to a patient having BBS is postaxial polydactyly and the development of retinal dystrophy. Retinal dystrophy is one of the most devastating symptoms of BBS leading to blindness within the second decade of life. 90% of individuals with BBS develop retinal dystrophy that develops as a rod-cone dystrophy. Symptoms start to show early in childhood with emerging night blindness that will progress to affect central vision as well (Klein and Ammann, 1969; Beales *et al.*, 1999; Forsythe and Beales, 2013). The retinal implications are heterogenic both in severity and phenotype and affects dark adaptation, the visual fields and the acuity of vision at varying degrees (Héon *et al.,* 2005; Azari *et al.,* 2006). 75% of affected individuals will progress to legal blindness with their second or third decade of life (Klein and Ammann, 1969; Forsythe and Beales, 2013). Many also become obese early in childhood, have learning disabilities and develop renal cysts (Forsythe and Beales, 2013).

Primary features	Secondary Features
Rod-cone dystrophy	Speech delay
Polydactyly	Developmental delay
Obesity	Diabetes mellitus
Genital anomalies	Dental anomalies
Learning difficulties	Congenital heart disease
Renal defects	Brachydactyly/syndactyly
	Ataxia/poor coordination
	Anosmia/hyposmia

Table 1 Overview of clinical BBS symptoms used for diagnostics.

Diagnosis of BBS is done based on clinical findings as well as screening for variants in the known BBS genes. Two categories were made based on observed phenotypic traits of BBS patients (see Table 1). To

make a clinical diagnosis, four primary features, or three primary and two secondary features should be observed preferably supported by a *BBS* gene variant (Forsythe and Beales, 2013).

The first link between BBS and cilia was found investigating BBS8. Ansley et al. show that BBS8 localizes to cilia in the retina and in lung epithelial cells (Ansley *et al.*, 2003). Today 23 genes have been associated with BBS all of which are linked to the cilium (See Table 2 Overview of name, localization and function of the 23 known BBS proteins.). The BBSome, which consists of BBS1, BBS2, BBS4, BBS5, BBS7, BBS8, BBS9, BBS17 and BBS18 (Nachury *et al.*, 2007; Jin *et al.*, 2010; Seo *et al.*, 2011), the chaperonin complex, consisting of BBS6, BBS10, and BBS12 (Seo *et al.*, 2010), BBS19 and BBS20 are localized in the cilium, and most of the remaining BBS proteins are located at the ciliary base (Suspitsin and Imyanitov, 2016). The BBSome facilitates export of IFT cargo and the chaperonin-complex assembles the BBSome (Álvarez-Satta, Castro-Sánchez and Valverde, 2017; Liu and Lechtreck, 2018). BBS3/ARL6 recruits the BBSome to the cilium and has a proposed role as a modulator of the Wnt pathway (Jin *et al.*, 2010; Wiens *et al.*, 2010; Mourão *et al.*, 2014). BBS11 is an E3 ubiquitin ligase whose ciliary connection is still being investigated (Chiang *et al.*, 2006; Novas *et al.*, 2015). BBS13, BBS15 and BBS16 all play a role in ciliogenesis (Dawe *et al.*, 2007; Leitch *et al.*, 2008; Tammachote *et al.*, 2009; S. K. Kim *et al.*, 2010; Schaefer *et al.*, 2010; Billingsley *et al.*, 2012; Airik *et al.*, 2016). BBS15 is also involved in cell movement through planar cell polarity (S. K. Kim *et al.*, 2010) and BBS16 is involved in Hedgehog (Hh) signaling (Schaefer *et al.*, 2010; Billingsley *et al.*, 2012; Airik *et al.*, 2016). Another BBS protein important for signaling is BBS17, that has been linked to both Hh signaling and Leptin signaling(Marion *et al.*, 2012; Wei *et al.*, 2018).

Protein	Gene	Localization	Function
BBS1	*BBS1*	BBSome: cilium/Basal Body	IFT adaptor, ciliary export
BBS2	*BBS2*	BBSome: cilium/Basal Body	IFT adaptor, ciliary export
BBS3	*ARL6*	Basal Body	Triggers BBSome coat formation
BBS4	*BBS4*	BBSome: cilium/Basal Body	IFT adaptor, ciliary export
BBS5	*BBS5*	BBSome: cilium/Basal Body	IFT adaptor, ciliary export
BBS6	*MKKS*	Chaperonin complex/basal body	Assembly of BBSome
BBS7	*BBS7*	BBSome: cilium/Basal Body	IFT adaptor, ciliary export
BBS8	*TTC8*	BBSome: cilium/Basal Body	IFT adaptor, ciliary export
BBS9	*BBS9*	BBSome: cilium/Basal Body	IFT adaptor, ciliary export
BBS10	*BBS10*	Chaperonin complex/basal body	Assembly of BBSome
BBS11	*TRIM32*	-	E3 ubiquitin ligase
BBS12	*BBS12*	Chaperonin complex/basal body	Assembly of BBSome
BBS13	*MKS1*	Basal Body	Ciliogenesis
BBS14	*CEP290*	Centrosome/cilium	Regulator of ciliary import and export of signaling molecules
BBS15	*WDPCP*	Basal Body	Ciliogenesis and cell migration
BBS16	*SDCCA8*	Centrosome	Ciliogenesis
BBS17	*LZTFL1*	BBSome: cilium/Basal Body	IFT adaptor, ciliary export
BBS18	*BBIP1*	BBSome: cilium/Basal Body	IFT adaptor, ciliary export
BBS19	*IFT27*	IFTB1 complex/cilium	IFT
BBS20	*IFT172*	IFTB1 complex/cilium	IFT
BBS21	*C8orf37*	Connecting cilium, photoreceptors	Unknown
BBS22	*SCLT1*	-	Unknown
BBS23	*CEP164*	-	Unknown

Table 2 Overview of name, localization and function of the 23 known BBS proteins. OMIM (Online Mendelian Inheritance in Man) database.

BBS14 acts as a modulator of ciliary import and export of signaling molecules (Leitch *et al.*, 2008; Shimada *et al.*, 2017). BBS19 and BBS20 are both part of the IFTB1 complex and thus function in ciliary transport

activities (Eguether *et al.*, 2014; Bujakowska *et al.*, 2015; Schaefer *et al.*, 2016). The function of BBS21 is still largely unknown, however we know that malfunctioning BBS21 protein leads to vision loss (Estrada-Cuzcano *et al.*, 2012; Heon *et al.*, 2016). BBS proteins have also been proposed as ciliary length regulators (Wiens *et al.*, 2010; Hernandez-Hernandez *et al.*, 2013; Patnaik *et al.*, 2019). SCLT1 and CEP164 have very recently been linked to BBS and their precise function in BBS remains to be determined (Shamseldin *et al.*, 2020).

The most commonly associated genes in Europe are *BBS1* and *BBS10* (Harville *et al.*, 2010) whereas in India and Saudi Arabia variants in *BBS3* and *BBS9* have a high prevalence (Abu Safieh *et al.*, 2010; Sathya Priya *et al.*, 2015). In total, variants in *BBS1-BB18* account for 70-80% of reported cases. The geological difference in the most commonly associated genes, underline the heterogeneity of BBS (Zaghloul and Katsanis, 2009; Muller *et al.*, 2010; M'hamdi *et al.*, 2014; Priya *et al.*, 2016). The ciliary connection with BBS explains why the observed phenotypic traits of this disease compromise so many different cell types and organs, as cilia are present in many cell types.

Many studies investigating the function of BBS proteins have been published – most of them use mouse models or immortalized cell lines with the gene of interest knocked out (Berbari *et al.*, 2008; Seo *et al.*, 2010; Zhang *et al.*, 2012; Hernandez-Hernandez *et al.*, 2013; Mourão *et al.*, 2014; Datta *et al.*, 2015; Airik *et al.*, 2016; Nozaki *et al.*, 2018).

Even though we have identified numerous BBS genes, there is currently no cure or treatment for this disease beside from symptomatic treatment. This is in part due to the number of associated genes, but also due to the rarity of some variants. This complicates the development of therapies for this disease. Development of gene therapy for the retinal phenotype is underway, but so far the work is in early stages focusing on *BBS1* variants in rodents (Forsythe *et al.*, 2018).

1.5. Signaling Pathways

The role of the cilium in regulating signaling has been established and BBS proteins has been linked to the transport of several signaling receptors (Anvarian *et al.*, 2019; Nachury and Mick, 2019). Hedgehog (Hh) signaling is important in embryonic development, and disturbances has been linked to tissue patterning defects (Briscoe and Thérond, 2013). Wnt signaling has been shown to be important when differentiating stem cells to RPE cells (see below) (May-Simera *et al.*, 2018).

In this section, an overview of Hh and Wnt signaling is given. Thorough reviews on the complex activation and regulations steps of both pathways exist but are beyond the scope of this dissertation. Focus in the following sections is on the key proteins and processes in these pathways important for getting an overview of the experimental work presented in section 5.

1.5.1. Hedgehog Signaling

Hedgehog (Hh) signaling is one of the most studied signaling pathways connected to the primary cilium. Hh determine self-renewal and cell fate in tissue homeostasis and during embryonic development (Briscoe and Thérond, 2013). The investigation of developmental defects in mice and other vertebrates connected IFT and the cilium to Hh during embryonic development (Huangfu *et al.*, 2003; Goetz and Anderson, 2010) and today we know that almost all involved proteins in Hh signaling are coupled to the cilium (Anvarian *et al.*, 2019). Activation and basal repression rely on ciliary trans-localization of several receptors, underlining the role of IFT in this pathway, and post-translational modifications of the GLI transcription factors (Eguether,

Cordelieres and Pazour, 2018; Anvarian *et al.*, 2019). See Figure 4 for a schematic presentation of the Hh pathway.

When the pathway is inactive/during basal repression, the seven trans-membrane receptor PATCHED1 (PTCH1) is localized at the ciliary membrane. GRP161, another negative regulator of Hh, is transported into the cilium through binding of tubby-like protein 3 (TULP3) and IFTA. This activates adenylyl cyclase that in turn increase the level of cyclic AMP (cAMP). Increased cAMP frees Protein kinase A (PKA) so it, together with glycogen synthase kinase 3β (GSK3β) and casein kinases (CK) can phosphorylate and promote proteolytic processing of full length GLI3 (GLIFL) leading to the formation of the truncated repressor form of GLI (GLIR) that prevents transcription of target genes. Suppressor of Fused (SUFU) is localized in the cytoplasm and act to restrain GLI3 there and promote processing into GLIR (Mukhopadhyay and Rohatgi, 2014; Anvarian *et al.*, 2019).

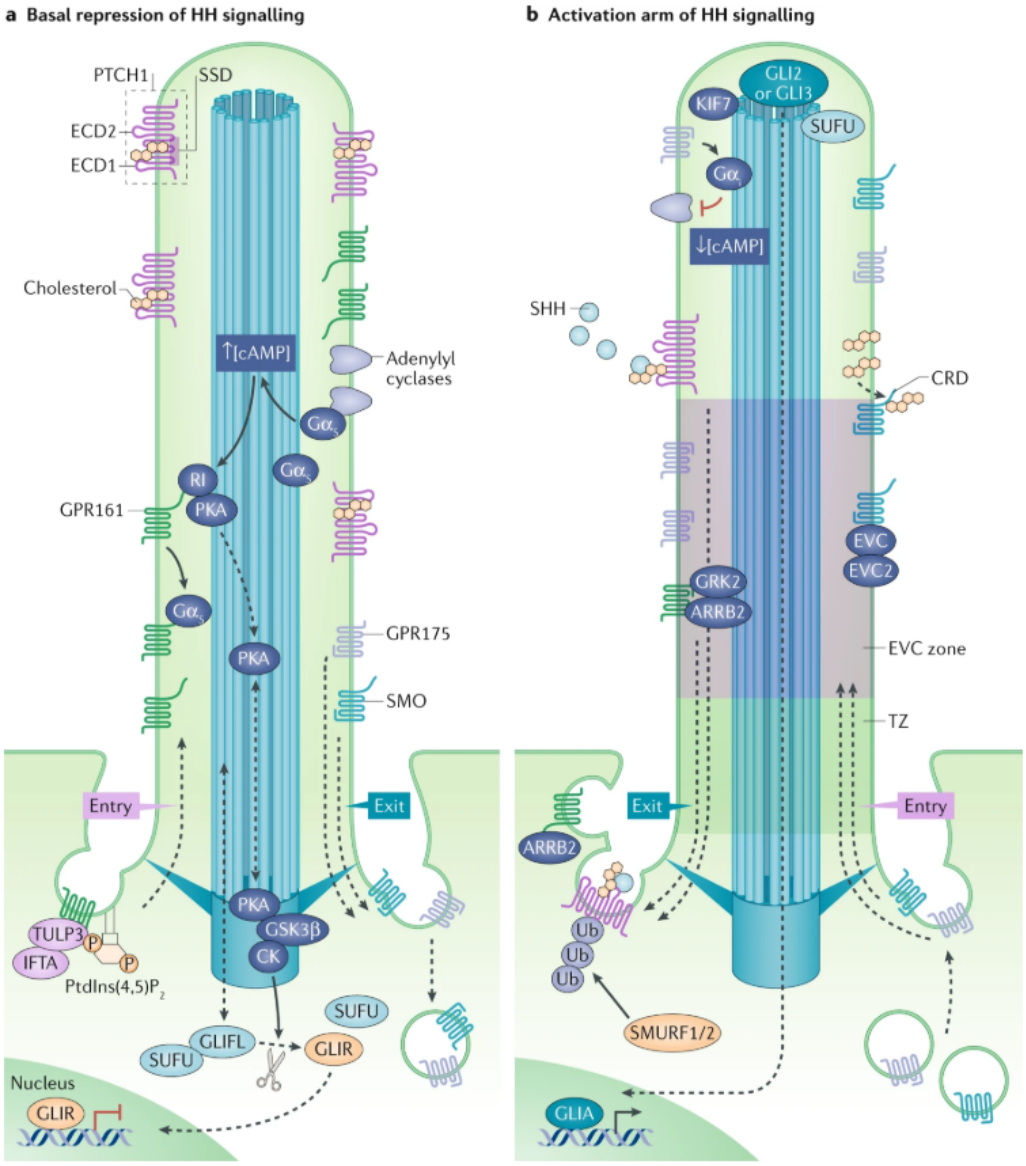

Figure 4 Schematic representation of Hh signaling. A: During Basal repression, PTCH1 and GPR161 is enriched in the ciliary membrane. This promotes the formation of cAMP through PKA and stimulates the processing of GLI transcription factors into their repressor form, GLIR. SMO and GPR175 that work in activating the pathway are exported from the cilium. B: When a ligand in

bound to PTCH, e.g. SHh, PTCH1 and GPR161 are transported out of the cilium through mechanisms involving GRK2 and ARRB2 and endocytosis allowing SMO to enter the cilium. This leads to a drop in cAMP and subsequently the GLI transcription factors are released from SUFU and processed into their activator forms, GLIA that turn on target gene expression. From (Anvarian *et al.*, 2019).

The availability of the PTCH1 receptor for ligand binding is regulated by cholesterol derivatives at the extra cellular domains (ECD).When the ligand Sonic Hh (SHh) binds PTCH1, PTCH1 is removed from the cilium through a coordinated process where it is ubiquitinylated (Ub) by E3 ligases SMURF1 and SMURF2 targeting PTCH1 for endocytosis by KIF13B and proteasomal degradation after trans-location to the transition zone of the cilium (Yue *et al.*, 2014; Schou *et al.*, 2017). This allows the receptor Smoothened (SMO) to be enriched in the ciliary membrane (Corbit *et al.*, 2005; Rohatgi, Milenkovic and Scott, 2007) promoting dissociation of SUFU from GLI. This leaves GLI free to be processed into the activator form of GLI (GLIA), by the phosphorylation of GLI2 at the ciliary tip and accumulation of KIF7 (Niewiadomski *et al.*, 2014). GLIA will subsequently translocate into the nucleus and activate transcription of target genes, such as GLI1. GLI2 and GLI3 can act as GLIR and GLIA but GLI1 can only act as GLIA (Liu, 2019).

Several other proteins add to the complexity of this signaling pathway and leave extra levels of regulation. After ciliary exit of GPR161, GPR175 enters the cilium and prevents the formation of cAMP, to further inhibit PKA activity (Singh, Wen and Scales, 2015). β-arrestin 2 (ARRB2) is thought to mediate ciliary exit in cooperation with the BBSome and IFT trains. It is thought to act as an adaptor between GPR161 and IFT and is recruited by GPCR kinase 2 (GRK2) (Pal *et al.*, 2016; Anvarian *et al.*, 2019). GPR2 can also induce Hh independently of GPR161 (Pusapati *et al.*, 2018). And finally, EVC and EVC2 complex mediate SMO-dependent activation of GLI2 (Dorn, Hughes and Rohatgi, 2012; Mukhopadhyay and Rohatgi, 2014). The IFTA complex itself has also been shown to have a regulatory role in Hh signaling (Liem *et al.*, 2012).

Aside from Shh, two other ligands for Hh signaling exist; Desert Hh (DHh) and Indian Hh (IHh). These ligands are tissue-specific to testis and growth plate chondrocytes respectively (Bitgood and McMahon, 1995). The above described type of Hh signaling is the canonical form but non-canonical Hh signaling has also been described that is either GLI or SMO independent. The exact function of this type of Hh signaling remains to be elucidated (Bijlsma and Roelink, 2010; Carballo *et al.*, 2018). Chemical compounds that modulate Hh signaling have been used to elucidate the mechanisms of this pathway. Cyclopamine, an antagonist of Hh, leads to SMO accumulation without activation of the pathway (Rohatgi *et al.*, 2009). Purmorphamine activates Hh signaling by binding directly to SMO and activating it (Sinha and Chen, 2006).

Several BBS components have also been linked to Hh signaling. The BBSome protein complex (see above) is involved in transport of GPCRs from the cilium back to the cell (Ye, Nager and Nachury, 2018). This process is important in Hh signaling, as both PTCH1 and GPR161 need to exit the cilium for Hh signaling to be activated. When the BBSome is not working, several proteins accumulate in the cilium, including SMO, leading to the disturbance of Hh signaling. Some of this disturbance may be rescued by ectosomal exit of ciliary proteins (Nager *et al.*, 2017). BBS16, BBS17 and BBS19 also regulate Hh (Marion *et al.*, 2012; Eguether *et al.*, 2014; Airik *et al.*, 2016). Dysregulation of Hh signaling has been linked to skeletal defects such as polydactyly, a feature commonly observed in BBS (Liu, 2019), highlighting the importance of this pathway.

1.5.2. Wnt Signaling

Two types of Wnt signaling exist; the canonical, working through β-catenin, affecting cell division, survival and differentiation, and the non-canonical or planar cell polarity subdivision, important for cell migration, that implicates a plethora of receptors depending on the desired downstream cellular events (MacDonald,

Tamai and He, 2009; Foulquier *et al.*, 2018; Anvarian *et al.*, 2019). The focus here will be on canonical-Wnt signaling. See Figure 5 for an overview of the pathway.

When the pathway is inactive, β-catenin is degraded by the β-catenin destruction complex consisting of adenomatous polypsis coli (APC), Axin, glycogen synthase kinase-3β (GSK3β) and casein kinase 1α (CK1α) binding and phosphorylating β-catenin which is then removed by the E3 ubiquitin-proteasome pathway ultimately leading do a decreased concentration of β-catenin in the cytoplasm (MacDonald, Tamai and He, 2009; Voronkov and Krauss, 2012).

The activation of Wnt happens when a ligand, the Wnt proteins, are acetylated by porcupine and subsequently bind to the receptor Frizzled (FRZ) and lipoprotein-receptor-related protein (LRP) 5/6 forming a complex at the plasma membrane. This in turn activates the Disheveled (DVL) proteins who bind to the c-terminus of FRZ while recruiting Axin, GSK3β and CK1 from the β-catenin-destruction complex. Once Axin has left the destruction complex the β-catenin destruction complex cannot form, leading to stabilized β-catenin that will accumulate and be transported to the nucleus where it activates transcription of target genes aided by transcription factors of the TCF/LEF family (Huelsken, 2002; MacDonald, Tamai and He, 2009; Valenta, Hausmann and Basler, 2012). Other mechanisms of β-catenin accumulation in the cytoplasm have been described that also act by disrupting the destruction complex (MacDonald and He, 2012; Guettler, 2016).

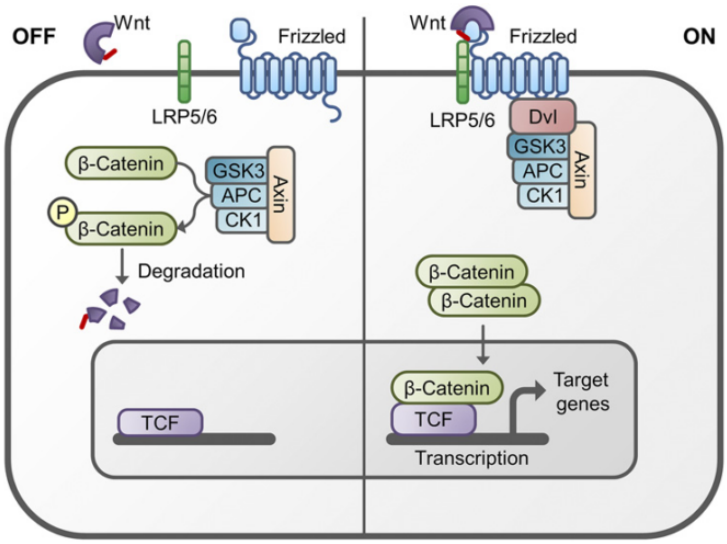

Figure 5 from (Foulquier *et al.*, 2018). *Schematic presentation of the Wnt signaling pathway. In the "OFF" state, the β-catenin destruction complex, consisting of GSK3, APC, CK1 and AXIN, targets β-catenin for degradation through the ubiquitin-proteasome pathway thus inhibiting transcription of target genes. In the "ON" state, Wnt ligand binds Frizzled forming a complex with LRP5/6, DVL, GSK3, APC, CK1 and Axin at the plasma membrane. This inhibits the activity of the β-catenin destruction complex ultimately leading to increased accumulation of β-catenin in the cytoplasm that enters the nucleus activating transcription of target genes aided by transcription factors from the TCF family.*

The cilium has been proposed as a regulator of Wnt signaling, but the literature is controversial even though several of the key Wnt pathway proteins have been shown to localize to cilia (Corbit *et al.*, 2008; He, 2008; Ocbina, Tuson and Anderson, 2009; Gerhardt *et al.*, 2016). One study found the cilium as a regulator of canonical Wnt – when they disrupted IFT, by depleting mouse embryos of KIF3A, Wnt activity was increased. A similar effect was seen in mouse embryonic fibroblasts when the entire cilium was disrupted as this led to hypersensitivity to the WNT3A ligand (Corbit *et al.*, 2008). But another one found Wnt activity to

be unchanged under similar conditions (Ocbina, Tuson and Anderson, 2009). Many other studies have tried to establish the function of the primary cilium in Wnt signaling but the mechanisms and overall role of the cilium is still unclear, further underlining the complexity of this pathway (Anvarian *et al.*, 2019).

Different agonists and antagonists have helped gain insight into Wnt signaling with different compounds targeting different parts of the Wnt signaling network. The Wnt activator CHIR99021 works by inhibiting GSK3β leaving the β-catenin destruction complex inactive and allowing β-catenin to accumulate in the cytoplasm (Bennett *et al.*, 2002). Dkk1 works as an inhibitor on Wnt signaling, as it binds LRP5/6 preventing the FRZ-receptor complex forming (Mao *et al.*, 2002). IWR-1 is another inhibitor of Wnt that targets tankyrases stabilizing Axin and the β-catenin destruction complex (Chen *et al.*, 2009; Martins-Neves *et al.*, 2018). IWP2 inhibits Porcupine activity hindering the secretion of Wnt ligands Wnt-1, Wnt2 and Wnt3a so the pathway is not activated (Wang *et al.*, 2013).

Suppression of BBS genes has previously been shown to stabilize β-catenin leading to a change in downstream effects (Gerdes *et al.*, 2007a; Wheway, Parry and Johnson, 2014). *BBS1*, *BBS3*, *BBS4* and *BBS6* have been implicated in Wnt signaling (Gerdes *et al.*, 2007b; Wiens *et al.*, 2010).

1.6. RAB28

In manuscript I, two brothers with a variant in the *RAB28* gene are described. Based on their clinical findings and from previously described variants in *RAB28*, the ciliary connection/function of RAB28 and the effects of the identified variant was investigated.

RAB28 belongs to the group of small GTPases of the Ras super family (Stenmark and Olkkonen, 2001). The Rab GTPases have been linked to intracellular vesicular trafficking processes. The ability of the small GTPases to be in an activated state (GTP-bound) or inactive state (GDP-bound) provides an opportunity for these proteins to act as regulators of vesicular trafficking as they change their conformation depending on their state and thus the ability for them to bind with effectors (Seixas *et al.*, 2013). To maintain the cilium's ability to mediate regulatory and sensory roles, it relies on IFT (See section above). Rab proteins have been linked to ciliary transport and ciliogenesis (Lim, Chua and Tang, 2011). Expression studies have revealed three isoforms of RAB28 expressed in different tissues, but all three was found in the retina (Brauers *et al.*, 1996; Roosing *et al.*, 2013). Roosing *et al.* found variants in *RAB28* in patients suffering from cone-rod dystrophy and showed that RAB28 protein localizes to ciliary rootlet and the basal body of photoreceptor cells in rats proposing an additional role for RAB28 in photoreceptor cell ciliary transport (Roosing *et al.*, 2013).

Even though we have learned more about the role of the RAB28 protein, only a handful of variants in the *RAB28* gene have been described (Roosing *et al.*, 2013; Riveiro-Álvarez *et al.*, 2015; Lee *et al.*, 2017), which makes the classification and evaluation of the effects of new variants found in this gene difficult. Two studies have used model organisms to elucidate the role of protein; Jensen et al. used *C. elegans* and Ying *et al.* a knock-out mouse model (Jensen *et al.*, 2016; Ying *et al.*, 2018).

Jensen *et al*. used whole organism RNA-Seq libraries of *C. elegans* to confirm RAB28 as a component of the cilium conserved amongst species. They saw that only ciliated neurons expressed RAB28 and that the active form undergoes bidirectional IFT through association with IFT trains in a BBSome dependent way (through interactions with BBS8). A *RAB28* severe loss-of-function/null allele resulted in grossly normal cilia and ciliary function hinting that RAB28 protein acts as an IFT cargo that may regulate IFT train docking (Jensen *et al.*, 2016). Ying *et al.* showed that *RAB28* knock-out mice had elongated cone photoreceptors with bulging tips indicating that *RAB28* is important for outer segment disc shedding by the photoreceptors and

phagocytosis by the retinal pigment epithelial (RPE) cells (see section below for more information about RPE cells) (Ying *et al.*, 2018).

These studies together with the discovered *RAB28* variants causing inherited retinal disease unveils a new player of regulation in the eye – it will indeed be interesting to follow if more variants in this gene will follow. As the expression of RAB28 protein has been shown to differ in tissues, the application of stem cell models presents an attractive system to pinpoint the exact cellular and ciliary function of RAB28 protein.

1.7. Stem Cells

The ability of stem cells to differentiate into cells of all three germ layers; endoderm, mesoderm and ectoderm, offers great promise to investigate embryonic development, carry out disease modeling and for drug screening purposes.

It was discovered in 1981, that cells derived from the inner cell mass of murine blastocysts were able to generate cells of all three germ layers and could self-renew indefinitely without losing this ability. These cells were termed embryonic stem cells (ESC), classified as pluripotent and these cells were successfully isolated and cultured. A while later, human embryonic stem cells were established and shown to have the same ability. This was groundbreaking, however, the use of ESCs was controversial, as the blastocyst they are derived from is an early stage embryo (for humans, day 4-5 post fertilization) (Evans and Kaufman, 1981; Thomson *et al.*, 1998). To circumvent some of the ethical issues with ESCs, it was attempted to make somatic cells pluripotent. Wilmut *et al*. successfully reverted somatic cells to an embryonic-like state exploiting an enucleated oocyte by transferring the nuclear contents of the somatic cell into this oocyte. This approach led to the first cloned animal, the sheep Dolly (Wilmut *et al.*, 1997). This method of creating stem cells is termed somatic cell nuclear transfer. Fusion of somatic cells and ESCs can also reprogram somatic cells to a pluripotent state (Cowan *et al.*, 2005). Although these discoveries were groundbreaking – they did not solve the core issue with having to use oocytes or ESCs. The experiments did serve as an inspiration to the major break-through that was achieved in 2006, when Yamanaka and Takahashi made the groundbreaking discovery that somatic cells can be reprogrammed back to a pluripotent stage using defined factors. First in mice and the year after several groups reported the same finding in human cells. These induced pluripotent stem cells (iPSC) have similar properties to embryonic stem cells; they can self-renew indefinitely while maintaining the ability to form cells of endoderm, mesoderm and ectoderm lineages, giving rise to almost all cell types of our body (Takahashi and Yamanaka, 2006; Takahashi *et al.*, 2007; Yu *et al.*, 2007). See Figure 6 for an overview of the different ways to turn somatic cells into stem cells and other sources for obtaining stem cells.

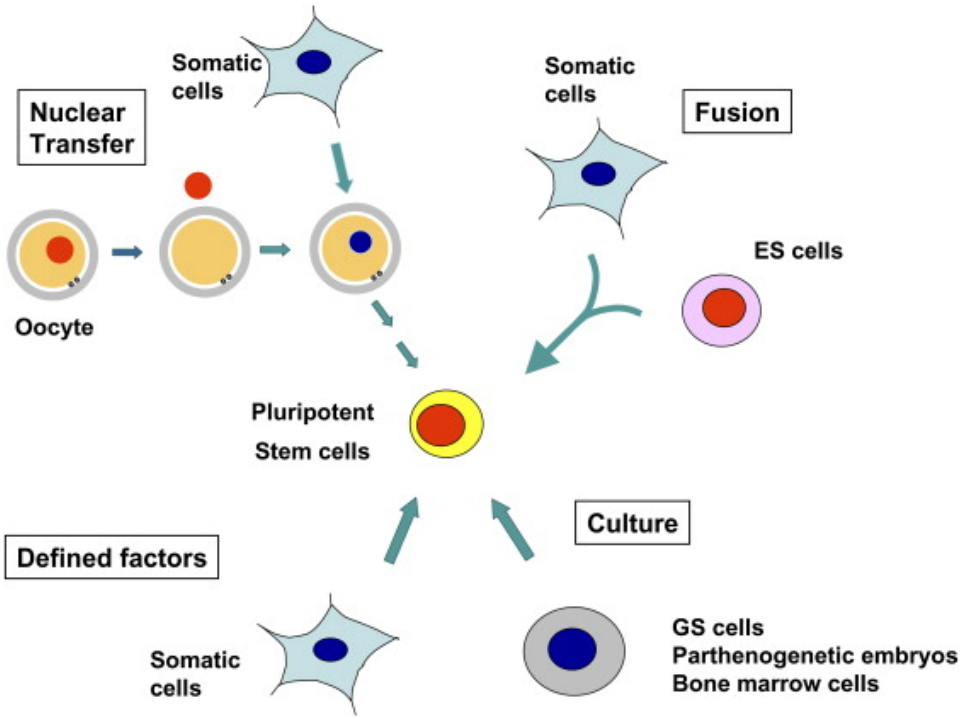

Figure 6 overview of ways to generate stem cells. The nucleus from a somatic cell can be transferred to an enucleated oocyte, Somatic cells can be fused with ES cells and defined factors can be used to induce pluripotency in somatic cells. Other sources of stem cells are from pathogenic embryos, bone marrow cells and from adult germ cells. Figure from (Yamanaka, 2007).

A core of three transcription factors are the main players responsible for maintaining the pluripotent stage; Oct3/4, Sox2 and Nanog (Nichols *et al.*, 1998; Avilion *et al.*, 2003; Mitsui *et al.*, 2003; Niwa, 2007). Takahashi and Yamanaka successfully reverted somatic cells of mice and humans to a pluripotent state by retroviral-insertion of an activated form of four genes; *OCT4*, *SOX2*, *KLF4* and *c-MYC* (also known as the OSKM factors) (Takahashi and Yamanaka, 2006; Takahashi *et al.*, 2007). The transcription factor Oct3/4 is in charge of maintaining the pluripotent stage whereas Sox2 regulates Oct3/4 expression. Sox2 and Oct3/4 activate Nanog and other important transcription factors for maintaining pluripotency (Masui *et al.*, 2007; Niwa *et al.*, 2009; Yoshida and Yamanaka, 2017). C-Myc is expendable for this process but increases efficiency as it opens up chromatin to give easier access to Sox2, Oct3/4 and Nanog. C-Myc has been reported to cause tumors but L-Myc can be used instead to avoid tumorigenic events without affecting reprogramming efficiency (Nakagawa *et al.*, 2008, 2010). Klf4 represses cell death and activates SOX2 (Niwa *et al.*, 2009).

The complete network of pluripotency remains to be elucidated but a lot of progress have been made when generating iPSC with the respect to culture conditions, delivery route of the reprogramming factors and even additional reprogramming factors. Some newer protocols add a short hairpin RNA targeting p53 to further suppress cell death (Takahashi and Yamanaka, 2006; Takahashi *et al.*, 2007; Yu *et al.*, 2007; Hong *et al.*, 2009; Okita *et al.*, 2011; Rasmussen *et al.*, 2014).

Once the combination of reprogramming factors has been decided upon, the next thing to consider when generating iPSC is how the reprogramming factors are introduced into the cells. Depending on the purpose of the iPSC, it is important to decide on a suitable vector; Lentiviruses and retroviruses were initially used to insert the OSKM factors as transgenes (Takahashi and Yamanaka, 2006; Takahashi *et al.*, 2007). However, this approach poses two potential problems; first, this type of virus will insert into the genome of the host

potentially causing harmful mutations to arise. Second, inserted transgenes can be re-activated which could lead to tumorigenesis. Methods to circumvent these issues have been developed. The use of the non-integrating adenovirus and the RNA-based Sendai virus proved that it was possible to generate iPSC with non-integrating viruses (Stadtfeld *et al.*, 2008; FUSAKI *et al.*, 2009; Seki *et al.*, 2010). Reprogramming can also be done using a protein expression vector that contain the reprogramming factors where this transgene can be removed using either the *Cre-LoxP* system or the piggyBac transposon system after successful iPSC reprogramming (Kaji *et al.*, 2009; Woltjen *et al.*, 2009; Yusa *et al.*, 2009). A combination of chemical compounds have also been proved to generate iPSC (Shi *et al.*, 2008; Hou *et al.*, 2013) as well as plasmid vectors (Okita *et al.*, 2008, 2011; Yu *et al.*, 2009). It is indeed possible to generate safe iPSC, but these described methods all vary in efficiency, workload and reproducibility so the choice ultimately depends on the purpose of the generated iPSC.

The last thing to discuss is what cell type to use. Several studies have reported that the donor cells can retain an epigenetic memory through their DNA methylation pattern that will make them more likely to differentiate into the cell type they used to be. It was debated if the donor cell type or the reprogramming method was the cause of this epigenetic memory and if this was something that was only observed in low passage iPSC (K. Kim *et al.*, 2010; Kim *et al.*, 2011; Lister *et al.*, 2011; Ohi *et al.*, 2011; Kajiwara *et al.*, 2012). One study compared both reprogramming methods and cell source and found that the observed epigenetic memory probably did not depend on reprogramming method or donor cell type but was more likely donor-specific (Kajiwara *et al.*, 2012). This means that easily available cells that require non-invasive procedures present an attractive donor cell source. Both dermal fibroblast cells and T cells from peripheral blood that can be obtained through minor procedures offer good donor choices (Seki *et al.*, 2010; Okita *et al.*, 2011).

The iPSC reprogramming method applied in this PhD project use human dermal fibroblasts as donor cell type, episomal plasmids as delivery system and the reprogramming factors OCT3/4, SOX2, KLF4, LIN28, L-MYC in combination with a short hairpin RNA targeting p53 delivered to the donor cells through electroporation (Okita *et al.*, 2011; Rasmussen *et al.*, 2014; Hey, Saltõkova, *et al.*, 2018; Hey, Saltõkowa, *et al.*, 2018a, 2018b). This method was chosen due to the efficiency and robustness in iPSC generation as well as available equipment.

1.8. RPE Cells

The retinal pigment epithelial (RPE) cells are implicated in several retinal diseases, including age-related macular degeneration, Stargardt disease and Best disease and the RPE cells often represent the starting point in retinal dystrophy. One reason for the fragility of the RPE cells, is because they are largely post-mitotic – So cells lost will not be replaced (Bok, 2005; Rattner and Nathans, 2006; Ambati, Atkinson and Gelfand, 2013). As mentioned above, blindness caused by BBS can be correlated to the loss of photoreceptor cells. However, another important ciliated cell type in the retina, the RPE cells, has recently been suggested affected as well (May-Simera *et al.*, 2018). The retina has a complex structure consisting of more than 55 cell types that work together to enable us to see (Masland, 2001; Foltz and Clegg, 2018; Langer *et al.*, 2018). Some of these cell types support the function of others and if these are stressed, this could have tremendous effects in this microenvironment which may ultimately lead to loss of vision.

1.8.1. RPE Cell Function

The RPE form a monolayer situated at the back of the eye right between the outer segments of the photoreceptors and Bruch's membrane in the retina (see Figure 7). It is a polarized epithelial cell layer where tight junctions help distinguish the apical and the basolateral membranes. The apical membrane has long

protrusions, or microvilli, that extend out and surround the photoreceptor outer segments and at the basolateral side, Bruch's membrane separates the RPE from the vessels of the choroid (Strauss, 2005).

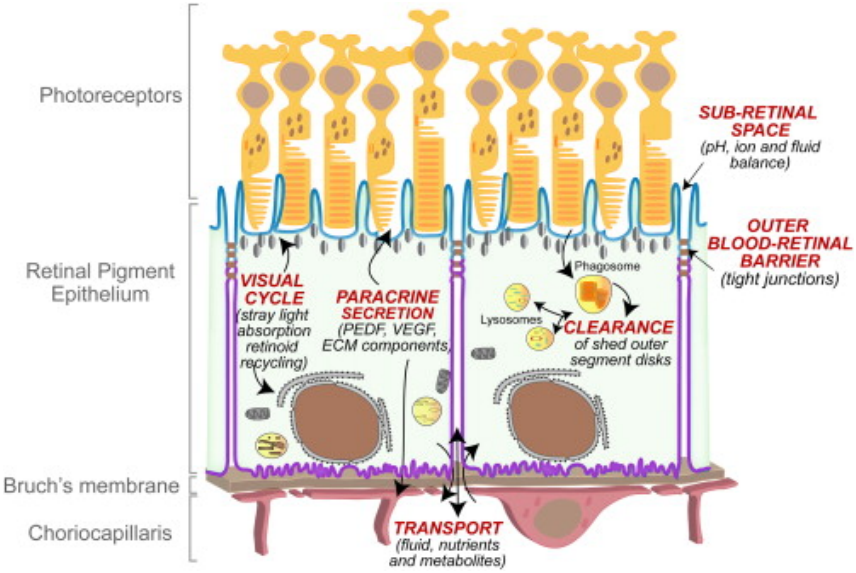

Figure 7 Schematic representation of localization of the RPE cells. The RPE extend apical micro-villi into subretinal space surrounding the outer segments of the photoreceptor cells and are able to support the function of photoreceptors through the visual cycle, paracrine secretion, transport, clearance and forming the outer blood-retinal barrier by apical tight junctions. Figure from (Toops, Tan and Lakkaraju, 2014).

The RPE cells have several important functions that can be divided into several topics; visual cycle, paracrine secretion, transport functions, clearance, blood-retinal barrier and subretinal space. In the visual cycle, stray light is absorbed by the pigmented melanosomes located at the apical membrane in the RPE cells and retinaldehyde (retinal) is recycled through the re-isomerization of all-*trans*-retinal back to 11-*cis*-retinal, which is essential, as the photoreceptors are unable to do this, and light transduction cannot happen without properly isomerized retinal (Bok, 1993; Marmorstein, 2001; Strauss, 2005; Rizzolo, 2007). The tight-junctions also form the outer blood-retinal barrier which is important in maintaining homeostasis of ions and fluids. This in turn also regulate the transport of metabolites, nutrients and fluids in and out of the retina and the ion-transport is important in keeping the photoreceptors excitable (Marmorstein, 2001; Rizzolo, 2007). The RPE take up nutrients from the blood that can be exchanged with the photoreceptor cells. Through paracrine secretion, growth factors such as vascular endothelial growth factor (VEGF) and pigment-derived epithelial-derived factor (PEDF) as well as components of the extracellular matrix. The growth factors can be used in the subretinal space to maintain tissues homeostasis (Strauss, 2005).

Pigmentation of the RPE cells occur through the maturation of melanosomes. Maturation levels of melanosomes can be divided into four stages, where especially stage I melanosomes show similarity to lysosomes and stage four have a highly structured matrix with fibrils containing dense melanin granules (Yamaguchi and Hearing, 2014).

When the RPE recycles retinal for the photoreceptors, it happens through the uptake, or phagocytosis, of shed outer segments from the photoreceptor cells. This process leads to the degeneration of the shed discs through the lysosomal/autophagosomal pathway. Five steps are characterized in this pathway; recognition and binding of the outer segment, ingestion, phagosome formation, lysosome fusion and digestion. Recognition happens through the binding of an "eat-me" signal consisting of phosphatidylserine (Wu, Tibrewal and Birge, 2006; Ferrington, Sinha and Kaarniranta, 2016) at the apical side of the RPE, triggering

the rest of the pathway. Mertk is involved in the engulfment process (Kevany and Palczewski, 2010). After ingestion, the outer segments are packed into phagosomes that are membrane bound and the phagosome is degraded through lysosomes in two steps; formation of phagolysosomes by fusion of phagosomes and lysosomes and then hydrolytic enzymes degrades the content of the phagolysosome at the basolateral side of the RPE (Bosch, Horwitz and Bok, 1993; Ferrington, Sinha and Kaarniranta, 2016). Close proximity between RPE and photoreceptors are needed for phagocytosis to happen (Matsumoto, Defoe and Besharse, 1987). Some of the key players in this process have been identified but we do not know the full story of how the phagosomes mature and the final steps in outer segment degradation yet (Ferrington, Sinha and Kaarniranta, 2016). Some overlap between phagocytosis and autophagy, the process of cell "self-eating" during times with restricted nutrients, have been observed but these are still two separate systems. A clear ciliary connection between phagocytosis have not been established yet, but it is known that several players of autophagy localize to cilia, so it may be possible that the cilium is involved in RPE phagocytosis events (Ferrington, Sinha and Kaarniranta, 2016; Morleo and Franco, 2019).

The RPE cells are essential for proper photoreceptor cell function and thus our vision – disturbance of just one of the described functions can ultimately lead to blindness.

1.8.2. RPE Cell Differentiation

RPE cells can arise through spontaneous differentiation of ESC and iPSC, however this process is slow and has low efficiency (about 1%) (Klimanskaya *et al.*, 2004; Buchholz *et al.*, 2009). Another option is to choose the directed differentiation approach, where it is attempted to mimic embryonic development through the temporal addition of growth factors and small molecules to speed up the differentiation process and increase efficiency.

During embryonic development, three germ layers are established that will give rise to all the cells in our body. The endoderm gives rise to cell types such as the lung cells, thyroid cells and pancreatic cells, the mesoderm to muscle cells and red blood cells and the ectoderm to cell types as the skin epidermis, neuronal cells of different types, and pigmented cells types such as the RPE cells (Gilbert, 2003). The RPE cells are derived from the optic neuroepithelium. During embryonic development, the eye field forms in the anterior neuroectoderm, which will give rise to the optic stalk, retina and the RPE cells (Fuhrmann, Zou and Levine, 2014). The events leading to the specification of the eye field, and later the RPE cells, rely on a temporal and complex coordination of signaling pathways and cell migration patterns. Several signaling pathways have been proved involved in this complex journey of development including Wnt, Hh and TGF-β signaling.

Directed differentiation using nicotinamide + Activin A yielded 33% efficiency and it took 6 weeks (Idelson *et al.*, 2009). And one study using bFGF, Noggin, retinoic acid and SHh yielded 60% in 60 days. This method was applied to control and retinal-specific patient iPSC (Zahabi *et al.*, 2012). Directed differentiation into neural retina took 21 days and had an efficiency of 80% using IGF-1, Noggin, Dkk1 and basic fibroblast growth factor (bFGF) (Lamba *et al.*, 2006). RPE cells and neural retina come from the same progenitor cells, so this differentiation strategy may be tweaked to yield RPE cells if some factors are changed or left out (Ramón Martínez-Morales, Rodrigo and Bovolenta, 2004; Buchholz *et al.*, 2013; Fuhrmann, Zou and Levine, 2014). It should be noted that some of these protocols have both suspension culture and adherent culture of the cells making them technically complicated.

The protocol described by Foltz and Clegg has combined these directed differentiation strategies to create a simple and highly efficient method for RPE differentiation (Buchholz *et al.*, 2013; Leach *et al.*, 2015; Foltz and Clegg, 2017). They use continuous adherent culture and add nicotinamide, Noggin, Dkk-1, IGF-1,

bFGF, Activin A, SU5402 and CHIR99021 at specific timepoint during an initial 14-day period followed by 3x 30 days of maturation (see Figure 8 for an overview of when the different compounds are added). This leaves a highly efficient system that is easy to work with. Initially the protocol did not include CHIR99021, but it was shown that activating Wnt in the last half of the period significantly increased the efficiency of the differentiation and in many cases made manual enrichment after the first maturation period of 30 days obsolete (Leach *et al.*, 2015).

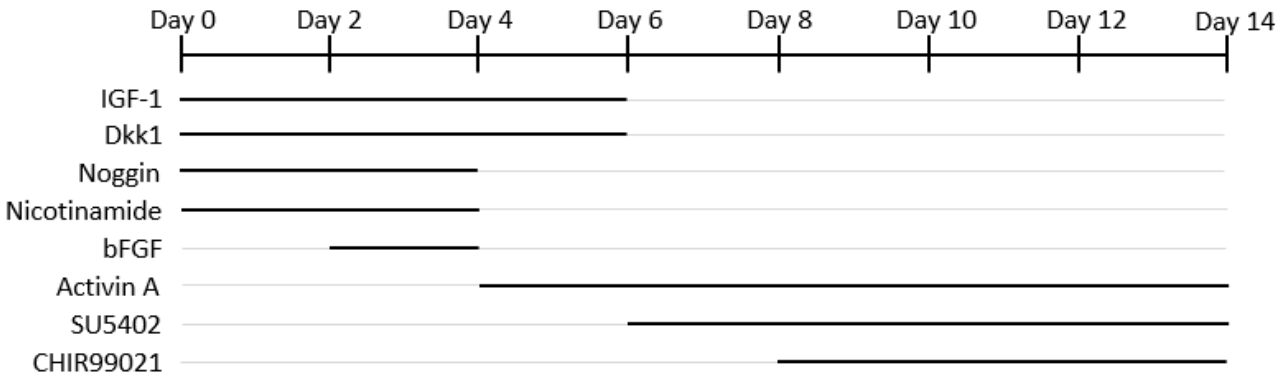

Figure 8 RPE differentiation. Overview of the initial 14-day period of RPE induction in the method developed by Leach et al. (Leach et al., 2015). Factors to induce early eye-field is added first, and then RPE cell fate is promoted by inhibiting formation of neural retina and promoting RPE cell formation through Wnt stimulation.

Leach *et al.* start out by adding factors that will specify the early eye field, such as IGF-1, Dkk1, Noggin, Nicotinamide, and bFGF. IGF-1 is a growth factor and addition promotes formation of three-dimensional ocular structures (Mellough *et al.*, 2015). Dkk1 is a Wnt inhibitor (for mode of action, see above). It promotes embryonic anterior neural development and is thus a promoter for early eye field-specification (Cruciat and Niehrs, 2013; Fujimura, 2016). Noggin is an antagonist of bone morphogenetic protein (BMP) and is added to induce neural lineage (Gerrard, Rodgers and Cui, 2005; Chambers *et al.*, 2009). Nicotinamide promotes differentiation and cell survival through kinase inhibition activities to induce early eye field differentiation (Buchholz *et al.*, 2013; Meng *et al.*, 2018) together with bFGF that promotes differentiation into neural retina and is also used to induce formation of early eye field (Klimanskaya *et al.*, 2004).

The next step is to promote the formation of RPE and inhibit neural retina formation. To achieve this, Activin A and SU5402 are added, and other factors are left out. Activin A is a member of the TGF- β family and has been shown to promote expression of genes specific to RPE cells (e.g. MITF) and repress differentiation into neural retina (Fuhrmann, Levine and Reh, 2000). SU5402 is a FGF inhibitor and also inhibits neural retina formation (Lamba *et al.*, 2006; Buchholz *et al.*, 2013). CHIR99021 is a Wnt activator (see above for mode of action) that promotes pigmentation and expression of MITF (Nakano *et al.*, 2012) to create mature RPE cells. Leach *et al.* are able to generate 97.7% mature RPE cells as a monolayer using this protocol (Leach *et al.*, 2015). If the RPE cell generated come from a person with e.g. BBS, then functional assays can be applied to investigate if the phenotype of the generated RPE cells is affected by the variant in one of the BBS genes.

2. Summary of Results

Research paper I, II and III: Describes the generation and characterization of patient-specific iPSC generated from people suffering from BBS with the variants c.1169T>;G/c.1135G>C in *BBS1*, c.271insT in *BBS10* and c.214G>A, p.(Gly72Ser) in *BBS5*. Episomal plasmids carrying the reprogramming factors OCT3/4, SOX2, KLF4, LIN28, L-MYC in combination with a short hairpin RNA targeting p53 was introduced by electroporation of fibroblast cells. Emerging iPSC colonies were harvested approximately 21 days post transfection and these cells were cultured until the reprogramming plasmids was lost from the cells. Subsequently, the iPSCs were investigated for stem cell markers OCT3/4, NANOG, SSEA3, SOX2, TRA-1-60 and TRA-1-81 using immunofluorescence microscopy and showed proper expression and localization patterns of the markers. Expression of several pluripotency-associated genes were investigated using real-time reverse transcriptase-PCR. All investigated genes had similar expression pattern in the generated iPSC lines as in a control iPSC line. Furthermore, a spontaneous differentiation experiment of the iPSC lines proved their ability to form cells of all 3 germ layers; endoderm, mesoderm and ectoderm thus establishing their true pluripotent status. Finally, the iPSCs identity were validated against their mother fibroblast cells through short tandem repeat (STR) analysis and chromosomal analysis confirmed normal karyotype.

Manuscript I: Variant evaluation and cellular consequence of the homozygous missense variant c.55G>A, p.(Gly19Arg) in *RAB28*. Two brothers with cone-rod dystrophy, polydactyly and myopia were investigated to provide a molecular genetic diagnosis. The discovered *RAB28* variant was found using targeted next generation sequencing in a large cohort of patients (n=667) of a retinal dystrophy gene panel consisting of 125 genes. Both individuals donated a skin biopsy and the obtained fibroblast cells were investigated for the subcellular localization of the RAB28 protein and number of cells with cilia was assessed. While no effect was seen on the number of ciliated cells, there was a significant reduction in RAB28 in cilia in both *RAB28* variant cell lines compared to control cells. These finding together with the DNA analysis confirm this missense variant as likely pathogenic.

Draft I: Investigation of fibroblast cells from 5 individuals suffering from BBS, harboring gene variants in *BBS1*, *BBS5* and *BBS10*, was investigated for Hh signaling and ciliary defects. Expression of the Hh target gene *GLI1* was examined in cells with and without serum depletion, to induce formation of the cilium, and with and without the Hh activator purmorphamine. A large reduction in *GLI1* expression was observed for all 5 BBS cell lines that did not show the ability to activate the Hh pathway properly compared to control cells. Some of the observed *GLI1* expression level was higher in the absence of serum depletion for the BBS cells indicating that this response is not cilia-specific. The underlaying mechanism was investigated, and accumulation of the Hh receptor SMO in cilia in unstimulated cells lead us to conclude that retrograde IFT is severely affected in these cells, as SMO should only accumulate in cilia after stimulation. Knock-down of *BBS1*, *BBS5* and *BBS10* using siRNA in hTERT-RPE1 cells validated the decreased *GLI1* response seen in the BBS fibroblast cells. Primary cilia length was also investigated in BBS fibroblast cells. Cells with a *BBS1* gene variant had significantly shorter cilia than control cells whereas *BBS5* and *BBS10* variant cells had significantly longer cilia and also had a tendency for increased length variability compared to control and *BBS1* cells.

Draft II: The above descried iPSC with a *BBS1* or *BBS10* gene variant were differentiated into RPE cells. The phenotype of these cells was compared to RPE cells derived from a control iPSC line. Data included derives from one experiment at this time, so these results are preliminary and should be interpreted with caution. The BBS-derived RPE cells showed incomplete maturation observed as a lack of tight junctions, and

expression of mature RPE-specific proteins. The BBS-RPE did develop some pigmentation, but it was lost from the cells at later stages. The BBS-RPE cells also showed Wnt and Hh signaling defects and long primary cilia. As an effort to mature the cells, Wnt and Hh agonist and antagonist were added in culture for a prolonged period. This had no effect on BBS-derived RPE cells but in control-RPE Wnt inhibition showed increased expression of mature RPE cell proteins and tight junctions. Regulation of Wnt signaling has previously been shown to be important for RPE cell maturation and the observed signaling defects in the BBS-RPE may be the underlaying cause for the inability of these cells to form mature RPE cells. We did not expect the inability of the BBS cells to differentiate into mature RPE cells as individuals with BBS are assumed to be born with a regular retina and normal sense of vision. The experiment needs to be replicated and more control assessments should be included. Furthermore, the RPE-differentiation protocol should be adapted to the BBS cell lines as this could improve their ability to differentiate into RPE cells.

3. Discussion, Perspectives and Conclusion

The ability to provide a molecular diagnosis is important for several reasons. First of all, it may affect how the involved disease is treated. Second, the person and family of the affected individual will benefit as they can be screened for the gene variant and third, they will benefit emotionally from knowing the cause of disease. Therefore, it is important to develop methods that can assist when gene variant analysis is difficult. Having the individual in question donate a skin biopsy is a good foundation to start functional assays on, as much can be learned from these cells as is evident in manuscript I, where a *RAB28* missense gene variant was classified likely pathogenic through combined DNA analysis and functional cell assays. This is a beautiful example of how powerful these methods can be when they are used together.

With the increasing availability of targeted next generation sequencing and of whole genome sequencing, this will likely lead to the discovery of more genes and gene variants of unknown significance. The development of methods for determining variant pathogenicity is more important than ever.

Not all gene variants express proteins that are important for fibroblast cell function, and in these cases the application of stem cell models can be useful as it is possible to generate any cell type of interest and to use cells derived from the affected individual. Several methods for generation of iPSCs from fibroblast cells exist and they all vary in efficiency, workload and genetic implications. It is important to choose a suitable system based on the application of the stem cell model. A study by Leach *et al.* compared several different methods for iPSC generation and two RPE differentiation protocols to see the implications of the chosen systems on the end product. They found that all iPSC types were able to generate RPE cells using the directed differentiation approach, whereas only 3 of 5 iPSC lines were able to differentiate into RPE cells using spontaneous differentiation which was the other tested RPE differentiation protocol (Leach *et al.*, 2016). This shows that choice of differentiation protocol is of great importance whereas the system for generating iPSC can be chosen more freely. The BBS proteins does not seem to affect the generation of iPSC as it was possible to reprogram cells from three individuals with pathogenic variants in *BBS1*, *BBS5* and *BBS10* respectively into iPSC.

The generation of iPSC and differentiation into cell type of interest takes time. Therefore, it is important to optimize applied methods. Episomal plasmids and electroporation was used to generate iPSC in this project. We have experienced that the obtained iPSCs need to be cultured for an extended period of time before losing the reprogramming plasmids. We have recently tested iPSC reprogramming using synthetic RNA and chemical transfection. The workload in this method is substantially smaller and so far, the method seems to be very efficient and the RNA vector is lost within few weeks of the transfection compared to almost 30 passages for some iPSC lines in our laboratory (unpublished data). Several iPSC lines never lost the reprogramming plasmids and had to be discarded.

Bardet-Biedl syndrome was chosen as a system to set up the RPE differentiation methods as we expected these cells to show a phenotype that could be distinguished from control cells. Surprisingly, we were not able to generate mature RPE cells at all from BBS-derived cells. This may be due to the observed signaling deficiencies observed in Hh and Wnt pathways (Zahabi *et al.*, 2012; May-Simera *et al.*, 2018) and thus the BBS proteins must be important in RPE cell differentiation and maturation. Individuals with BBS are born with a sense of vision that is assumes to be normal, so the finding that iPSC from such individuals are unable to form mature RPE cells is very surprising. It may be worth investigating the health of the retina further in very young individuals with BBS, as persons are usually referred for an exam after development of vision loss. It should be noted that the observed RPE phenotype of the BBS-RPE cells may translate more severe in a cell culture dish than in humans. This is the first report of RPE cells generated from cells derived from

individuals with these *BBS* gene variants. Other studies focusing on RPE cells in BBS have mainly used mouse models or iPSC. Several studies have seen defects in RPE cells when BBS proteins are malfunctioning and one study even saw effects in RPE cells before the photoreceptor cells were affected (May-Simera *et al.*, 2018; Patnaik *et al.*, 2019). In BBS the cause of photoreceptor degeneration is generally assumed to be the result of defective ciliary trafficking between the inner and outer. It may be possible that the RPE cells actually contribute to this phenotype in BBS. The RPE cells may be healthy enough to sustain the photoreceptors for several years. It is important to establish the exact role of the RPE cells in this and to investigate if vision loss can be delayed through treatment of these cells.

The study presented in manuscript 1 contains basic research to elucidate the pathogenicity status of the investigated *RAB28* gene variant. The literature links RAB28 to transport of GLUT-4 and NF-κB and to regulation of endocytic trafficking and subsequent degradation (Lumb *et al.*, 2011; Jiang *et al.*, 2013; Zhou *et al.*, 2017). Further studies that enlighten how the variant affects cellular signaling should be carried out to determine if RAB28 is a regulator of trafficking other signaling proteins in different pathways. Preliminary experiments have been carried out investigating Hh signaling in the RAB28 patient cell lines along with knock-down of *RAB28* in immortalized human hTERT-RPE1 cells that all showed normal Hh signaling behavior (unpublished data). This is surprising, as the patients that donated the cells had polydactyly and, on this basis, we expected Hh signaling to be disturbed. Other cilia-coupled signaling pathways, such as Wnt signaling, should be investigated as well. So far, we do not know the localization of RAB28 in RPE cells and photoreceptor cells derived from the patient cell lines. Previous studies have shown RAB28 to be localized at the basal body in rat photoreceptor cells (Roosing *et al.*, 2013) and Ying *et al.* saw that RAB28 was needed for the phagocytosis of shed outer segments (Ying *et al.*, 2018). IPSC should be generated from the patient cell lines and the gene variant should be introduced in control iPSC and these should be differentiated into RPE and photoreceptor cells to see how RAB28 localizes and if they are able to carry out phagocytosis. The ability to shed outer segments from photoreceptor cells was linked to RAB28. In Rab28 knock-out mice large balloon-like structures formed at the RPE-facing tips of the photoreceptor cells, like they were unable to shed the used discs (Ying *et al.*, 2018). It therefore may be that other forms of vesicular transport and ciliary export may be disturbed in the RAB28 patient cells, for instance ectocytosis. Further studies are needed to dissect the exact role of RAB28 in cellular signaling and ciliary transport events.

In conclusion, the aims of the PhD project have been fulfilled. Functional investigation of a gene variant in an individual with retinal dystrophy was carried out on a missense variant in *RAB28.* This led to the variant classification likely pathogenic. Several iPSC lines were generated from three different individuals with BBS, two of which were differentiated into RPE cells. Fibroblast cells from the individuals with BBS were investigated for signaling defects and these results have been compared to the results obtained in RPE cells from the same individuals.

4. References

Abu Safieh, L. *et al.* (2010) 'Clinical and molecular characterisation of Bardet-Biedl syndrome in consanguineous populations: the power of homozygosity mapping', *Journal of Medical Genetics*, 47(4), pp. 236–241. doi: 10.1136/jmg.2009.070755.

Adzhubei, I. A. *et al.* (2010) 'A method and server for predicting damaging missense mutations', *Nature Methods*. Nature Publishing Group, 7(4), pp. 248–249. doi: 10.1038/nmeth0410-248.

Airik, R. *et al.* (2016) 'SDCCAG8 Interacts with RAB Effector Proteins RABEP2 and ERC1 and Is Required for Hedgehog Signaling', *PLOS ONE*. Edited by Y. Komarova, 11(5), p. e0156081. doi: 10.1371/journal.pone.0156081.

Álvarez-Satta, M., Castro-Sánchez, S. and Valverde, D. (2017) 'Bardet-Biedl Syndrome as a Chaperonopathy: Dissecting the Major Role of Chaperonin-Like BBS Proteins (BBS6-BBS10-BBS12)', *Frontiers in Molecular Biosciences*, 4(July 2017), pp. 1–7. doi: 10.3389/fmolb.2017.00055.

Ambati, J., Atkinson, J. P. and Gelfand, B. D. (2013) 'Immunology of age-related macular degeneration', *Nature Reviews Immunology*. Nature Publishing Group, 13(6), pp. 438–451. doi: 10.1038/nri3459.

Ansley, S. J. *et al.* (2003) 'Basal body dysfunction is a likely cause of pleiotropic Bardet–Biedl syndrome', *Nature*, 425(6958), pp. 628–633. doi: 10.1038/nature02030.

Anvarian, Z. *et al.* (2019) 'Cellular signalling by primary cilia in development, organ function and disease', *Nature Reviews Nephrology*, 15(4), pp. 199–219. doi: 10.1038/s41581-019-0116-9.

Avasthi, P. and Marshall, W. F. (2012) 'Stages of ciliogenesis and regulation of ciliary length', *Differentiation*. Elsevier, 83(2), pp. S30–S42. doi: 10.1016/j.diff.2011.11.015.

Avilion, A. A. *et al.* (2003) 'Multipotent cell lineages in early mouse development depend on SOX2 function.', *Genes & development*, 17(1), pp. 126–40. doi: 10.1101/gad.224503.

Azari, A. A. *et al.* (2006) 'Retinal disease expression in Bardet-Biedl syndrome-1 (BBS1) is a spectrum from maculopathy to retina-wide degeneration', *Investigative Ophthalmology and Visual Science*, 47(11), pp. 5004–5010. doi: 10.1167/iovs.06-0517.

Badgandi, H. B. *et al.* (2017) 'Tubby family proteins are adapters for ciliary trafficking of integral membrane proteins', *The Journal of cell biology*, 216(3), pp. 743–760. doi: 10.1083/jcb.201607095.

Bardet, G. (1995) 'ON CONGENITAL OBESITY SYNDROME WITH POLYDACTYLY AND RETINITIS PIGMENTOSA (A CONTRIBUTION TO THE STUDY OF CLINICAL FORMS OF HYPOPHYSEAL OBESITY) Thesis, for the degree of Doctor of Medicine', *Obesity Research*, 3(4), pp. 387–399. doi: 10.1002/j.1550-8528.1995.tb00165.x.

Beales, P. L. *et al.* (1999) 'New criteria for improved diagnosis of Bardet-Biedl syndrome: Results of a population survey', *Journal of Medical Genetics*, 36(6), pp. 437–446. doi: 10.1136/jmg.36.6.437.

Behal, R. H. *et al.* (2012) 'Subunit Interactions and Organization of the Chlamydomonas reinhardtii Intraflagellar Transport Complex A Proteins', *Journal of Biological Chemistry*, 287(15), pp. 11689–11703. doi: 10.1074/jbc.M111.287102.

Bennett, C. N. *et al.* (2002) 'Regulation of Wnt Signaling during Adipogenesis', *Journal of Biological Chemistry*, 277(34), pp. 30998–31004. doi: 10.1074/jbc.M204527200.

Berbari, N. F. *et al.* (2008) 'Bardet-Biedl syndrome proteins are required for the localization of G protein-coupled receptors to primary cilia', *Proceedings of the National Academy of Sciences*, 105(11), pp. 4242–

4246. doi: 10.1073/pnas.0711027105.

Bhogaraju, S. *et al.* (2013) 'Molecular Basis of Tubulin Transport Within the Cilium by IFT74 and IFT81', *Science*, 341(6149), pp. 1009–1012. doi: 10.1126/science.1240985.

Biedl, A. (1995) 'A Pair of Siblings with Adiposo-Genital Dystrophy', *Obesity Research*, 3(4), pp. 404–404. doi: 10.1002/j.1550-8528.1995.tb00167.x.

Bijlsma, M. F. and Roelink, H. (2010) 'Non-cell-autonomous signaling by Shh in tumors: challenges and opportunities for therapeutic targets', *Expert Opinion on Therapeutic Targets*, 14(7), pp. 693–702. doi: 10.1517/14728222.2010.497488.

Billingsley, G. *et al.* (2012) 'Mutational Analysis of SDCCAG8 in Bardet-Biedl Syndrome Patients with Renal Involvement and Absent Polydactyly', *Ophthalmic Genetics*, 33(3), pp. 150–154. doi: 10.3109/13816810.2012.689411.

Bitgood, M. J. and McMahon, A. P. (1995) 'Hedgehog and Bmp Genes Are Coexpressed at Many Diverse Sites of Cell–Cell Interaction in the Mouse Embryo', *Developmental Biology*, 172(1), pp. 126–138. doi: 10.1006/dbio.1995.0010.

Bok, D. (1993) 'The retinal pigment epithelium: a versatile partner in vision', *Journal of Cell Science*, 1993(Supplement 17), pp. 189–195. doi: 10.1242/jcs.1993.Supplement_17.27.

Bok, D. (2005) 'Evidence for an inflammatory process in age-related macular degeneration gains new support', *Proceedings of the National Academy of Sciences*, 102(20), pp. 7053–7054. doi: 10.1073/pnas.0502819102.

Bosch, E., Horwitz, J. and Bok, D. (1993) 'Phagocytosis of outer segments by retinal pigment epithelium: phagosome-lysosome interaction.', *Journal of Histochemistry & Cytochemistry*, 41(2), pp. 253–263. doi: 10.1177/41.2.8419462.

Brauers, A. *et al.* (1996) 'Alternative mRNA splicing of the novel GTPase Rab28 generates isoforms with different C-termini', *European Journal of Biochemistry*, 237(3), pp. 833–840. doi: 10.1111/j.1432-1033.1996.0833p.x.

Briscoe, J. and Thérond, P. P. (2013) 'The mechanisms of Hedgehog signalling and its roles in development and disease', *Nature Reviews Molecular Cell Biology*, 14(7), pp. 416–429. doi: 10.1038/nrm3598.

Broekhuis, J. R., Leong, W. Y. and Jansen, G. (2013) 'Regulation of Cilium Length and Intraflagellar Transport', in *International Review of Cell and Molecular Biology*. Elsevier, pp. 101–138. doi: 10.1016/B978-0-12-407697-6.00003-9.

Buchholz, D. E. *et al.* (2009) 'Derivation of Functional Retinal Pigmented Epithelium from Induced Pluripotent Stem Cells', *Stem Cells*, 27(10), pp. 2427–2434. doi: 10.1002/stem.189.

Buchholz, D. E. *et al.* (2013) 'Rapid and Efficient Directed Differentiation of Human Pluripotent Stem Cells Into Retinal Pigmented Epithelium', *STEM CELLS Translational Medicine*, 2(5), pp. 384–393. doi: 10.5966/sctm.2012-0163.

Bujakowska, K. M. *et al.* (2015) 'Mutations in IFT172 cause isolated retinal degeneration and Bardet–Biedl syndrome', *Human Molecular Genetics*, 24(1), pp. 230–242. doi: 10.1093/hmg/ddu441.

Cao, M. *et al.* (2015) 'Uni-directional ciliary membrane protein trafficking by a cytoplasmic retrograde IFT motor and ciliary ectosome shedding', *eLife*, 2015(4), pp. 1–15. doi: 10.7554/eLife.05242.

Carballo, G. B. *et al.* (2018) 'A highlight on Sonic hedgehog pathway', *Cell Communication and Signaling*.

Cell Communication and Signaling, 16(1), p. 11. doi: 10.1186/s12964-018-0220-7.

Chambers, S. M. *et al.* (2009) 'Highly efficient neural conversion of human ES and iPS cells by dual inhibition of SMAD signaling', *Nature Biotechnology*, 27(3), pp. 275–280. doi: 10.1038/nbt.1529.

Chen, B. *et al.* (2009) 'Small molecule–mediated disruption of Wnt-dependent signaling in tissue regeneration and cancer', *Nature Chemical Biology*, 5(2), pp. 100–107. doi: 10.1038/nchembio.137.

Chiang, A. P. *et al.* (2006) 'Homozygosity mapping with SNP arrays identifies TRIM32, an E3 ubiquitin ligase, as a Bardet-Biedl syndrome gene (BBS11)', *Proceedings of the National Academy of Sciences*, 103(16), pp. 6287–6292. doi: 10.1073/pnas.0600158103.

Corbit, K. C. *et al.* (2005) 'Vertebrate Smoothened functions at the primary cilium', *Nature*, 437(7061), pp. 1018–1021. doi: 10.1038/nature04117.

Corbit, K. C. *et al.* (2008) 'Kif3a constrains β-catenin-dependent Wnt signalling through dual ciliary and non-ciliary mechanisms', *Nature Cell Biology*, 10(1), pp. 70–76. doi: 10.1038/ncb1670.

Cowan, C. A. *et al.* (2005) 'Nuclear Reprogramming of Somatic Cells After Fusion with Human Embryonic Stem Cells', *Science*, 309(5739), pp. 1369–1373. doi: 10.1126/science.1116447.

Van Cruchten, S. *et al.* (2017) 'Pre- and Postnatal Development of the Eye: A Species Comparison', *Birth Defects Research*, 109(19), pp. 1540–1567. doi: 10.1002/bdr2.1100.

Cruciat, C.-M. and Niehrs, C. (2013) 'Secreted and Transmembrane Wnt Inhibitors and Activators', *Cold Spring Harbor Perspectives in Biology*, 5(3), pp. a015081–a015081. doi: 10.1101/cshperspect.a015081.

Datta, P. *et al.* (2015) 'Accumulation of non-outer segment proteins in the outer segment underlies photoreceptor degeneration in Bardet–Biedl syndrome', *Proceedings of the National Academy of Sciences*, 112(32), pp. E4400–E4409. doi: 10.1073/pnas.1510111112.

Dawe, H. R. *et al.* (2007) 'The Meckel-Gruber Syndrome proteins MKS1 and meckelin interact and are required for primary cilium formation', *Human Molecular Genetics*, 16(2), pp. 173–186. doi: 10.1093/hmg/ddl459.

Dorn, K. V., Hughes, C. E. and Rohatgi, R. (2012) 'A Smoothened-Evc2 Complex Transduces the Hedgehog Signal at Primary Cilia', *Developmental Cell*. Elsevier Inc., 23(4), pp. 823–835. doi: 10.1016/j.devcel.2012.07.004.

Eguether, T. *et al.* (2014) 'IFT27 Links the BBSome to IFT for Maintenance of the Ciliary Signaling Compartment', *Developmental Cell*. Elsevier Inc., 31(3), pp. 279–290. doi: 10.1016/j.devcel.2014.09.011.

Eguether, T., Cordelieres, F. P. and Pazour, G. J. (2018) 'Intraflagellar transport is deeply integrated in hedgehog signaling', *Molecular Biology of the Cell*, 29(10), pp. 1178–1189. doi: 10.1091/mbc.E17-10-0600.

Estrada-Cuzcano, A. *et al.* (2012) 'Mutations in C8orf37, encoding a ciliary protein, are associated with autosomal-recessive retinal dystrophies with early macular involvement', *American Journal of Human Genetics*, 90(1), pp. 102–109. doi: 10.1016/j.ajhg.2011.11.015.

Evans, M. J. and Kaufman, M. H. (1981) 'Establishment in culture of pluripotential cells from mouse embryos', *Nature*, 292(5819), pp. 154–156. Available at: http://dx.doi.org/10.1038/292154a0.

Ferrington, D. A., Sinha, D. and Kaarniranta, K. (2016) 'Defects in retinal pigment epithelial cell proteolysis and the pathology associated with age-related macular degeneration', *Progress in Retinal and Eye Research*, 51(3), pp. 69–89. doi: 10.1016/j.preteyeres.2015.09.002.

Foltz, L. P. and Clegg, D. O. (2017) 'Rapid, Directed Differentiation of Retinal Pigment Epithelial Cells from Human Embryonic or Induced Pluripotent Stem Cells', *Journal of Visualized Experiments*, e56274(128). doi: 10.3791/56274.

Foltz, L. P. and Clegg, D. O. (2018) 'Patient-derived induced pluripotent stem cells for modelling genetic retinal dystrophies', *Progress in Retinal and Eye Research*. Elsevier, (September), pp. 1–13. doi: 10.1016/j.preteyeres.2018.09.002.

Forsythe, E. *et al.* (2018) 'Managing Bardet-Biedl syndrome-now and in the future', *Frontiers in Pediatrics*, 6(February), pp. 1–8. doi: 10.3389/fped.2018.00023.

Forsythe, E. and Beales, P. L. (2013) 'Bardet-Biedl syndrome', *European Journal of Human Genetics*, 21(1), pp. 8–13. doi: 10.1038/ejhg.2012.115.

Foulquier, S. *et al.* (2018) 'WNT Signaling in Cardiac and Vascular Disease', *Pharmacological Reviews*. Edited by M. C. Michel, 70(1), pp. 68–141. doi: 10.1124/pr.117.013896.

Fu, W. *et al.* (2016) 'Role for the IFT-A Complex in Selective Transport to the Primary Cilium', *Cell Reports*, 17(6), pp. 1505–1517. doi: 10.1016/j.celrep.2016.10.018.

Fuhrmann, S., Levine, E. M. and Reh, T. A. (2000) 'Extraocular mesenchyme patterns the optic vesicle during early eye development in the embryonic chick', *Development*, 127(21), pp. 4599–4609.

Fuhrmann, S., Zou, C. and Levine, E. M. (2014) 'Retinal pigment epithelium development, plasticity, and tissue homeostasis', *Experimental Eye Research*. Elsevier Ltd, 123, pp. 141–150. doi: 10.1016/j.exer.2013.09.003.

Fujimura, N. (2016) 'WNT/β-Catenin Signaling in Vertebrate Eye Development', *Frontiers in Cell and Developmental Biology*, 4(NOV), pp. 1–7. doi: 10.3389/fcell.2016.00138.

FUSAKI, N. *et al.* (2009) 'Efficient induction of transgene-free human pluripotent stem cells using a vector based on Sendai virus, an RNA virus that does not integrate into the host genome', *Proceedings of the Japan Academy, Series B*, 85(8), pp. 348–362. doi: 10.2183/pjab.85.348.

Garcia-Gonzalo, F. R. and Reiter, J. F. (2017) 'Open Sesame: How transition fibers and the transition zone control ciliary composition', *Cold Spring Harbor Perspectives in Biology*, 9(2). doi: 10.1101/cshperspect.a028134.

Gerdes, J. M. *et al.* (2007a) 'Disruption of the basal body compromises proteasomal function and perturbs intracellular Wnt response', *Nature Genetics*, 39(11), pp. 1350–1360. doi: 10.1038/ng.2007.12.

Gerdes, J. M. *et al.* (2007b) 'Disruption of the basal body compromises proteasomal function and perturbs intracellular Wnt response', *Nature Genetics*, 39(11), pp. 1350–1360. doi: 10.1038/ng.2007.12.

Gerhardt, C. *et al.* (2016) 'The cilia-regulated proteasome and its role in the development of ciliopathies and cancer', *Cilia*. BioMed Central, 5(1), pp. 1–14. doi: 10.1186/s13630-016-0035-3.

Gerrard, L., Rodgers, L. and Cui, W. (2005) 'Differentiation of Human Embryonic Stem Cells to Neural Lineages in Adherent Culture by Blocking Bone Morphogenetic Protein Signaling', *Stem Cells*, 23(9), pp. 1234–1241. doi: 10.1634/stemcells.2005-0110.

Gilbert, S. F. (2003) 'The morphogenesis of evolutionary developmental biology.', *The International journal of developmental biology*, 47(7–8), pp. 467–77. Available at: papers2://publication/uuid/B5FE20B7-4D8E-4621-9F57-5AA32FBC75AB.

Goetz, S. C. and Anderson, K. V. (2010) 'The primary cilium: a signalling centre during vertebrate

development', *Nature Reviews Genetics*. Nature Publishing Group, 11(5), pp. 331–344. doi: 10.1038/nrg2774.

Guettler, S. (2016) 'AXIN Shapes Tankyrase ARChitecture', *Structure*. Elsevier Ltd, 24(10), pp. 1625–1627. doi: 10.1016/j.str.2016.09.003.

Harville, H. M. *et al.* (2010) 'Identification of 11 novel mutations in eight BBS genes by high-resolution homozygosity mapping', *Journal of Medical Genetics*, 47(4), pp. 262–267. doi: 10.1136/jmg.2009.071365.

He, X. (2008) 'Cilia put a brake on Wnt signalling', *Nature Cell Biology*, 10(1), pp. 11–13. doi: 10.1038/ncb0108-11.

Heon, E. *et al.* (2016) 'Mutations in C8ORF37 cause Bardet Biedl syndrome (BBS21)', 25(11), pp. 2283–2294. doi: 10.1093/hmg/ddw096.

Héon, E. *et al.* (2005) 'Ocular phenotypes of three genetic variants of Bardet-Biedl syndrome', *American Journal of Medical Genetics*, 132 A(3), pp. 283–287. doi: 10.1002/ajmg.a.30466.

Hernandez-Hernandez, V. *et al.* (2013) 'Bardet–Biedl syndrome proteins control the cilia length through regulation of actin polymerization', *Human Molecular Genetics*, 22(19), pp. 3858–3868. doi: 10.1093/hmg/ddt241.

Hey, C. A. B., Saltõkova, K. B., *et al.* (2018) 'Comparison of two different culture conditions for derivation of early hiPSC', *Cell Biology International*, 42(11), pp. 1467–1473. doi: 10.1002/cbin.10966.

Hey, C. A. B., Saltõkowa, K. B., *et al.* (2018a) 'Generation of induced pluripotent stem cells, KCi001-A derived from a Bardet-Biedl syndrome patient compound heterozygous for the BBS1 variants c.1169T>G/c.1135G>C', *Stem Cell Research*. Elsevier, 31(February), pp. 235–239. doi: 10.1016/j.scr.2018.08.005.

Hey, C. A. B., Saltõkowa, K. B., *et al.* (2018b) 'Generation of induced pluripotent stem cells, KCi002-A derived from a patient with Bardet-Biedl syndrome homozygous for the BBS10 variant c.271insT', *Stem Cell Research*. Elsevier, 33(February), pp. 46–50. doi: 10.1016/j.scr.2018.09.013.

Hey, C. A. B. *et al.* (2019) 'Generation and characterization of three isogenic induced pluripotent stem cell lines from a patient with Bardet-Biedl syndrome and homozygous for the BBS5 variant', *Stem Cell Research*. Elsevier, 41(September), p. 101594. doi: 10.1016/j.scr.2019.101594.

Heydeck, W. *et al.* (2018) 'The complexity of the cilium: spatiotemporal diversity of an ancient organelle', *Current Opinion in Cell Biology*. Elsevier Ltd, 55, pp. 139–149. doi: 10.1016/j.ceb.2018.08.001.

Hirano, T. *et al.* (2017) 'Intraflagellar transport - A complex mediates ciliary entry and retrograde trafficking of ciliary G protein-coupled receptors', *Molecular Biology of the Cell*, 28(3), pp. 429–439. doi: 10.1091/mbc.E16-11-0813.

Hjortshøj, T. D. *et al.* (2010) 'Bardet-Biedl syndrome in Denmark-report of 13 novel sequence variations in six genes', *Human Mutation*, 31(4), pp. 429–436. doi: 10.1002/humu.21204.

Hong, H. *et al.* (2009) 'Suppression of induced pluripotent stem cell generation by the p53-p21 pathway', *Nature*. Macmillan Publishers Limited. All rights reserved, 460(7259), pp. 1132–1135. Available at: http://dx.doi.org/10.1038/nature08235.

Hou, P. *et al.* (2013) 'Pluripotent Stem Cells Induced from Mouse Somatic Cells by Small-Molecule Compounds', *Science*, 341(6146), pp. 651–654. doi: 10.1126/science.1239278.

Huangfu, D. *et al.* (2003) 'Hedgehog signalling in the mouse requires intraflagellar transport proteins',

Nature, 426(6962), pp. 83–87. doi: 10.1038/nature02061.

Huelsken, J. (2002) 'The Wnt signalling pathway', *Journal of Cell Science*, 115(21), pp. 3977–3978. doi: 10.1242/jcs.00089.

Idelson, M. *et al.* (2009) 'Directed Differentiation of Human Embryonic Stem Cells into Functional Retinal Pigment Epithelium Cells', *Cell Stem Cell*. Elsevier Ltd, 5(4), pp. 396–408. doi: 10.1016/j.stem.2009.07.002.

Jensen, V. L. *et al.* (2016) 'Whole-Organism Developmental Expression Profiling Identifies RAB-28 as a Novel Ciliary GTPase Associated with the BBSome and Intraflagellar Transport', *PLoS Genetics*, 12(12), pp. 1–29. doi: 10.1371/journal.pgen.1006469.

Jespersgaard, C. *et al.* (2020) 'A Missense Mutation in RAB28 in a Family with Cone-Rod Dystrophy and Postaxial Polydactyly Prevents Localization of RAB28 to the Primary Cilium', *Investigative ophthalmology & visual science*, 61(2), p. 29. doi: 10.1167/iovs.61.2.29.

Jiang, J. *et al.* (2013) 'Involvement of Rab28 in NF-κB Nuclear Transport in Endothelial Cells', *PLoS ONE*, 8(2), pp. 1–9. doi: 10.1371/journal.pone.0056076.

Jin, H. *et al.* (2010) 'The conserved bardet-biedl syndrome proteins assemble a coat that traffics membrane proteins to Cilia', *Cell*. Elsevier Ltd, 141(7), pp. 1208–1219. doi: 10.1016/j.cell.2010.05.015.

Kaji, K. *et al.* (2009) 'Virus-free induction of pluripotency and subsequent excision of reprogramming factors', *Nature*. Macmillan Publishers Limited. All rights reserved, 458(7239), pp. 771–775. Available at: http://dx.doi.org/10.1038/nature07864.

Kajiwara, M. *et al.* (2012) 'Donor-dependent variations in hepatic differentiation from human-induced pluripotent stem cells', *Proceedings of the National Academy of Sciences of the United States of America*, 109(31), pp. 12538–12543. doi: 10.1073/pnas.1209979109.

Karczewski, K. J. *et al.* (2017) 'The ExAC browser: Displaying reference data information from over 60 000 exomes', *Nucleic Acids Research*, 45(D1), pp. D840–D845. doi: 10.1093/nar/gkw971.

Keady, B. T. *et al.* (2012) 'IFT25 Links the Signal-Dependent Movement of Hedgehog Components to Intraflagellar Transport', *Developmental Cell*. Elsevier Inc., 22(5), pp. 940–951. doi: 10.1016/j.devcel.2012.04.009.

Kevany, B. M. and Palczewski, K. (2010) 'Phagocytosis of Retinal Rod and Cone Photoreceptors', *Physiology*, 25(1), pp. 8–15. doi: 10.1152/physiol.00038.2009.

Kim, K. *et al.* (2010) 'Epigenetic memory in induced pluripotent stem cells', *Nature*, 467(7313), pp. 285–290. doi: 10.1038/nature09342.

Kim, K. *et al.* (2011) 'Donor cell type can influence the epigenome and differentiation potential of human induced pluripotent stem cells', *Nature Biotechnology*, 29(12), pp. 1117–1119. doi: 10.1038/nbt.2052.

Kim, S. K. *et al.* (2010) 'Planar Cell Polarity Acts Through Septins to Control Collective Cell Movement and Ciliogenesis', *Science*, 329(5997), pp. 1337–1340. doi: 10.1126/science.1191184.

Klein, D. and Ammann, F. (1969) 'The syndrome of Laurence-Moon-Bardet-Biedl and allied diseases in Switzerland. Clinical, genetic and epidemiological studies', *Journal of the Neurological Sciences*, 9(3), pp. 479–513. doi: 10.1016/0022-510X(69)90091-4.

Klimanskaya, I. *et al.* (2004) 'Derivation and Comparative Assessment of Retinal Pigment Epithelium from Human Embryonic Stem Cells Using Transcriptomics', *Cloning and Stem Cells*, 6(3), pp. 217–245. doi: 10.1089/clo.2004.6.217.

Kostic, C. and Arsenijevic, Y. (2016) 'Animal modelling for inherited central vision loss', *The Journal of Pathology*, 238(2), pp. 300–310. doi: 10.1002/path.4641.

Kozminski, K. G., Beech, P. L. and Rosenbaum, J. L. (1995) 'The Chlamydomonas kinesin-like protein FLA10 is involved in motility associated with the flagellar membrane', *Journal of Cell Biology*, 131(6 I), pp. 1517–1527. doi: 10.1083/jcb.131.6.1517.

Lamba, D. A. *et al.* (2006) 'Efficient generation of retinal progenitor cells from human embryonic stem cells', *Proceedings of the National Academy of Sciences*, 103(34), pp. 12769–12774. doi: 10.1073/pnas.0601990103.

Langer, K. B. *et al.* (2018) 'Retinal Ganglion Cell Diversity and Subtype Specification from Human Pluripotent Stem Cells', *Stem Cell Reports*. ElsevierCompany., 10(4), pp. 1282–1293. doi: 10.1016/j.stemcr.2018.02.010.

LAURENCE, J. Z. and MOON, R. C. (1995) 'FOUR CASES OF "RETINITIS PIGMEN-TOSA"" OCCURRING IN THE SAME FAMILY, AND ACCOMPANIED BY GENERAL IMPERFECTIONS OF DEVELOPMENT."', *Obesity Research*, 3(4), pp. 400–403. doi: 10.1002/j.1550-8528.1995.tb00166.x.

Leach, L. L. *et al.* (2015) 'Canonical/ -Catenin Wnt Pathway Activation Improves Retinal Pigmented Epithelium Derivation From Human Embryonic Stem Cells', *Investigative Ophthalmology & Visual Science*, 56(2), pp. 1002–1013. doi: 10.1167/iovs.14-15835.

Leach, L. L. *et al.* (2016) 'Induced Pluripotent Stem Cell-Derived Retinal Pigmented Epithelium: A Comparative Study Between Cell Lines and Differentiation Methods', *Journal of Ocular Pharmacology and Therapeutics*, 32(5), pp. 317–330. doi: 10.1089/jop.2016.0022.

Lechtreck, K. F. *et al.* (2009) 'The Chlamydomonas reinhardtii BBSome is an IFT cargo required for export of specific signaling proteins from flagella', *Journal of Cell Biology*, 187(7), pp. 1117–1132. doi: 10.1083/jcb.200909183.

Lechtreck, K. F. *et al.* (2013) 'Cycling of the signaling protein phospholipase D through cilia requires the BBSome only for the export phase', *Journal of Cell Biology*, 201(2), pp. 249–261. doi: 10.1083/jcb.201207139.

Lechtreck, K. F. (2015) 'IFT–Cargo Interactions and Protein Transport in Cilia', *Trends in Biochemical Sciences*. Elsevier Ltd, 40(12), pp. 765–778. doi: 10.1016/j.tibs.2015.09.003.

Lee, G.-I. *et al.* (2017) 'A novel likely pathogenic variant in the RAB28 gene in a Korean patient with cone–rod dystrophy', *Ophthalmic Genetics*. Taylor & Francis, 38(6), pp. 587–589. doi: 10.1080/13816810.2017.1301965.

Leitch, C. C. *et al.* (2008) 'Hypomorphic mutations in syndromic encephalocele genes are associated with Bardet-Biedl syndrome', *Nature Genetics*, 40(4), pp. 443–448. doi: 10.1038/ng.97.

Liem, K. F. *et al.* (2012) 'The IFT-A complex regulates Shh signaling through cilia structure and membrane protein trafficking', *Journal of Cell Biology*, 197(6), pp. 789–800. doi: 10.1083/jcb.201110049.

Lim, Y. S., Chua, C. E. L. and Tang, B. L. (2011) 'Rabs and other small GTPases in ciliary transport', *Biology of the Cell*, 103(5), pp. 209–221. doi: 10.1042/BC20100150.

Lister, R. *et al.* (2011) 'Hotspots of aberrant epigenomic reprogramming in human induced pluripotent stem cells', *Nature*. Nature Publishing Group, 471(7336), pp. 68–73. doi: 10.1038/nature09798.

Liu, A. (2019) 'Proteostasis in the Hedgehog signaling pathway', *Seminars in Cell & Developmental Biology*. Elsevier, 93(July 2018), pp. 153–163. doi: 10.1016/j.semcdb.2018.10.009.

Liu, P. and Lechtreck, K. F. (2018) 'The Bardet–Biedl syndrome protein complex is an adapter expanding the cargo range of intraflagellar transport trains for ciliary export', *Proceedings of the National Academy of Sciences*, 115(5), pp. E934–E943. doi: 10.1073/pnas.1713226115.

Lucker, B. F. *et al.* (2005) 'Characterization of the Intraflagellar Transport Complex B Core', *Journal of Biological Chemistry*, 280(30), pp. 27688–27696. doi: 10.1074/jbc.M505062200.

Lucker, B. F. *et al.* (2010) 'Direct interactions of intraflagellar transport complex B proteins IFT88, IFT52, and IFT46', *Journal of Biological Chemistry*, 285(28), pp. 21508–21518. doi: 10.1074/jbc.M110.106997.

Lumb, J. H. *et al.* (2011) 'Rab28 function in trypanosomes: interactions with retromer and ESCRT pathways', *Journal of Cell Science*, 124(22), pp. 3771–3783. doi: 10.1242/jcs.079178.

M'hamdi, O. *et al.* (2014) 'Clinical and genetic characterization of Bardet-Biedl syndrome in Tunisia: Defining a strategy for molecular diagnosis', *Clinical Genetics*, 85(2), pp. 172–177. doi: 10.1111/cge.12129.

MacDonald, B. T. and He, X. (2012) 'Frizzled and LRP5/6 Receptors for Wnt/ -Catenin Signaling', *Cold Spring Harbor Perspectives in Biology*, 4(12), pp. a007880–a007880. doi: 10.1101/cshperspect.a007880.

MacDonald, B. T., Tamai, K. and He, X. (2009) 'Wnt/β-Catenin Signaling: Components, Mechanisms, and Diseases', *Developmental Cell*. Elsevier Inc., 17(1), pp. 9–26. doi: 10.1016/j.devcel.2009.06.016.

Mao, B. *et al.* (2002) 'Kremen proteins are Dickkopf receptors that regulate Wnt/β-catenin signalling', *Nature*, 417(6889), pp. 664–667. doi: 10.1038/nature756.

Marion, V. *et al.* (2012) 'Exome sequencing identifies mutations in LZTFL1 , a BBSome and smoothened trafficking regulator, in a family with Bardet–Biedl syndrome with situs inversus and insertional polydactyly', *Journal of Medical Genetics*, 49(5), pp. 317–321. doi: 10.1136/jmedgenet-2012-100737.

Marmorstein, A. D. (2001) 'The Polarity of the Retinal Pigment Epithelium', *Traffic*, 2(12), pp. 867–872. doi: 10.1034/j.1600-0854.2001.21202.x.

Martins-Neves, S. R. *et al.* (2018) 'IWR-1, a tankyrase inhibitor, attenuates Wnt/β-catenin signaling in cancer stem-like cells and inhibits in vivo the growth of a subcutaneous human osteosarcoma xenograft', *Cancer Letters*, 414, pp. 1–15. doi: 10.1016/j.canlet.2017.11.004.

Masland, R. H. (2001) 'The fundamental plan of the retina', *Nature Neuroscience*, 4(9), pp. 877–886. doi: 10.1038/nn0901-877.

Masui, S. *et al.* (2007) 'Pluripotency governed by Sox2 via regulation of Oct3/4 expression in mouse embryonic stem cells', *Nature Cell Biology*, 9(6), pp. 625–635. doi: 10.1038/ncb1589.

Mathe, E. *et al.* (2006) 'Computational approaches for predicting the biological effect of p53 missense mutations: a comparison of three sequence analysis based methods', *Nucleic Acids Research*, 34(5), pp. 1317–1325. doi: 10.1093/nar/gkj518.

Matsumoto, B., Defoe, D. M. and Besharse, J. C. (1987) 'Membrane turnover in rod photoreceptors: ensheathment and phagocytosis of outer segment distal tips by pseudopodia of the retinal pigment epithelium', *Proceedings of the Royal Society of London. Series B. Biological Sciences*, 230(1260), pp. 339–354. doi: 10.1098/rspb.1987.0023.

May-Simera, H. L. *et al.* (2018) 'Primary Cilium Mediated Retinal Pigment Epithelium Maturation is Retarded in Ciliopathy Patient Cells', *Cell Reports*. ElsevierCompany., 22(1), pp. 189–205. doi: 10.1016/j.celrep.2017.12.038.

Mellough, C. B. *et al.* (2015) 'IGF-1 Signaling Plays an Important Role in the Formation of Three-

Dimensional Laminated Neural Retina and Other Ocular Structures from Human Embryonic Stem Cells', *Stem Cells*, 33(8), pp. 2416–2430. doi: 10.1002/stem.2023.

Meng, Y. *et al.* (2018) 'Nicotinamide Promotes Cell Survival and Differentiation as Kinase Inhibitor in Human Pluripotent Stem Cells', *Stem Cell Reports*. ElsevierCompany., 11(6), pp. 1347–1356. doi: 10.1016/j.stemcr.2018.10.023.

Mitsui, K. *et al.* (2003) 'The Homeoprotein Nanog Is Required for Maintenance of Pluripotency in Mouse Epiblast and ES Cells', *Cell*, 113(5), pp. 631–642. doi: 10.1016/S0092-8674(03)00393-3.

Morleo, M. and Franco, B. (2019) 'The Autophagy-Cilia Axis: An Intricate Relationship', *Cells*, 8(8), p. 905. doi: 10.3390/cells8080905.

Morthorst, S. K., Christensen, S. T. and Pedersen, L. B. (2018) 'Regulation of ciliary membrane protein trafficking and signalling by kinesin motor proteins', *The FEBS Journal*, 285(24), pp. 4535–4564. doi: 10.1111/febs.14583.

Mourão, A. *et al.* (2014) 'Structural basis for membrane targeting of the BBSome by ARL6', *Nature Structural & Molecular Biology*, 21(12), pp. 1035–1041. doi: 10.1038/nsmb.2920.

Mourão, A., Christensen, S. T. and Lorentzen, E. (2016) 'The intraflagellar transport machinery in ciliary signaling', *Current Opinion in Structural Biology*, 41, pp. 98–108. doi: 10.1016/j.sbi.2016.06.009.

Moyer, J. *et al.* (1994) 'Candidate gene associated with a mutation causing recessive polycystic kidney disease in mice', *Science*, 264(5163), pp. 1329–1333. doi: 10.1126/science.8191288.

Mukhopadhyay, S. *et al.* (2010) 'TULP3 bridges the IFT-A complex and membrane phosphoinositides to promote trafficking of G protein-coupled receptors into primary cilia', *Genes & Development*, 24(19), pp. 2180–2193. doi: 10.1101/gad.1966210.

Mukhopadhyay, S. and Rohatgi, R. (2014) 'G-protein-coupled receptors, Hedgehog signaling and primary cilia', *Seminars in Cell & Developmental Biology*. Elsevier Ltd, 33, pp. 63–72. doi: 10.1016/j.semcdb.2014.05.002.

Muller, J. *et al.* (2010) 'Identification of 28 novel mutations in the Bardet–Biedl syndrome genes: the burden of private mutations in an extensively heterogeneous disease', *Human Genetics*, 127(5), pp. 583–593. doi: 10.1007/s00439-010-0804-9.

Nachury, M. V. *et al.* (2007) 'A Core Complex of BBS Proteins Cooperates with the GTPase Rab8 to Promote Ciliary Membrane Biogenesis', *Cell*, 129(6), pp. 1201–1213. doi: 10.1016/j.cell.2007.03.053.

Nachury, M. V. (2018) 'The molecular machines that traffic signaling receptors into and out of cilia', *Current Opinion in Cell Biology*. Elsevier Ltd, 51, pp. 124–131. doi: 10.1016/j.ceb.2018.03.004.

Nachury, M. V. and Mick, D. U. (2019) 'Establishing and regulating the composition of cilia for signal transduction', *Nature Reviews Molecular Cell Biology*. Springer US, 20(7), pp. 389–405. doi: 10.1038/s41580-019-0116-4.

Nager, A. R. *et al.* (2017) 'An Actin Network Dispatches Ciliary GPCRs into Extracellular Vesicles to Modulate Signaling', *Cell*, 168(1–2), pp. 252-263.e14. doi: 10.1016/j.cell.2016.11.036.

Nakagawa, M. *et al.* (2008) 'Generation of induced pluripotent stem cells without Myc from mouse and human fibroblasts', *Nature Biotechnology*, 26(1), pp. 101–106. doi: 10.1038/nbt1374.

Nakagawa, M. *et al.* (2010) 'Promotion of direct reprogramming by transformation-deficient Myc', *Proceedings of the National Academy of Sciences*, 107(32), pp. 14152–14157. doi:

10.1073/pnas.1009374107.

Nakano, T. *et al.* (2012) 'Self-Formation of Optic Cups and Storable Stratified Neural Retina from Human ESCs', *Cell Stem Cell*. Elsevier, 10(6), pp. 771–785. doi: 10.1016/j.stem.2012.05.009.

Nash, B. M. *et al.* (2015) 'Retinal dystrophies, genomic applications in diagnosis and prospects for therapy.', *Translational pediatrics*, 4(2), pp. 139–63. doi: 10.3978/j.issn.2224-4336.2015.04.03.

Nichols, J. *et al.* (1998) 'Formation of Pluripotent Stem Cells in the Mammalian Embryo Depends on the POU Transcription Factor Oct4', *Cell*, 95(3), pp. 379–391. doi: 10.1016/S0092-8674(00)81769-9.

Niewiadomski, P. *et al.* (2014) 'Gli Protein Activity Is Controlled by Multisite Phosphorylation in Vertebrate Hedgehog Signaling', *Cell Reports*. The Authors, 6(1), pp. 168–181. doi: 10.1016/j.celrep.2013.12.003.

Niwa, H. (2007) 'How is pluripotency determined and maintained?', *Development*, 134(4), pp. 635–646. doi: 10.1242/dev.02787.

Niwa, H. *et al.* (2009) 'A parallel circuit of LIF signalling pathways maintains pluripotency of mouse ES cells', *Nature*, 460(7251), pp. 118–122. doi: 10.1038/nature08113.

Novas, R. *et al.* (2015) 'Bardet-Biedl syndrome: Is it only cilia dysfunction?', *FEBS Letters*, 589(22), pp. 3479–3491. doi: 10.1016/j.febslet.2015.07.031.

Nozaki, S. *et al.* (2018) 'BBS1 is involved in retrograde trafficking of ciliary GPCRs in the context of the BBSome complex', *PLoS ONE*, 13(3), pp. 1–17. doi: 10.1371/journal.pone.0195005.

Ocbina, P. J. R., Tuson, M. and Anderson, K. V. (2009) 'Primary Cilia Are Not Required for Normal Canonical Wnt Signaling in the Mouse Embryo', *PLoS ONE*. Edited by C.-P. Heisenberg, 4(8), p. e6839. doi: 10.1371/journal.pone.0006839.

Ohi, Y. *et al.* (2011) 'Incomplete DNA methylation underlies a transcriptional memory of somatic cells in human iPS cells', *Nature Cell Biology*. Nature Publishing Group, 13(5), pp. 541–549. doi: 10.1038/ncb2239.

Okita, K. *et al.* (2008) 'Generation of Mouse Induced Pluripotent Stem Cells Without Viral Vectors', *Science*, 322(5903), pp. 949–953. doi: 10.1126/science.1164270.

Okita, K. *et al.* (2011) 'A more efficient method to generate integration-free human iPS cells', *Nature Methods*. Nature Publishing Group, 8(5), pp. 409–412. doi: 10.1038/nmeth.1591.

Ou, G. *et al.* (2005) 'Functional coordination of intraflagellar transport motors', *Nature*, 436(7050), pp. 583–587. doi: 10.1038/nature03818.

Pal, K. *et al.* (2016) 'Smoothened determines β-arrestin–mediated removal of the G protein–coupled receptor Gpr161 from the primary cilium', *The Journal of Cell Biology*, 212(7), pp. 861–875. doi: 10.1083/jcb.201506132.

Patnaik, S. R. *et al.* (2019) 'Bardet–Biedl Syndrome proteins regulate cilia disassembly during tissue maturation', *Cellular and Molecular Life Sciences*. Springer International Publishing, 76(4), pp. 757–775. doi: 10.1007/s00018-018-2966-x.

Pazour, G. J. *et al.* (2000) 'Chlamydomonas IFT88 and its mouse homologue, polycystic kidney disease gene Tg737, are required for assembly of cilia and flagella', *Journal of Cell Biology*, 151(3), pp. 709–718. doi: 10.1083/jcb.151.3.709.

Pazour, G. J., Dickert, B. L. and Witman, G. B. (1999) 'The DHC1b (DHC2) isoform of cytoplasmic dynein is required for flagellar assembly', *Journal of Cell Biology*, 144(3), pp. 473–481. doi: 10.1083/jcb.144.3.473.

Pazour, G. J., Wilkerson, C. G. and Witman, G. B. (1998) 'A dynein light chain is essential for the retrograde particle movement of intraflagellar transport (IFT)', *Journal of Cell Biology*, 141(4), pp. 979–992. doi: 10.1083/jcb.141.4.979.

Pedersen, L. B. *et al.* (2005) 'Chlamydomonas IFT172 Is Encoded by FLA11, Interacts with CrEB1, and Regulates IFT at the Flagellar Tip', *Current Biology*, 15(3), pp. 262–266. doi: 10.1016/j.cub.2005.01.037.

Porter, M. E. *et al.* (1999) 'Cytoplasmic dynein heavy chain 1b is required for flagellar assembly in Chlamydomonas', *Molecular Biology of the Cell*, 10(3), pp. 693–712. doi: 10.1091/mbc.10.3.693.

Prevo, B., Scholey, J. M. and Peterman, E. J. G. (2017) 'Intraflagellar transport: mechanisms of motor action, cooperation, and cargo delivery', *FEBS Journal*, 284(18), pp. 2905–2931. doi: 10.1111/febs.14068.

Priya, S. *et al.* (2016) 'Bardet-Biedl syndrome: Genetics, molecular pathophysiology, and disease management', *Indian Journal of Ophthalmology*, 64(9), pp. 620–627. doi: 10.4103/0301-4738.194328.

Pusapati, G. V *et al.* (2018) 'G protein–coupled receptors control the sensitivity of cells to the morphogen Sonic Hedgehog', *Science Signaling*, 11(516), p. eaao5749. doi: 10.1126/scisignal.aao5749.

Ramón Martínez-Morales, J., Rodrigo, I. and Bovolenta, P. (2004) 'Eye development: a view from the retina pigmented epithelium', *BioEssays*, 26(7), pp. 766–777. doi: 10.1002/bies.20064.

Rasmussen, M. A. *et al.* (2014) 'Transient p53 Suppression Increases Reprogramming of Human Fibroblasts without Affecting Apoptosis and DNA Damage', *Stem Cell Reports*, 3(3), pp. 404–413. doi: 10.1016/j.stemcr.2014.07.006.

Rattner, A. and Nathans, J. (2006) 'Macular degeneration: recent advances and therapeutic opportunities', *Nature Reviews Neuroscience*, 7(11), pp. 860–872. doi: 10.1038/nrn2007.

Rentzsch, P. *et al.* (2019) 'CADD: Predicting the deleteriousness of variants throughout the human genome', *Nucleic Acids Research*. Oxford University Press, 47(D1), pp. D886–D894. doi: 10.1093/nar/gky1016.

Richards, S. *et al.* (2015) 'Standards and guidelines for the interpretation of sequence variants: a joint consensus recommendation of the American College of Medical Genetics and Genomics and the Association for Molecular Pathology', *Genetics in Medicine*, 17(5), pp. 405–423. doi: 10.1038/gim.2015.30.

Riveiro-Álvarez, R. *et al.* (2015) 'New mutations in the rab28 gene in 2 spanish families with cone-rod dystrophy ', *JAMA Ophthalmology*, 133(2), pp. 133–139. Available at: http://dx.doi.org/10.1001/jamaophthalmol.2014.4266.

Rizzolo, L. J. (2007) 'Development and Role of Tight Junctions in the Retinal Pigment Epithelium', in *International Review of Cytology*, pp. 195–234. doi: 10.1016/S0074-7696(07)58004-6.

Rohatgi, R. *et al.* (2009) 'Hedgehog signal transduction by Smoothened: Pharmacologic evidence for a 2-step activation process', *Proceedings of the National Academy of Sciences*, 106(9), pp. 3196–3201. doi: 10.1073/pnas.0813373106.

Rohatgi, R., Milenkovic, L. and Scott, M. P. (2007) 'Patched1 Regulates Hedgehog Signaling at the Primary Cilium', *Science*, 317(5836), pp. 372–376. doi: 10.1126/science.1139740.

Roosing, S. *et al.* (2013) 'Mutations in RAB28, Encoding a Farnesylated Small GTPase, Are Associated with Autosomal-Recessive Cone-Rod Dystrophy', *The American Journal of Human Genetics*. The American Society of Human Genetics, 93(1), pp. 110–117. doi: 10.1016/j.ajhg.2013.05.005.

Santos, N. and Reiter, J. F. (2008) 'Building it up and taking it down: The regulation of vertebrate ciliogenesis', *Developmental Dynamics*, 237(8), pp. 1972–1981. doi: 10.1002/dvdy.21540.

Sathya Priya, C. *et al.* (2015) 'Mutation spectrum in BBS genes guided by homozygosity mapping in an Indian cohort', *Clinical Genetics*, 87(2), pp. 161–166. doi: 10.1111/cge.12342.

Satir, P. and Christensen, S. T. (2007) 'Overview of Structure and Function of Mammalian Cilia', *Annual Review of Physiology*, 69(1), pp. 377–400. doi: 10.1146/annurev.physiol.69.040705.141236.

Schaefer, E. *et al.* (2010) 'Mutations in SDCCAG8/NPHP10 Cause Bardet-Biedl Syndrome and Are Associated with Penetrant Renal Disease and Absent Polydactyly', *Molecular Syndromology*, 1(6), pp. 273–281. doi: 10.1159/000331268.

Schaefer, E. *et al.* (2016) 'Identification of a novel mutation confirms the implication of IFT172 (BBS20) in Bardet–Biedl syndrome', *Journal of Human Genetics*, 61(5), pp. 447–450. doi: 10.1038/jhg.2015.162.

Schou, K. B. *et al.* (2017) 'KIF13B establishes a CAV1-enriched microdomain at the ciliary transition zone to promote Sonic hedgehog signalling', *Nature Communications*, 8(1), p. 14177. doi: 10.1038/ncomms14177.

Schwarz, J. M. *et al.* (2010) 'MutationTaster evaluates disease-causing potential of sequence alterations', *Nature Methods*. Nature Publishing Group, 7(8), pp. 575–576. doi: 10.1038/nmeth0810-575.

Seixas, E. *et al.* (2013) 'Rab and Arf proteins in genetic diseases', *Traffic*, 14(8), pp. 871–885. doi: 10.1111/tra.12072.

Seki, T. *et al.* (2010) 'Generation of Induced Pluripotent Stem Cells from Human Terminally Differentiated Circulating T Cells', *Cell Stem Cell*. Elsevier Ltd, 7(1), pp. 11–14. doi: 10.1016/j.stem.2010.06.003.

Seo, S. *et al.* (2010) 'BBS6, BBS10, and BBS12 form a complex with CCT/TRiC family chaperonins and mediate BBSome assembly', *Proceedings of the National Academy of Sciences*, 107(4), pp. 1488–1493. doi: 10.1073/pnas.0910268107.

Seo, S. *et al.* (2011) 'A novel protein LZTFL1 regulates ciliary trafficking of the BBSome and smoothened', *PLoS Genetics*, 7(11). doi: 10.1371/journal.pgen.1002358.

Shamseldin, H. E. *et al.* (2020) 'The morbid genome of ciliopathies: an update', *Genetics in Medicine*. Springer US, 0(0), pp. 1–10. doi: 10.1038/s41436-020-0761-1.

Shi, Y. *et al.* (2008) 'Induction of Pluripotent Stem Cells from Mouse Embryonic Fibroblasts by Oct4 and Klf4 with Small-Molecule Compounds', *Cell Stem Cell*, 3(5), pp. 568–574. doi: 10.1016/j.stem.2008.10.004.

Shimada, H. *et al.* (2017) 'In Vitro Modeling Using Ciliopathy-Patient-Derived Cells Reveals Distinct Cilia Dysfunctions Caused by CEP290 Mutations', *Cell Reports*. ElsevierCompany., 20(2), pp. 384–396. doi: 10.1016/j.celrep.2017.06.045.

Singh, J., Wen, X. and Scales, S. J. (2015) 'The Orphan G Protein-coupled Receptor Gpr175 (Tpra40) Enhances Hedgehog Signaling by Modulating cAMP Levels', *Journal of Biological Chemistry*, 290(49), pp. 29663–29675. doi: 10.1074/jbc.M115.665810.

Sinha, S. and Chen, J. K. (2006) 'Purmorphamine activates the Hedgehog pathway by targeting Smoothened', *Nature Chemical Biology*, 2(1), pp. 29–30. doi: 10.1038/nchembio753.

Sorokin, S. (1962) 'CENTRIOLES AND THE FORMATION OF RUDIMENTARY CILIA BY FIBROBLASTS AND SMOOTH MUSCLE CELLS', *The Journal of Cell Biology*, 15(2), pp. 363–377. doi: 10.1083/jcb.15.2.363.

Sorokin, S. P. (1968) 'Reconstructions of centriole formation and ciliogenesis in mammalian lungs.', *Journal of cell science*, 3(2), pp. 207–30. Available at: http://www.ncbi.nlm.nih.gov/pubmed/5661997.

Stadtfeld, M. *et al.* (2008) 'Induced Pluripotent Stem Cells Generated Without Viral Integration', *Science*, 322(5903), pp. 945–949. doi: 10.1126/science.1162494.

Stenmark, H. and Olkkonen, V. M. (2001) 'The Rab GTPase family', *Genome Biology*, 2(5), p. reviews3007.1. doi: 10.1186/gb-2001-2-5-reviews3007.

Strauss, O. (2005) 'The Retinal Pigment Epithelium in Visual Function', *Physiological Reviews*, 85(3), pp. 845–881. doi: 10.1152/physrev.00021.2004.

Sung, C.-H. and Leroux, M. R. (2013) 'The roles of evolutionarily conserved functional modules in cilia-related trafficking', *Nature Cell Biology*. Nature Publishing Group, 15(12), pp. 1387–1397. doi: 10.1038/ncb2888.

Suspitsin, E. N. and Imyanitov, E. N. (2016) 'Bardet-Biedl Syndrome', *Molecular Syndromology*, 7(2), pp. 62–71. doi: 10.1159/000445491.

Takahashi, K. *et al.* (2007) 'Induction of pluripotent stem cells from adult human fibroblasts by defined factors', *cell*. Elsevier, 131(5), pp. 861–872.

Takahashi, K. and Yamanaka, S. (2006) 'Induction of pluripotent stem cells from mouse embryonic and adult fibroblast cultures by defined factors', *cell*. Elsevier, 126(4), pp. 663–676.

Tammachote, R. *et al.* (2009) 'Ciliary and centrosomal defects associated with mutation and depletion of the Meckel syndrome genes MKS1 and MKS3', *Human Molecular Genetics*, 18(17), pp. 3311–3323. doi: 10.1093/hmg/ddp272.

Taschner, M. *et al.* (2011) 'Biochemical mapping of interactions within the intraflagellar transport (IFT) B core complex: IFT52 binds directly to four other IFT-B subunits', *Journal of Biological Chemistry*, 286(30), pp. 26344–26352. doi: 10.1074/jbc.M111.254920.

Taschner, M. *et al.* (2014) 'Crystal structures of IFT70/52 and IFT52/46 provide insight into intraflagellar transport B core complex assembly', *Journal of Cell Biology*, 207(2), pp. 269–282. doi: 10.1083/jcb.201408002.

Taschner, M. *et al.* (2016) 'IFT-B 2 complex', *The EMBO journal*, 35(7), pp. 1–18.

Taschner, M. and Lorentzen, E. (2016) 'The Intraflagellar Transport Machinery', *Cold Spring Harbor Perspectives in Biology*, 8(10), p. a028092. doi: 10.1101/cshperspect.a028092.

Tavtigian, S. V. *et al.* (2006) 'Comprehensive statistical study of 452 BRCA1 missense substitutions with classification of eight recurrent substitutions as neutral', *Journal of Medical Genetics*, 43(4), pp. 295–305. doi: 10.1136/jmg.2005.033878.

Thomson, J. A. *et al.* (1998) 'Embryonic stem cell lines derived from human blastocysts.', *Science (New York, N.Y.)*, 282(5391), pp. 1145–7. doi: 10.1126/science.282.5391.1145.

Toops, K. A., Tan, L. X. and Lakkaraju, A. (2014) 'A detailed three-step protocol for live imaging of intracellular traffic in polarized primary porcine RPE monolayers', *Experimental Eye Research*. Elsevier Ltd, 124, pp. 74–85. doi: 10.1016/j.exer.2014.05.003.

Tucker, R. W., Pardee, A. B. and Fujiwara, K. (1979) 'Centriole ciliation is related to quiescence and DNA synthesis in 3T3 cells', *Cell*, 17(3), pp. 527–535. doi: 10.1016/0092-8674(79)90261-7.

Valenta, T., Hausmann, G. and Basler, K. (2012) 'The many faces and functions of β-catenin', *The EMBO Journal*, 31(12), pp. 2714–2736. doi: 10.1038/emboj.2012.150.

Vaser, R. *et al.* (2016) 'SIFT missense predictions for genomes', *Nature Protocols*. Nature Publishing Group, 11(1), pp. 1–9. doi: 10.1038/nprot.2015.123.

Vashishtha, M., Walther, Z. and Hall, J. L. (1996) 'The kinesin-homologous protein encoded by the Chlamydomonas FLA10 gene is associated with basal bodies and centrioles', *Journal of Cell Science*, 109(3), pp. 541–549.

Voronkov, A. and Krauss, S. (2012) 'Wnt/beta-Catenin Signaling and Small Molecule Inhibitors', *Current Pharmaceutical Design*, 19(4), pp. 634–664. doi: 10.2174/13816128130406.

Walther, Z. (1994) 'The Chlamydomonas FLA10 gene encodes a novel kinesin-homologous protein', *The Journal of Cell Biology*, 126(1), pp. 175–188. doi: 10.1083/jcb.126.1.175.

Wang, X. *et al.* (2013) 'The Development of Highly Potent Inhibitors for Porcupine', *Journal of Medicinal Chemistry*, 56(6), pp. 2700–2704. doi: 10.1021/jm400159c.

Wei, Q. *et al.* (2018) 'Lztfl1/BBS17 controls energy homeostasis by regulating the leptin signaling in the hypothalamic neurons', *Journal of Molecular Cell Biology*, 10(5), pp. 402–410. doi: 10.1093/jmcb/mjy022.

Wheway, G., Parry, D. A. and Johnson, C. A. (2014) 'The role of primary cilia in the development and disease of the retina', *Organogenesis*, 10(1), pp. 69–85. doi: 10.4161/org.26710.

Wiens, C. J. *et al.* (2010) 'Bardet-Biedl Syndrome-associated Small GTPase ARL6 (BBS3) Functions at or near the Ciliary Gate and Modulates Wnt Signaling', *Journal of Biological Chemistry*, 285(21), pp. 16218–16230. doi: 10.1074/jbc.M109.070953.

Willoughby, C. E. *et al.* (2010) 'Anatomy and physiology of the human eye: effects of mucopolysaccharidoses disease on structure and function - a review', *Clinical & Experimental Ophthalmology*, 38(SUPPL. 1), pp. 2–11. doi: 10.1111/j.1442-9071.2010.02363.x.

Wilmut, I. *et al.* (1997) 'Viable offspring derived from fetal and adult mammalian cells', *Nature*, 385(6619), pp. 810–813. doi: 10.1038/385810a0.

Woltjen, K. *et al.* (2009) 'piggyBac transposition reprograms fibroblasts to induced pluripotent stem cells', *Nature*. Macmillan Publishers Limited. All rights reserved, 458(7239), pp. 766–770. Available at: http://dx.doi.org/10.1038/nature07863.

Wood, C. R. *et al.* (2013) 'The cilium secretes bioactive ectosomes', *Current Biology*. Elsevier Ltd, 23(10), pp. 906–911. doi: 10.1016/j.cub.2013.04.019.

Wu, Y., Tibrewal, N. and Birge, R. B. (2006) 'Phosphatidylserine recognition by phagocytes: a view to a kill', *Trends in Cell Biology*, 16(4), pp. 189–197. doi: 10.1016/j.tcb.2006.02.003.

Yamaguchi, Y. and Hearing, V. J. (2014) 'Melanocytes and Their Diseases', *Cold Spring Harbor Perspectives in Medicine*, 4(5), pp. a017046–a017046. doi: 10.1101/cshperspect.a017046.

Yamanaka, S. (2007) 'Strategies and New Developments in the Generation of Patient-Specific Pluripotent Stem Cells', *Cell Stem Cell*, 1(1), pp. 39–49. doi: 10.1016/j.stem.2007.05.012.

Ye, F., Nager, A. R. and Nachury, M. V. (2018) 'BBSome trains remove activated GPCRs from cilia by enabling passage through the transition zone', *The Journal of Cell Biology*, 217(5), pp. 1847–1868. doi: 10.1083/jcb.201709041.

Ying, G. *et al.* (2018) 'The small GTPase Rab28 is required for phagocytosis of cone outer segments by the murine retinal pigmented epithelium', *Journal of Biological Chemistry*, p. jbc.RA118.005484. doi: 10.1074/jbc.RA118.005484.

Yoshida, Y. and Yamanaka, S. (2017) 'Induced Pluripotent Stem Cells 10 Years Later', *Circulation Research*, 120(12), pp. 1958–1968. doi: 10.1161/CIRCRESAHA.117.311080.

Yu, J. *et al.* (2007) 'Induced Pluripotent Stem Cell Lines Derived from Human Somatic Cells', *Science*, 318(5858), pp. 1917–1920. Available at: http://science.sciencemag.org/content/318/5858/1917.abstract.

Yu, J. *et al.* (2009) 'Human Induced Pluripotent Stem Cells Free of Vector and Transgene Sequences', *Science*, 324(5928), p. 797. Available at: http://science.sciencemag.org/content/324/5928/797.abstract.

Yue, S. *et al.* (2014) 'Requirement of Smurf-mediated endocytosis of Patched1 in sonic hedgehog signal reception', *eLife*, 3(3), pp. 1–25. doi: 10.7554/eLife.02555.

Yusa, K. *et al.* (2009) 'Generation of transgene-free induced pluripotent mouse stem cells by the piggyBac transposon', *Nature Methods*, 6(5), pp. 363–369. doi: 10.1038/nmeth.1323.

Zaghloul, N. A. and Katsanis, N. (2009) 'Mechanistic insights into Bardet-Biedl syndrome, a model ciliopathy', *Journal of Clinical Investigation*, 119(3), pp. 428–437. doi: 10.1172/JCI37041.

Zahabi, A. *et al.* (2012) 'A New Efficient Protocol for Directed Differentiation of Retinal Pigmented Epithelial Cells from Normal and Retinal Disease Induced Pluripotent Stem Cells', *Stem Cells and Development*, 21(12), pp. 2262–2272. doi: 10.1089/scd.2011.0599.

Zhang, Q. *et al.* (2012) 'BBS proteins interact genetically with the IFT pathway to influence SHH-related phenotypes', *Human Molecular Genetics*, 21(9), pp. 1945–1953. doi: 10.1093/hmg/dds004.

Zhou, Z. *et al.* (2017) 'Rab28 is a TBC1D1/TBC1D4 substrate involved in GLUT4 trafficking', *FEBS Letters*, 591(1), pp. 88–96. doi: 10.1002/1873-3468.12509.

5. Enclosed Papers

Research Paper I

Generation of induced pluripotent stem cells, KCi001-A derived from a Bardet-Biedl syndrome patient compound heterozygous for the *BBS1* variants c.1169T>G/c.1135G>C

Stem Cell Research 31 (2018) 235–239

Contents lists available at ScienceDirect

Stem Cell Research

journal homepage: www.elsevier.com/locate/scr

Lab resource: Stem Cell Line

Generation of induced pluripotent stem cells, KCi001-A derived from a Bardet-Biedl syndrome patient compound heterozygous for the *BBS1* variants *c.1169T > G/c.1135G > C*

Caroline Amalie Brunbjerg Hey, Katarina Beata Saltõkowa, Lasse Jonsgaard Larsen, Zeynep Tümer, Karen Brøndum-Nielsen, Karen Grønskov, Tina Duelund Hjortshøj, Lisbeth Birk Møller*

Applied Human Molecular Genetics, Kennedy Center, Department of Clinical Genetics, Copenhagen University Hospital, Rigshospitalet, Gl. Landevej 7, 2600 Glostrup, Denmark

A B S T R A C T

Bardet-Biedl syndrome (BBS) is an autosomal recessive ciliopathy with a wide range of symptoms including obesity, retinal dystrophy, polycystic kidney disease, polydactyly, hypogonadism and learning difficulties. Here we describe the successful generation of an induced pluripotent stem cell (iPSC) KCi001-A from a BBS patient compound heterozygous for two disease causing *BBS1* variants c.1169T > G, p. (Met390Arg)/c.1135G > C, p.(Gly370Arg).

Resource table

Unique stem cell line identifier	KCi001-A
Alternative name(s) of stem cell line	BBS1 Clone10
Institution	Kennedy Center, Rigshospitalet
Contact information of distributor	Lisbeth Birk Møller, Lisbeth.Birk.Moeller@regionh.dk
Type of cell line	Induced pluripotent stem cell line (iPSC)
Origin	Human
Additional origin info	Female, Caucasian
Cell source	Dermal fibroblasts
Clonality	Clonal
Method of reprogramming	Nucleofection with non-integrating episomal plasmids carrying *OCT3/4, SOX2, KLF4, L-MYC, LIN28* and *shP53*
Genetic modification	NA
Type of modification	NA
Associated disease	Autosomal recessive Bardet-Biedl syndrome
Gene/locus	*BBS1,* Chr11: g.66293652 T > G, p.(Met390Arg); g.66293618G > C, p.(Gly379Arg); compound heterozygous. Ref sequence: NM_024649.4
Method of modification	NA
Name of transgene or resistance	NA
Inducible/constitutive system	NA
Date archived/stock date	25-01-2018
Cell line repository/bank	NA
Ethical approval	The study was approved by the regional scientific ethical committee in the Capital Region of Denmark (H-3-2014-140). Written informed consent was obtained from the patients.

* Corresponding author.
E-mail address: Lisbeth.birk.moeller@regionh.dk (L.B. Møller).

https://doi.org/10.1016/j.scr.2018.08.005
Received 24 February 2018; Received in revised form 19 July 2018; Accepted 8 August 2018
Available online 10 August 2018

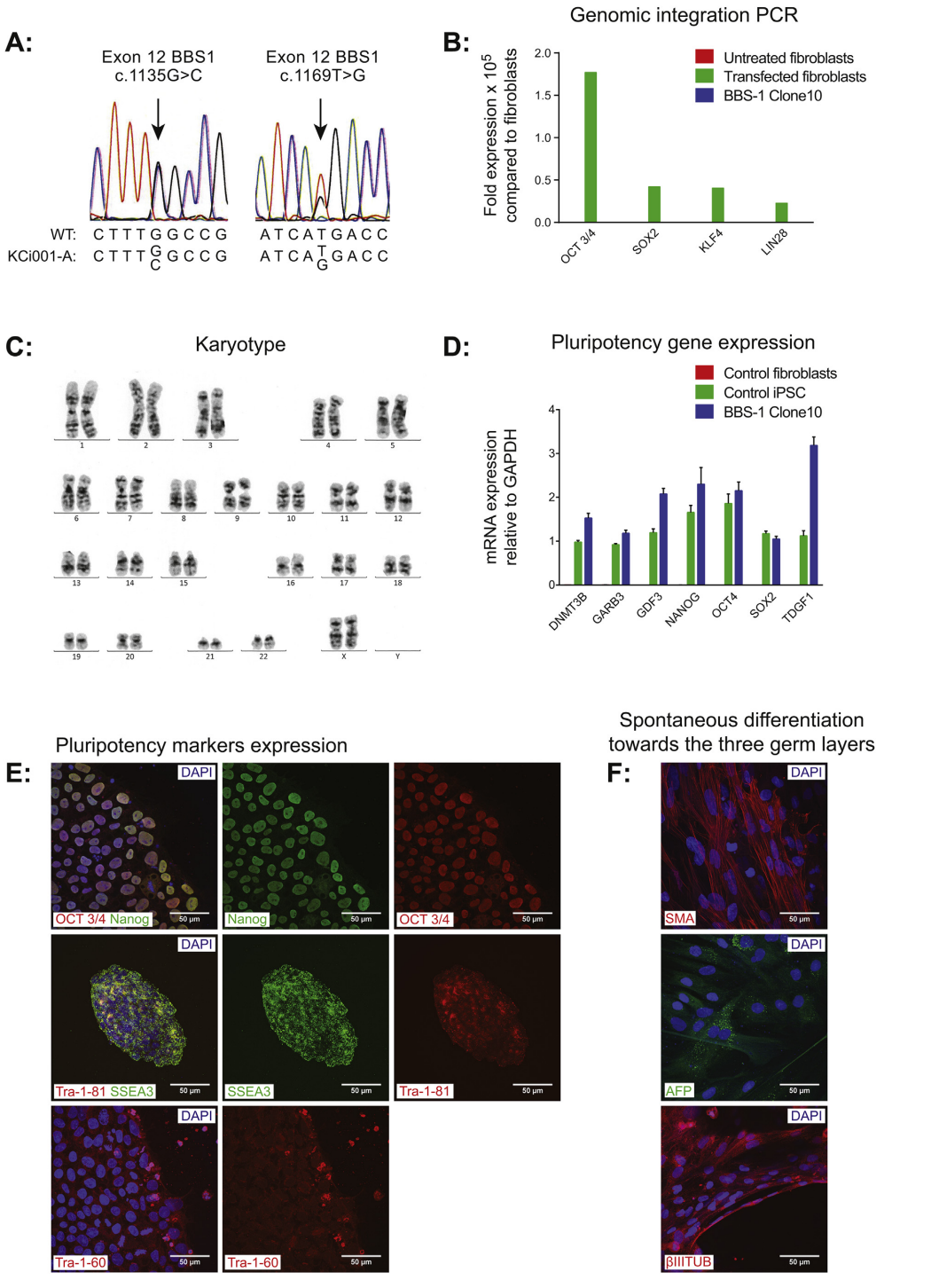

(caption on next page)

Fig. 1. Characterization of BBS1 Clone 10 line (KCi001-A). A. WT sequences and mutations in KCi001-A in the same regions of the BBS1 gene. B. Quantitative real time PCR showing absence of episomal plasmids in BBS1 Clone 10 (KCi001-A) and control fibroblasts and presence of plasmids in transfected fibroblasts. C. Karyotype of representative metaphase showing normal 46 chromosomes (XX). D. mRNA expression of pluripotency markers in control iPSC line and in BBS1 Clone 10 (KCi001-A). E. Confocal images showing immunodetection of pluripotency-associated markers in BBS1 Clone 10 (KCi001-A). F. Immunofluorescence analysis of in vitro differentiation of BBS1 Clone 10 (KCi001-A) EBs using specific antibodies against the mesodermal marker α-smooth muscle actin (SMA), endodermal marker α-fetoprotein (AFP) and the ectodermal marker βIII-tubulin (βtub). Nuclei were stained with DAPI. Scale bar 50μM.

1. Resource utility

Bardet-Biedl syndrome BBS is characterized by defective cilia function. The *BBS1* encoded protein is a member of the BBSome complex, which is important for trafficking of membrane proteins in the cilium. The generated iPSC line represents a useful source to investigate the effect of *BBS1* in the pathophysiology of BBS.

2. Resource details

BBS is a rare, autosomal recessive disorder, where cellular, cilium-dependent signalling is affected. It has an estimated prevalence of 1/59000 in Denmark (Hjortshøj et al., 2010). Primary cilia are microtubule-based organelles, extending from the surface of most quiescent vertebrate cells. The BBS1 protein is part of a protein complex termed the BBSome and is thought to have a function in intra flagellar transport (IFT) in the primary cilium and in the connecting cilium, a specialized primary cilium in photoreceptors. Previous studies have shown defective IFT as a result of pathogenic variants in the genes encoding the proteins of the BBSome complex (Nager et al., 2017), but few studies have focused on the function of BBS1 even though it is one of the most frequently affected protein in BBS (Forsythe and Beales, 2012).

Fibroblasts were obtained from a skin biopsy of a patient with classic BBS symptoms, and compound heterozygous for the *BBS1* variants: c.1169T > G, p.(Met390Arg) and c.1135G > C, p. (Gly370Arg). The fibroblasts were reprogrammed into iPSC by nucleofection of three non-integrating episomal plasmids, encoding the human genes; *OCT3/4*, *SOX2*, *KLF4*, *L-MYC*, *LIN28* and a p53 knock down *shP53*. Successful isolation of the iPSC clone, KCi001-A was achieved and sequencing of genomic DNA from KCi001-A confirmed the retention of the *BBS1* variants (Fig. 1A). Absence of integration of the episomal plasmids in genomic DNA in KCi001-A, were verified by quantitative RT-PCR analysis (Applied Biosystems 7500 Fast system) using plasmid specific primers for *OCT3/4*, *SOX-2*, *KLF4*, *LIN28* and *L-MYC* (Table 2), in the presence of SYBR green (Fig. 1B). DNA from control fibroblast 72 h post transfection and DNA from un-transfected fibroblasts were used as a positive and negative control, respectively (Fig. 1B). Primers for the corresponding endogenous genes were included as positive controls (not shown). Normal karyotype of the generated iPSC was preserved (46,XX) (Fig. 1C). Short tandem repeat (STR)-PCR profile analysis, where 22 different loci were analysed, showed 100% identity match between the parental fibroblast cell line and KCi001-A (submitted in archive with journal). Pluripotency was confirmed by expression of the genes, *OCT4*, *NANOG*, *SOX-2*, *TDGF1*, *DNMT3B*, *GDF3*and *GARB3*, analysed by RT-qPCR using Taq-man probes (Fig. 1D). The mRNA level of the different genes, were normalized to *GAPDH* mRNA. RNA from untreated fibroblasts and from a control iPSC line was included as a negative and a positive control, respectively (Fig. 1D). Pluripotency was further supported by immunocytochemistry (ICC) demonstrating the presence of the proteins Nanog and Oct4 in the nucleus, and the surface epitopes recognized by SSEA3, Tra-1-60 and Tra-1-81 antibodies in the cytoplasm (Fig. 1E). Furthermore, the capability of KCi001-A to differentiate into cells of all three germ layers was carried out by spontaneous differentiation, initiated by embryoid body formation, followed by adherent culture for a total of 21 days. The iPSC line showed positive ICC staining for mesodermal (α-smooth muscle actin (SMA)), endodermal (α-fetoprotein (AFP)) and ectodermal markers (βIII-tubulin (βtub)) (Fig. 1F). All together these data show that we have successfully created a BBS1 iPSC line; KCi001-A (Table 1).

3. Materials and methods

3.1. Reprogramming

Fibroblasts, were grown in DMEM-F12 + GlutaMAX (Gibco), 10% foetal bovine serum (FBS), 1% penicillin-streptomycin (Gibco) in a 37 °C humidified 5%-CO_2 incubator. 5×10^5 cells were transfected with 1,25 ng of each of the three plasmids; hOct3/4, hSK, hUL (Addgene plasmids #27077, #27078, #27080) in Primary Mammalian Fibroblasts buffer (Lonza), using Amaxa Nucleofector™ 2b/program V-

Table 1
Characterization and validation.

Classification	Test	Result	Data
Morphology	Photography	Normal ES-like morphology	Not shown
Phenotype	Immunocytochemistry	Positive for cell surface markers; Oct4, Nanog, SSEA3, Tra-1-60, Tra-1-81	Fig. 1 panel E
	RT-qPCR (TaqMan probes; Applied Biosystems 7500 Fast system)	Positive for; OCT4, NANOG, SOX2, TDGF1, DNMT3B, GARB3 and GDF3	Fig. 1 panel D
Genotype	Karyotype (G-banding) and resolution	46,XX, resolution 450–500	Fig. 1 panel C
Identity	Microsatellite PCR (mPCR)	NA	NA
	STR analysis Elucigene QST*R PLUSv2	22 sites were tested. 100% identity match between parental fibroblasts and KCi001-A	submitted in archive with journal
Variant analysis	Sanger sequencing	GENE: *BBS1* Compound heterozygous Chr11: g.66293652 T > G, p.(Met390Arg)/g.66293618G > C, p.(Gly379Arg)	Fig. 1 panel A
	Southern Blot OR WGS	NA	NA
Microbiology and virology	Mycoplasma	Mycoplasma testing by RT-PCR (negative)	Supplementary File 1
Differentiation potential	Embryoid body formation	Presence of the proteins α-smooth muscle actin (SMA), α-fetoprotein (AFP) and βIII-tubulin (βtub) were used to confirm formation of the three germ layers.	Fig. 1 panel F
Donor screening	HIV 1 + 2 Hepatitis B, Hepatitis C	NA	NA
Genotype additional info	Blood group genotyping	NA	NA
	HLA tissue typing	NA	NA

024 and seeded on gelatine coated dishes (Sigma) in fibroblast medium without antibiotics for 24 h followed by culturing in standard fibroblast medium. On day 6 after transfection, iPSCs were seeded on ESC grade Matrigel (Corning) coated dishes, 50–80 × 10^3 cells/well, in mTeSR1 media (stem cell Technology) in an atmosphere of 5% CO_2, 5% O_2, 90% N_2 at 37 °C. From day 20 iPSC colonies were manually dissected. The iPSCs were split using 0,5 mM ultrapure EDTA (Gibco) at 70% confluency and frozen in mTeSR1 with 10% DMSO.

3.2. Karyotyping

Cells were treated with KaryoMAX colcemid for 45 min, dissociated and treated with hypotonic solution followed by fixation in freshly mixed 75% methanol: 25% acetic acid. Metaphase chromosomes were stained with Giemsa for cytogenic analysis.

3.3. Genomic DNA isolation, integration, genotyping and short tandem repeat (STR) analyses

DNA was purified using DNeasy Blood and Tissue kit (QIAGEN). Integration analysis was performed by Quantitative PCR using plasmid specific primers in the presence of SYBR green (Table 2). Data were analysed using the ΔΔCT method and the amounts were normalized to GAPDH. To confirm the identity of the cell-line, genotyping was performed with BBS1 specific primers and STR was performed using Elucigene QST*R PLUSv2.

3.4. Quantitative real time reverse transcriptase polymerase chain reaction (RT-qPCR)

RNA was harvested using RNeasy kit (QIAGEN), treated with DNase I (Invitrogen,) and cDNA synthesized using high capacity cDNA kit (Applied Biosystems). Taqman probes (Table 2) were used. Relative standard curves were used for data analysed and amounts normalized to GAPDH mRNA.

3.5. In vitro differentiation

The iPSC were treated with 0,5 mM ultrapure EDTA (Gibco) and plated in ultra-low adhesion plates (CORNING) in mTeSR1 media with ROCK inhibitor, to induce formation of embryoid bodies. On day two media was changed to DMEM-F12 + GlutaMAX (Gibco), 20% knock-out serum replacement (Gibco), 1 × non-essential amino acids (Sigma), 0,1 mM 2-mecaptoethanol (Sigma) and 1% pen/strep After one week of suspension culture the aggregates were transferred to adherent culture in DMEM F-12 with GlutaMAX, 10% FBS and 1% pen/strep media on

Table 2
Reagents details.

Antibodies used for immunocytochemistry

	Antibody	Dilution	Company Cat # and RRID
Pluripotency marker	Rabbit anti-NANOG	1:500	PeproTech Cat# 500-P236, RRID: AB_1268805
Pluripotency marker	Mouse anti-OCT3/4	1:200	Santa Cruz Biotechnology Cat# sc5279, RRID: AB_628051
Pluripotency marker	Rat anti SSEA3	1:200	BioLegend Cat# 330302, RRID: AB_1236554
Pluripotency marker	Mouse anti-TRA-1-60	1:200	BioLegend Cat# 330602, RRID: AB_1186144
Pluripotency marker	Mouse anti-TRA-1-81	1:200	BioLegend Cat# 330702, RRID: AB_1089240
Differentiation marker, Mesoderm	Mouse anti- α-smooth muscle actin (SMA)	1:500	Dako Cat# M0851, RRID: AB_2223500
Differentiation marker, Endoderm	Rabbit anti-α-fetoprotein (AFP)	1:500	Dako Cat# A0008, RRID: AB_2650473
Differentiation marker, Ectoderm	Mouse anti-βIII tubulin (βtub)	1:4000	Sigma-Aldrich Cat# T8660, RRID: AB_477590
Secondary antibody	Alexa Flour Goat Anti-Rabbit 488	1:800	Life Technologies Cat# A11008, RRID: AB_143165
Secondary antibody	Alexa Flour Donkey Anti-Mouse 546	1:800	Life Technologies Cat# A10036, RRID: AB_2534012
Secondary antibody	Alexa Flour Rabbit Anti-Rat 488	1:800	Molecular Probes Cat# A-21210, RRID: AB_2535796

Primers

	Target	Forward/Reverse primer (5′-3′)
Episomal Plasmids (qPCR)	OCT3/4 Plasmid	CATTCAAACTGAGGTAAGGG/TAGCGTAAAAGGAGCAACATAG
Endogenous (qPCR)	OCT3/4 Endogenous	CCCCAGGGCCCCATTTTGGTACC/ACCTCAGTTTGAATGCATGGGAGAGC
Episomal Plasmids (qPCR)	KLF4 Plasmid	CCACCTCGCCTTACACATGAAGA/TAGCGTAAAAGGAGCAACATAG
Endogenous (qPCR)	KLF4 Endogenous	ACCCATCCTTCCTGCCCGATCAGA/TTGGTAATGGAGCGGCGGGACTTG
Episomal Plasmids (qPCR)	SOX2 Plasmid	TTCACATGTCCCAGCACTACCAGA/TTTGTTTGACAGGAGCGACAAT
Endogenous (qPCR)	SOX2 Endogenous	TTCACATGTCCCAGCACTACCAGA/TCACATGTGTGAGAGGGGCAGTGTGC
Episomal Plasmids (qPCR)	L-MYC Plasmid	GGCTGAGAAGAGGATGGCTAC/TTTGTTTGACAGGAGCGACAAT
Endogenous (qPCR)	L-MYC Endogenous	GCGAACCCAAGACCCAGGCCTGCTCC/CAGGGGGTCTGCTCGCACCGTGATG
Episomal Plasmids (qPCR)	LIN28 Plasmid	AGCCATATGGTAGCCTCATGTCCGC/TAGCGTAAAAGGAGCAACATAG
Endogenous (qPCR)	LIN28 Endogenous	AGCCATATGGTAGCCTCATGTCCGC/TCAATTCTGTGCCTCCGGGAGCAGGGTAGG
House-Keeping Gene (qPCR)	GAPDH (1)	ACCACAGTCCATGCCATCAC/TCCACCACCCTGTTGCTGTA
BBS1 patogenic variants (Seq.)	BBS1 ex 12	GTGAGATTGGAGGGGAGATG/GGGATGCTGGGTGAACTAGA

Taqman probes

	Target	Assay ID
Pluripotency marker (RT-qPCR)	POU5F1/OCT4	Thermo Fisher Scientific Hs04260367_g1
Pluripotency marker (RT-qPCR)	NANOG	Thermo Fisher Scientific Hs04260366_g1
Pluripotency marker (RT-qPCR)	SOX2	Thermo Fisher Scientific Hs01053049_s1
Pluripotency marker (RT-qPCR)	TDGF1	Thermo Fisher Scientific Hs02339497_g1
Pluripotency marker (RT-qPCR)	DNMT3B	Thermo Fisher Scientific Hs00171876_m1
Pluripotency marker (RT-qPCR)	GARB3	Thermo Fisher Scientific Hs00241459_m1
Pluripotency marker (RT-qPCR)	GDF3	Thermo Fisher Scientific Hs00220998_m1
House-Keeping Gene (RT-qPCR)	GAPDH	Thermo Fisher Scientific Hs99999905_m1

gelatine (Sigma) coated coverslips. Morphological changes were observed and after two weeks of adherent culture the cells were fixed and investigated by immunocytochemistry.

3.6. Immunocytochemistry

Cells grown on gelatine or matrigel (for pluripotency) coated coverslips were fixed with 4% paraformaldehyde (Hounisen) for 15 min, and permeabilized with 0,2% TritonX-100 in PBS for 15 min. Slides were incubated in blocking buffer for 1 h (3% BSA, 0,2% TritonX-100 in PBS). Incubation with primary antibodies diluted in blocking buffer, was performed for 2 h at RT or overnight at 5 °C followed by incubation with secondary antibodies in blocking buffer (Table 2). Nuclei were stained using DAPI.

Acknowledgments

We thank Eva Pihl and Pia Skovgaard for technical support and Jette Bune Rasmussen for assistance with generating the figures. The study was supported by grants from Rigshospitalet (R76-A2852) and Velux foundation (VELUX32700).

Appendix A. Supplementary data

Supplementary data to this article can be found online at https://doi.org/10.1016/j.scr.2018.08.005.

References

Forsythe, E., Beales, P.L., 2012. Bardet-Biedl syndrome. Eur. J. Hum. Genet. 21, 8. https://doi.org/10.1038/ejhg.2012.115.

Hjortshøj, T.D., Grønskov, K., Philp, A.R., Nishimura, D.Y., Riise, R., Sheffield, V.C., Rosenberg, T., Brøndum-Nielsen, K., 2010. Bardet-Biedl syndrome in Denmark - report of 13 novel sequence variations in six genes. Hum. Mutat. 31 (4), 429–436. https://doi.org/10.1002/humu.21204.

Nager, A.R., Goldstein, J.S., Herranz-Pérez, V., Portran, D., Ye, F., Garcia-Verdugo, J.M., Nachury, M.V., 2017. An actin network dispatches ciliary GPCRs into extracellular vesicles to modulate signaling. Cell 168 (1), 252–263. http://www.sciencedirect.com/science/article/pii/S0092867416316087.

Research Paper II

Generation of induced pluripotent stem cells, KCi002-A derived from a patient with Bardet-Biedl syndrome homozygous for the *BBS10* variant c.271insT

Stem Cell Research 33 (2018) 46–50

Contents lists available at ScienceDirect

Stem Cell Research

journal homepage: www.elsevier.com/locate/scr

Lab resource: Stem Cell Line

Generation of induced pluripotent stem cells, KCi002-A derived from a patient with Bardet-Biedl syndrome homozygous for the BBS10 variant c.271insT

Caroline Amalie Brunbjerg Hey, Katarina Beata Saltõkowa, Lasse Jonsgaard Larsen, Zeynep Tümer, Karen Brøndum-Nielsen, Karen Grønskov, Tina Duelund Hjortshøj, Lisbeth Birk Møller*

Applied Human Molecular Genetics, Kennedy Center, Department of Clinical Genetics, Copenhagen University Hospital, Rigshospitalet, Gl. Landevej 7, 2600 Glostrup, Denmark

A B S T R A C T

Bardet-Biedl syndrome (BBS) is genetically heterogeneous with at least 21 genes involved, and *BBS10* encodes, together with *BBS6* and *BBS12*, chaperonin-like proteins which are important for the assembly of the multiprotein complex, the BBSome encoded by other BBS genes. Here we describe the successful generation of an induced pluripotent stem cell (iPSC) line *KCi002-A* from a male with BBS, homozygous for the disease causing variant c.271insT, p.(Cys91fsX95) in *BBS10*.

Resource table

Unique stem cell line identifier	KCi002-A
Alternative name(s) of stem cell line	BBS10 Clone1A
Institution	Rigshospitalet, Kennedy Center
Contact information of distributor	Lisbeth Birk Møller, Lisbeth.Birk.Moeller@regionh.dk
Type of cell line	induced pluripotent stem cell (iPSC)
Origin	Human
Additional origin info	Male, Caucasian
Cell source	Dermal fibroblasts
Clonality	Clonal
Method of reprogramming	Nucleofection with non-integrating episomal plasmids carrying *OCT3/4*, *SOX2*, *KLF4*, *L-MYC*, *LIN28* and *shP53*
Genetic modification	NA
Type of modification	NA
Associated disease	Autosomal recessive Bardet-Biedl syndrome
Gene/locus	*BBS10*, Chr 12: g.7674149insT, p.(Cys91fsX95), homozygous. Ref sequence: NM_024685.3
Method of modification	NA
Name of transgene or resistance	NA
Inducible/constitutive system	NA
Date archived/stock date	25-01-2018
Cell line repository/bank	NA
Ethical approval	The study was approved by the regional scientific ethical committee in the Capital Region of Denmark (H-3-2014-140). Written informed consent was obtained from the patients.

* Corresponding author.
E-mail address: Lisbeth.birk.moeller@regionh.dk (L.B. Møller).

https://doi.org/10.1016/j.scr.2018.09.013
Received 24 February 2018; Received in revised form 25 August 2018; Accepted 18 September 2018
Available online 20 September 2018

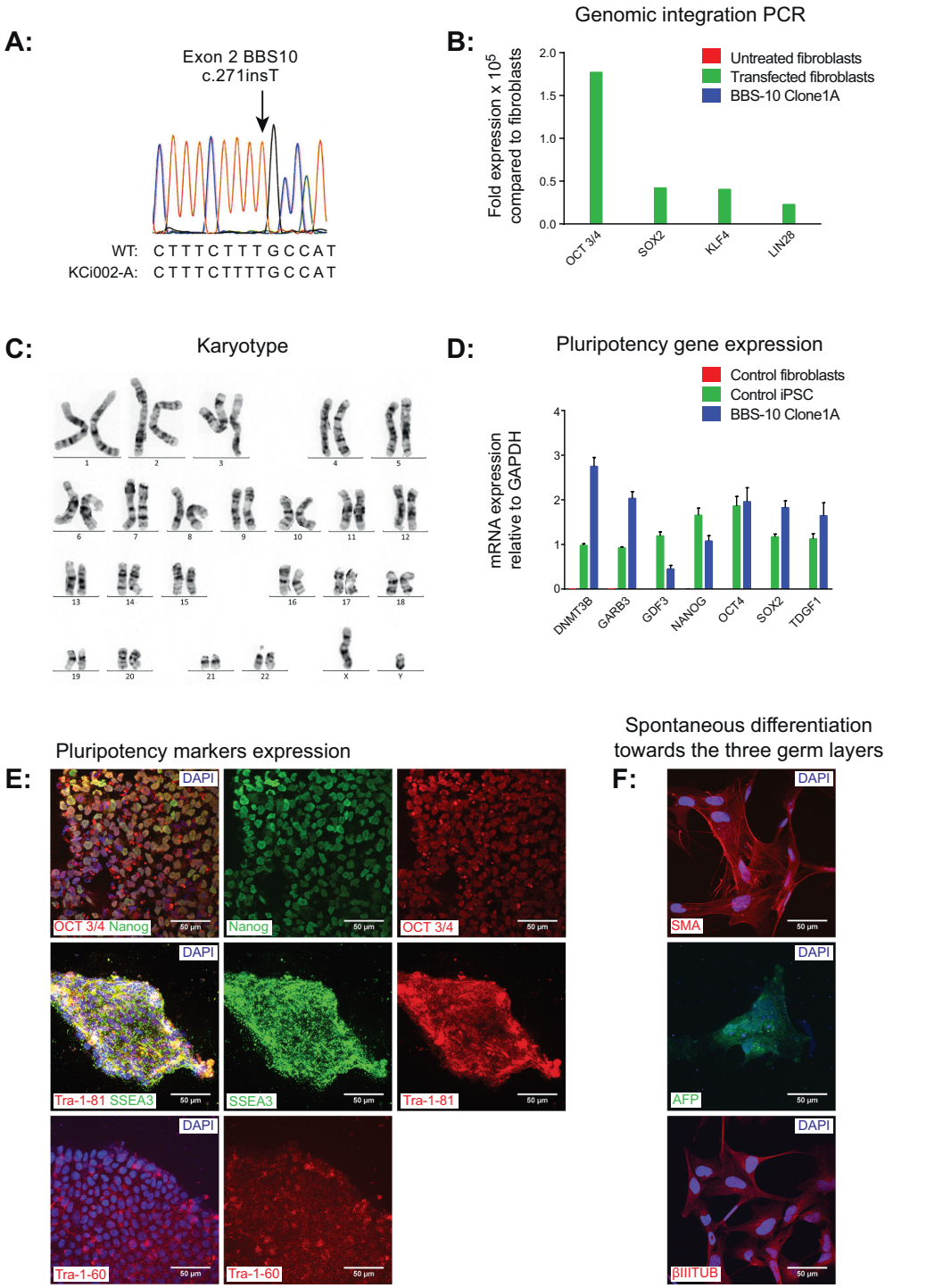

(caption on next page)

Fig. 1. Characterization of BBS10 Clone 1A line (KCi002-A). A. WT sequences and mutation in KCi002-A in the same regions of the BBS10 gene. B. Quantitative real time PCR showing absence of episomal plasmids in BBS10 Clone 1A (KCi002-A) and control fibroblasts and presence of plasmids in transfected fibroblasts. C. Karyotype of representative metaphase showing normal 46 chromosomes (XY). D. mRNA expression of pluripotency markers in control iPSC line and in BBS10 Clone 1A (KCi002-A). E. Confocal images showing immunodetection of pluripotency-associated markers in BBS10 Clone 10 (KCi002-A). F. Immunofluorescence analysis of *in vitro* differentiation of BBS10 Clone 1A (KCi002-A) EBs using specific antibodies against the mesodermal marker α-smooth muscle actin (SMA), endodermal marker α-fetoprotein (AFP) and the ectodermal marker βIII-tubulin (βtub). Nuclei were stained with DAPI. Scale bar 50 μM.

Resource utility

BBS is a ciliopathy and a chaperonopathy. *BBS10* encodes a chaperonin-like protein, which participates in the assembly of the BBSome. The generated iPSC line represents a useful source to investigate the effect of the chaperonin complex on the pathophysiology of BBS, including assembly of the BBSome, in different tissues.

Resource details

Bardet-Biedl syndrome (BBS) is a rare autosomal recessive disorder having an estimated prevalence in Denmark of 1/59.000 (Hjortshøj et al. 2010). BBS is a ciliopathy, defined as diseases caused by defects in ciliary structure and/or function. Today 21 different genes involved in BBS are known. Because three genes *BBS6*, *BBS10* and *BBS12* encode chaperonin-like proteins, BBS is now also considered to belong to the group of diseases termed chaperonopathies (Seo et al. 2010; Stoetzel et al. 2006). The chaperonin-like proteins form the chaperonin-complex which localize to the ciliary basal body and centrosomes. The complex is important for assembly of another BBS protein complex called the BBSome. It has been shown that disease causing variants in *BBS6*, *BBS10* and *BBS12* result in a malfunctioning BBSome (Zhang et al. 2012). To investigate the role of *BBS10* in ciliary function, an iPSC line from a patient homozygous for the pathogenic variant c.271insT, p.Cys91fsX95 in the *BBS10* gene was created.

Patient specific human dermal fibroblasts from a male homozygous for the variant c.271insT, p.(Cys91fsX95), in *BBS10*, were reprogrammed to iPSC by nucleofection of three episomal plasmids expressing the human genes *OCT3/4, SOX2, KLF4, L-MYC, LIN 28* and a short hairpin RNA against P53 (*shP53*). Sequencing of the generated iPSC line *KCi002-A,* confirmed the presence of the variant (Fig. 1A). Investigation for the episomal plasmids in genomic DNA from *KCi002-A* by quantitative PCR (Applied Biosystems 7500 Fast system), using plasmid specific primers for *OCT3/4*, *SOX-2*, *KLF4*, *LIN28* and *L-MYC* (Table 2), using SYBR green, confirmed that none of the three episomal plasmids were integrated into the genome (Fig. 1B). DNA from control fibroblast 72 h post transfection and DNA from un-transfected fibroblasts were used as a positive and negative control (Fig. 1B). Primers for the corresponding endogenous genes were included as controls (not shown). Investigation of the generated iPSC demonstrated a normal karyotype (46,XY) (Fig. 1C). Short tandem repeat (STR)-PCR profile analysis, where 22 different loci were analysed, showed 100% identity match between the parental fibroblast cell line and *KCi002-A* (submitted in archive with journal). The pluripotency status of *KCi002-A* was verified by RT-qPCR increased expression of *OCT4*, *NANOG*, *SOX2*, *TDGF1*, *DNMT3B*, *GARB3* and *GDF3* (Fig. 1D) using Taq-man probes (Table 2). The mRNA level of the different genes, were normalized to *GAPDH* mRNA. RNA from untreated fibroblasts and from a control iPSC line was included as a negative and positive control. These results were further underlined by immunochemical demonstration of Oct 3/4 and Nanog proteins in the nucleus, and presence of the pluripotency surface markers recognized by TRA-1-60, TRA-1-81 and SSEA3 antibodies in the cytoplasm (Fig. 1E). The differentiation potential of the generated iPSC line was investigated by spontaneous differentiation. Immunochemical examination after three weeks of differentiation demonstrated expression of the mesodermal marker, α-smooth-muscle actin (SMA), the endodermal marker, α-feto protein (AFP) and the ectodermal marker, β-III-tubulin (β-tub) (Fig. 1F). All together these data show that we have successfully created an iPSC line, *KCi002-A* (Table 1).

Materials and methods

Reprogramming

Fibroblast were cultivated in DMEM-F12 with GlutaMAX, 10% foetal bovine serum, 1% penicillin-streptomycin, (all from Gibco), in a 37 °C humidified 5%-CO_2 incubator. Amaxa Nucleofector™ 2b/program V-024 was used for the transfection in the Primary Mammalian Fibroblasts buffer (Lonza) with 1,25 ng of each of the reprogramming plasmids; hOct3/4, hSK, hUL (Addgene #27077, #27078, #27080) for 5×10^5 cells. Transfected cells were seeded on gelatine (Sigma) coated dishes without antibiotics for 24 h followed by cultivation using standard fibroblast conditions. Day 6 post transfection cells were transferred to Corning ESC grade Matrigel coated dishes in mTeSR1 medium (stem cell) in 5% CO_2, 5% O_2 and 90% N_2. The iPSC colonies were harvested from day 20. The iPSC were split using 0,5 mM ultrapure EDTA (Gibco) at around 70% confluency and cryopreserved in mTeSR1 supplemented with 10% DMSO.

Karyotyping

iPSC were incubated for 45 min with KaryoMAX colcemid, dissociated with 0,5 mM ultrapure EDTA (Gibco), treated with hypotonic solution, and then fixed with fresh 75% methanol and 25% acetic acid. The karyotyping was performed on metaphase chromosomes using Giemsa staining.

Genomic DNA isolation, Integration, Genotyping and Short tandem Repeat (STR) analyses

DNA was purified using DNeasy Blood and Tissue kit (QIAGEN). Integration analysis was performed by Quantitative PCR using plasmid specific primers in combination with SYBR green (Table 2). Data were analysed using the ΔΔCT method and the amounts were normalized to GAPDH. To confirm the identity of the cell-line, genotyping and STR analysis were performed using *BBS10* specific primers and Elucigene QST*R PLUSv2 respectively.

Quantitative real time reverse transcriptase polymerase chain reaction (RT-qPCR)

RNA purified by RNeasy kit (Qiagen) was DNase treated (DNase I,Invitrogen) followed by cDNA synthesis (High Capacity cDNA kit,Applied Biosystems). Taqman probes were used (Table 2). Data was analysed using relative standard curve method. Expression level was normalization to GAPDH.

In vitro differentiation

iPSC were dissociated to small aggregates using 0,5 mM ultrapure EDTA (Gibco) and seeded in ultra-low adhesion plates (CORNING) in mTeSR1 supplemented with ROCK inhibitor to induce embryoid body formation. Day two after seeding, media was changed to DMEM-F12 + GlutaMAX (Gibco) supplemented with 20% knock-out serum replacement (Gibco), 1 × non-essential amino acids (Sigma), 0,1 mM 2-

Table 1
Characterization and validation.

Classification	Test	Result	Data
Morphology	Photography	Normal	Not shown
Phenotype	Immunocytochemistry	Positive for Oct3/4, Nanog, SSEA3, Tra-1-60, Tra-1-81	Fig. 1 panel E
	RT-qPCR (TaqMan probes; Applied Biosystems 7500 Fast system)	Positive expression of OCT4, NANOG, SOX2, TDGF1, DNMT3B, GARB3 and GDF3	Fig. 1 panel D
Genotype	Karyotype (G-banding) and resolution	46,XY, resolution 450–500	Fig. 1 panel C
Identity	Microsatellite PCR (mPCR)	NA	NA
	STR analysis Elucigene QST*R PLUSv2	22 sites were tested. 100% identity match between parental fibroblasts and KCi002-A	Submitted in archive with journal
Variant analysis	Sanger sequencing	GENE: *BBS10* Homozygous Chr12: g.7674149insT, p.(Cys91fs*95)	Fig. 1 panel A
	Southern Blot OR WGS	NA	NA
Microbiology and virology	Mycoplasma	Mycoplasma testing by RT-PCR; Negative	Supplementary File 1
Differentiation potential	Embryoid body formation	Presence of α-smooth muscle actin (SMA), α-fetoprotein (AFP) and βIII-tubulin (βtub) were used to confirm formation of the three germ layers.	Fig. 1 panel F
Donor screening	HIV 1 + 2 Hepatitis B, Hepatitis C	NA	NA
Genotype additional info	Blood group genotyping	NA	NA
	HLA tissue typing	NA	NA

Table 2
Reagents details.

Antibodies used for immunocytochemistry

	Antibody	Dilution	Company Cat # and RRID
Pluripotency marker	Rabbit anti-NANOG	1:500	PeproTech Cat# 500-P236, RRID: AB_1268805
Pluripotency marker	Mouse anti-OCT3/4	1:200	Santa Cruz Biotechnology Cat# sc5279, RRID: AB_628051
Pluripotency marker	Rat anti SSEA3	1:200	BioLegend Cat# 330302, RRID: AB_1236554
Pluripotency marker	Mouse anti-TRA-1-60	1:200	BioLegend Cat# 330602, RRID: AB_1186144
Pluripotency marker	Mouse anti-TRA-1-81	1:200	BioLegend Cat# 330702, RRID: AB_1089240
Differentiation marker, Mesoderm	Mouse anti- α-smooth muscle actin (SMA)	1:500	Dako Cat# M0851, RRID: AB_2223500
Differentiation marker, Endoderm	Rabbit anti-α-fetoprotein (AFP)	1:500	Dako Cat# A0008, RRID: AB_2650473
Differentiation marker, Ectoderm	Mouse anti-βIII tubulin (βtub)	1:4000	Sigma-Aldrich Cat# T8660, RRID: AB_477590
Secondary antibody	Alexa Flour Goat Anti-Rabbit 488	1:800	Life Technologies Cat# A11008, RRID: AB_143165
Secondary antibody	Alexa Flour Donkey Anti-Mouse 546	1:800	Life Technologies Cat# A10036, RRID: AB_2534012
Secondary antibody	Alexa Flour Rabbit Anti-Rat 488	1:800	Molecular Probes Cat# A-21210, RRID: AB_2535796

Primers

	Target	Forward/Reverse primer (5′-3′)
Episomal Plasmids (qPCR)	OCT3/4 Plasmid (Pla)	CATTCAAACTGAGGTAAGGG/TAGCGTAAAAGGAGCAACATAG
Episomal Plasmids (qPCR)	OCT3/4 Endogenous (CDS)	CCCCAGGGCCCCATTTTGGTACC/ACCTCAGTTTGAATGCATGGGAGAGC
Episomal Plasmids (qPCR)	KLF4 Plasmid	CCACCTCGCCTTACACATGAAGA/TAGCGTAAAAGGAGCAACATAG
Episomal Plasmids (qPCR)	KLF4 Endogenous	ACCCATCCTTCCTGCCCGATCAGA/TTGGTAATGGAGCGGCGGGACTTG
Episomal Plasmids (qPCR)	SOX2 Plasmid	TTCACATGTCCCAGCACTACCAGA/TTTGTTTGACAGGAGCGACAAT
Episomal Plasmids (qPCR)	SOX2 Endogenous	TTCACATGTCCCAGCACTACCAGA/TCACATGTGTGAGAGGGGCAGTGTGC
Episomal Plasmids (qPCR)	L-MYC Plasmid	GGCTGAGAAGAGGATGGCTAC/TTTGTTTGACAGGAGCGACAAT
Episomal Plasmids (qPCR)	L-MYC Endogenous	GCGAACCCAAGACCCAGGCCTGCTCC/CAGGGGGTCTGCTCGCACCGTGATG
Episomal Plasmids (qPCR)	LIN28 Plasmid	AGCCATATGGTAGCCTCATGTCCGC/TAGCGTAAAAGGAGCAACATAG
Episomal Plasmids (qPCR)	LIN28 Endogenous	AGCCATATGGTAGCCTCATGTCCGC/TCAATTCTGTGCCTCCGGGAGCAGGGTAGG
House-Keeping Gene (qPCR)	GAPDH (1)	ACCACAGTCCATGCCATCAC/TCCACCACCCTGTTGCTGTA
Patient variant (Seq.)	*BBS10* ex 2	AGCCAGCCTTCTGAAAATGA/TTCTTCCCACTCTTCCACAAA

Taqman probes

	Target	Assay Id
Pluripotency marker (RT-qPCR)	POU5F1/OCT4	Thermo Fisher Scientific Hs04260367_g1
Pluripotency marker (RT-qPCR)	NANOG	Thermo Fisher Scientific Hs04260366_g1
Pluripotency marker (RT-qPCR)	SOX2	Thermo Fisher Scientific Hs01053049_s1
Pluripotency marker (RT-qPCR)	TDGF1	Thermo Fisher Scientific Hs02339497_g1
Pluripotency marker (RT-qPCR)	DNMT3B	Thermo Fisher Scientific Hs00171876_m1
Pluripotency marker (RT-qPCR)	GARB3	Thermo Fisher Scientific Hs00241459_m1
Pluripotency marker (RT-qPCR)	GDF3	Thermo Fisher Scientific Hs00220998_m1
House-Keeping Gene (RT-qPCR)	GAPDH	Thermo Fisher Scientific Hs99999905_m1

mecaptoethanol (Sigma) and 1% pen/strep (Gibco). After 1 week of suspension culture the aggregates were transferred to adherent culture in DMEM F-12 with GlutaMAX, 10% FBS and 1% pen/strep media on gelatine (Sigma,) coated coverslips. Changes in morphology were followed for two weeks, after which the cells were fixed and investigated by immunocytochemistry.

Immunocytochemistry

The iPSC grown on gelatine or matrigel (for pluripotency) coated coverslips were fixed using 4% paraformaldehyde (Hounisen) for 15 min, permeabilized using 0,2% TritonX-100 in PBS for 15 min. Followed by incubation in blocking buffer (3% BSA, 0,2% TritonX-100 in PBS) for 1 h. Incubation with primary antibodies was performed for 2 h, followed by incubation with secondary antibodies for 45 min, all diluted in blocking buffer at RT – Nuclei were visualized using DAPI. Antibodies are specified in Table 2.

Acknowledgments

We thank Eva Pihl, Pia Skovgaard and Pia Hougaard for technical support and Jette Bune Rasmussen for assistance with generating the figures. The study was supported by grants from Rigshospitalet (R76-A2852) and Velux foundation (VELUX32700).

Appendix A. Supplementary data

Supplementary data to this article can be found online at https://doi.org/10.1016/j.scr.2018.09.013.

References

Hjortshøj, T.D., Grønskov, K., Philp, A.R., Nishimura, D.Y., Riise, R., Sheffield, V.C., Rosenberg, T., Brøndum-Nielsen, K., 2010. Bardet-Biedl syndrome in Denmark, report of 13 novel sequence variations in six genes. Hum. Mutat. 31 (4), 429–436. https://doi.org/10.1002/humu.21204.

Seo, S., Baye, L.M., Schulz, N.P., Beck, J.S., Zhang, Q., Slusarski, D.C., Sheffield, V.C., 2010. BBS6, BBS10, and BBS12 form a complex with CCT/TRiC family chaperonins and mediate BBSome assembly. Proc. Natl. Acad. Sci. 107 (4), 1488–1493. https://doi.org/10.1073/pnas.0910268107.

Stoetzel, C., et al., 2006. BBS10 encodes a vertebrate-specific chaperonin-like protein and is a major BBS locus. Nat. Genet. 38, 521. https://doi.org/10.1038/ng1771.

Zhang, Q., Yu, D., Seo, S., Stone, E.M., Sheffield, V.C., 2012. Intrinsic protein-protein interaction-mediated and chaperonin-assisted sequential assembly of stable Bardet-Biedl syndrome protein complex, the BBSome. J. Biol. Chem. 287 (24), 20625–20635. https://doi.org/10.1074/jbc.M112.341487.

Research Paper III

Generation and characterization of three isogenic induced pluripotent stem cell lines from a patient with Bardet-Biedl syndrome homozygous for the *BBS5* variant; c.214G>A, p.(Gly72Ser).

Stem Cell Research 41 (2019) 101594

Contents lists available at ScienceDirect

Stem Cell Research

journal homepage: www.elsevier.com/locate/scr

Lab resource: Stem Cell Line

Generation and characterization of three isogenic induced pluripotent stem cell lines from a patient with Bardet-Biedl syndrome and homozygous for the *BBS5* variant

Caroline Amalie Brunbjerg Hey[a], Lasse Jonsgaard Larsen[a], Zeynep Tümer[a,b], Karen Brøndum-Nielsen[a], Karen Grønskov[a], Tina Duelund Hjortshøj[a], Lisbeth Birk Møller[a,*]

[a] Kennedy Center, Department of Clinical Genetics, Copenhagen University Hospital, Rigshospitalet, Gl. Landevej 7, 2600 Glostrup, Denmark
[b] Department of Clinical Medicine, Faculty of Health and Medical Sciences, University of Copenhagen, 2200N Copenhagen, Denmark

A B S T R A C T

Bardet-Biedl syndrome (BBS), an autosomal recessive disease, is associated with non-functional primary cilia. BBS5 is part of the protein complex termed the BBSome. The BBSome associates with intra flagellar transport (IFT) particles and mediates trafficking of membrane proteins in the cilium, a process important for cilia-mediated signal transduction. Here we describe the generation of three induced pluripotent stem cell (iPSC) lines, KCi003-A, KCi003-B and KCi003-C from a patient with BBS and homozygous for the disease causing variant c.214G > A, p.(Gly72Ser) in BBS5. The iPSC lines can be used for investigation of IFT in different cell types differentiated from the iPSC line.

Resource table

Unique stem cell lines identifier	KCi003-A KCi003-B KCi003-C
Alternative names of stem cell lines	BBS5 cl. 3A (KCi003-A) BBS5 cl. 4A (KCi003-B) BBS5 cl. 5A (KCi003-C)
Institution	Kennedy Center, Rigshospitalet
Contact information of distributor	Lisbeth Birk Møller, Lisbeth.Birk.Moeller@regionh.dk
Type of cell lines	iPSC
Origin	Human
Cell Source	Dermal fibroblasts (KC-85)
Clonality	Clonal
Method of reprogramming	Nucleofection with non-integrating episomal plasmids carrying *OCT3/4, SOX2, KLF4, L-MYC, LIN28* and *shP53*
Multiline rationale	Isogenic clones
Genetic Modification	NA
Type of Modification	NA
Associated disease	Autosomal recessive Bardet-Biedl syndrome
Gene/locus	*BBS5*, Chr2: g.170344321G > A, p.(Gly72Ser), homozygous Ref sequence: NM_152384.2
Method of modification	NA
Name of transgene or resistance	NA
Inducible/constitutive system	NA
Date archived/stock date	01–03–2019
Cell line repository/bank	NA
Ethical approval	The study was approved by the regional scientific ethical committee in the Capital Region of Denmark (H-3-2014-140). Written informed consent was obtained from the patients.

1. Resource utility

To gain further insight into the complicated mechanisms of the ciliopathy disorder, Bardet-Biedl syndrome (BBS), and the implications of variants discovered in the proteins of the BBSome complex, induced pluripotent stem cells (iPSC) were generated from a patient homozygous for the *BBS5* variant: c.214G > A, p.(Gly72Ser).

2. Resource details

BBS is a autosomal recessive disorder with an estimated incidence between 1:13,500 and 1:160,000 depending on the geographic location (Forsythe and Beales, 2013; Hjortshøj et al., 2010). BBS5 is part of the protein complex termed the BBSome. The BBSome associates with intra flagellar transport (IFT) particles and mediates trafficking of membrane proteins in the cilium, a process important for primary cilia-mediated movement and signal transduction (Mourão et al., 2016; Nachury et al.,

* Corresponding author.
E-mail address: Lisbeth.Birk.Moeller@regionh.dk (L.B. Møller).

https://doi.org/10.1016/j.scr.2019.101594
Received 22 July 2019; Received in revised form 15 September 2019; Accepted 19 September 2019
Available online 04 November 2019

2007). The primary cilium, a membrane protrusion present on most quiescent cells. The cilium is important for coordinating certain cellular processes. Due to non-functional cilia in BBS patients, the patients are characterized by systemic manifestations including obesity, renal cysts, polydactyly, retinal dystrophy, learning difficulties and hypogonadism.

A fibroblasts culture were established from a skin biopsy obtained from a patient with Bardet-Biedl syndrome homozygous for the *BBS5* variant: c.214G > A, p.(Gly72Ser). Low-passage fibroblasts were reprogramed into iPSC using episomal plasmids coding for the human genes *OCT3/4, SOX2, KLF4,* L-*MYC, LIN28* and a short hairpin RNA targeting p53, resulting in generation of three iPSC lines KCi003-A, KCi003-B and KCi003-C (Table 1). Sanger sequencing showed presence of the variant *BBS5*: c.214G > A, p.(Gly72Ser) in all three generated iPSC lines (Fig. 1A and Supl. Fig. 1A and B) and STR analysis comparing 22 sites between the original fibroblast culture, KCi003-A, KCi003-B and KCi003-C gave 100% identity match confirming the origin of KCi003-A, KCi003-B and KCi003-C (Table 2, supplementary file). The karyotype was confirmed to be normal (46,XY) in all three iPSC lines (Fig. 1B). Expression of pluripotency-related genes *OCT* 3/*4, NANOG, SOX2* and *TRA*-1–60 was investigated using immunofluorescence microscopy. Nuclear localization of OCT3/4, NANOG and SOX2 was confirmed and TRA-1–60 was visible in the membrane of the investigated colonies of KCi003-A, KCi003-B and KCi003-C (Fig. 1C). Expression level of seven pluripotency-associated genes was investigated by real-time quantitative RT-PCR (qRT-PCR) using taqman probes and primers (Table 3). Similar levels of expression were obtained for KCi003-A, KCi003-B, KCi003-C and a control iPSC line (Fig. 1D), whereas fibroblasts had zero expression of the tested genes (not shown). The absence of genomic integrated plasmids was validated by quantitative PCR (q-PCR) using genomic DNA from KCi003-A, KCi003-B and KCi003-C together with SYBR green and primers specific for the reprogramming plasmids (Pla). DNA from fibroblasts 72 h post transfection was used as a positive control. Quantitative PCR using primers specific for the coding sequence (CDS) of *OCT, SOX2, KLF4* and *LIN28* (Table 3) confirmed the presence of the endogenous genes in the three iPSC clones and the control IPSC. As these primers detect both endogenous and plasmid-derived genes (Okita et al., 2011) the highest signal was obtained in DNA from fibroblasts, 72 h post transfection (Fig. 1E). The ability to form cells of all three germ layers was tested by embryoid body formation followed by adherent culture and immunofluorescence analysis of smooth muscle actin (SMA), α-fetoprotein (AFP) and βIII-tubulin (βtub). KCi003-A, KCi003-B and KCi003-C show clear expression of SMA, AFP and βtub, confirming the ability to differentiate into cells of all three germ layers (Fig. 1F). Altogether these results confirm the origin and pluripotent state of KCi003-A, KCi003-B and KCi003-C.

3. Materials and methods

3.1. Cell culture and reprogramming

Fibroblast cells were maintained at 37 °C and 5%-CO_2 in DMEM-F12 + GlutaMAX with 10% foetal bovine serum and 1% penicillin-streptomycin (all Gibco). Addgene episomal plasmids #27077, #27078, #27080 (1.25 ng of each for 5×10^5 cells) were transfected into low passage cells using Primary Mammalian Fibroblasts buffer (Lonza) and program V-024 on Amaxa Nucleofector™ 2b. Cells were seeded on gelatine coated dishes post transfection, in culture medium without antibiotics for the first 24 h. Cells were transferred to ESC grade Matrigel (Corning) 6-well coated dishes on day 6 post transfection ($50–80 \times 10^3$ cells per 6-well) and cultured in mTeSR1 (Stemcell Technologies) with a gas composition of 5% CO_2, 5% O_2, 90% N_2 at 37 °C. Gentle cell Dissociation Reagent (Stemcell Technologies) was used for passaging and cells were frozen in mTeSR1 supplemented with 10% DMSO (Sigma-Aldrich).

3.2. DNA isolation and analyses

To purify DNA, the kit DNeasy Blood and Tissue kit (QIAGEN) was used. DNA was used for plasmid integration analysis, genotyping and Short tandem Repeat (STR) analysis. Primers used for integration, genotyping and STR analysis are listed in Table 3. SYBR green reagents were used for integration analysis and the ΔΔCT method applied with amounts normalized to GAPDH. STR analysis was carried out using Elucigene QST*R PLUSv2.

3.3. Karyotyping

Cells (passage 10 or higher) were treated with KaryoMAX colcemid for 45 min, dissociated, treated with hypotonic solution and fixed in fresh 75% methanol and 25% acetic acid. Two metaphase chromosomes stained with Giemsa were investigated per clone.

3.4. Gene expression analysis

RNA was harvested using the RNeasy kit (QIAGEN). RNA was DNase treated with DNase I (Invitrogen) before cDNA synthesis with high capacity cDNA kit (Applied Biosystems). Taqman probes are listed in Table 3. Data was analysed using the ΔΔCT method. Amounts were normalized to GAPDH and a control iPSC.

Table 1
Summary of lines.

iPSC line names	Abbreviation in figures	Gender	Age	Ethnicity	Genotype of locus	Disease
KCi003-A	KCi003-A	Male	39	Somali	*BBS5,* Chr2: g.170344321G > A, p.(Gly72Ser)	Bardet-Biedl syndrome
KCi003-B	KCi003-B	Male	39	Somali	*BBS5,* Chr2: g.170344321G > A, p.(Gly72Ser)	Bardet-Biedl syndrome
KCi003-C	KCi003-C	Male	39	Somali	*BBS5,* Chr2: g.170344321G > A, p.(Gly72Ser)	Bardet-Biedl syndrome

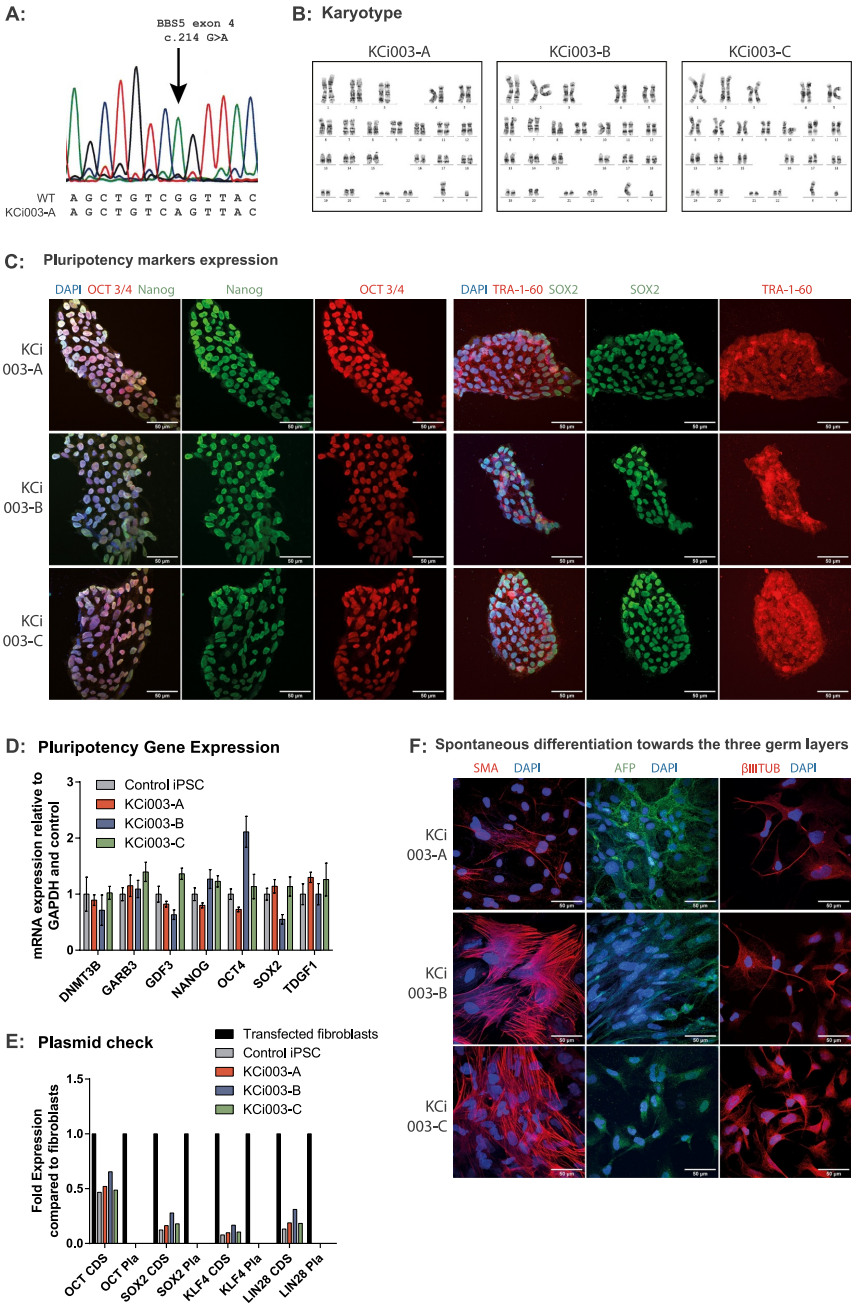

Fig. 1. Characterization and validation of three BBS5 iPSC lines.

Table 2
Characterization and validation.

Classification	Test	Result	Data
Morphology	Photography	Normal ES-like morphology	Not shown
Phenotype	Immunocytochemistry	Positive for cell surface markers; OCT4, NANOG, SOX2, TRA-1-60	Fig. 1 panel C
	Quantitative Real-Time PCT (TaqMan probes; Applied Biosystems 7500 Fast system)	Positive for; OCT4, NANOG, SOX2, TDGF1, DNMT3B, GARB3 and GDF3	Fig. 1 panel D
Genotype	Karyotype (G-banding) and resolution	46,XY, Resolution 450–500	Fig. 1 panel B
Identity	DNA Profiling STR analysis	DNA Profiling not performed	NA
		22 sites were tested. 100% identity match between parental fibroblasts and KCi003-A, KCi00-B and KCi003-C.	Submitted in archive with journal
Variant analysis	Sanger sequencing	*BBS5*: c.214G > A, p.(Gly72Ser) homozygous	Fig. 1 panel A and Supplementary Fig. 1A and B
	Southern Blot OR WGS	NA	NA
Microbiology and virology	Mycoplasma	Mycoplasma testing by RT-PCR (negative)	Supplementary Files 1, 2 and 3
Differentiation potential	Embryoid body formation followed by spontaneous differentiation		
	Presence of the proteins α-smooth muscle actin (SMA), α-fetoprotein (AFP) and βIII-tubulin (βtub) were used to confirm formation of the three germ layers.	Fig. 1 panel F	
Donor screening	HIV 1 + 2 Hepatitis B, Hepatitis C	NA	NA
Genotype additional info	Blood group genotyping	NA	NA
	HLA tissue typing	NA	NA

3.5. In vitro spontaneous differentiation

Spontaneous differentiation was initiated by embryoid body formation in suspension culture for one week followed by adherent culture for two weeks. The first day of suspension culture, cell aggregates were performed in mTeSR1 with ROCK inhibitor. The following 6 days the cells were cultured in differentiation medium (DMEM-F12 + GlutaMAX (Gibco), 20% knock-out serum replacement (Gibco), 1x non-essential amino acids (Sigma), 0,1 mM 2-mecaptoethanol (Sigma) and 1% penicillin-streptomycin (Gibco). For adherent culture, the cell aggregates were cultured in fibroblast medium on gelatine (Sigma) coated dishes. Morphology was observed, and at the end of the protocol cells were analysed using immunocytochemistry (see below).

3.6. Immunocytochemistry

To fixate the cells, incubation with 4% paraformaldehyde (Hounisen) at RT for 15 min was carried out. Then, the cells were incubated with 0,2% TritonX-100 in PBS for 15 min to permeabilize the cells. The cells were treated with blocking buffer consisting of 3% BSA (Tocris) and 0,2% TritonX-100 (Sigma) in PBS for one hour. Primary antibody incubation was carried out for two hours at RT or 5 °C overnight. Secondary antibody incubation was 45 min at RT. DAPI diluted in PBS was used to visualize nuclei. All used antibodies were diluted in blocking buffer and antibody details are found in Table 3.

Table 3
Reagents details.

Antibodies used for immunocytochemistry

	Antibody	Dilution	Company Cat # and RRID
Pluripotency Marker	Rabbit anti-NANOG	1:500	PeproTech Cat# 500-P236, RRID: AB_1268805
Pluripotency Marker	Mouse anti-OCT3/4	1:200	Santa Cruz Biotechnology Cat# sc5279, RRID: AB_628051
Pluripotency Marker	Rabbit anti-SOX2	1:200	ThermoFisher Cat# PA1-094, RRID: AB_ 2539862
Pluripotency Marker	Mouse anti–TRA–1–60	1:200	BioLegend Cat# 330,602, RRID: AB_1186144
Differentiation Marker, Mesoderm	Mouse anti- α-smooth muscle actin (SMA)	1:500	Dako Cat# M0851, RRID: AB_2223500
Differentiation Marker, Endoderm	Rabbit anti-α-fetoprotein (AFP)	1:500	Dako Cat# A0008, RRID: AB_2650473
Differentiation Marker, Ectoderm	Mouse anti-βIII tubulin (βtub)	1:4000	Sigma-Aldrich Cat# T8660, RRID: AB_477590
Secondary antibody	Alexa Flour Goat Anti-Rabbit 488	1:800	Life Technologies Cat# A11008 RRID: AB_143165
Secondary antibody	Alexa Flour Donkey Anti-Mouse 546	1:800	Life Technologies Cat# A10036 RRID: AB_2534012
Secondary antibody	Alexa Flour Rabbit Anti-Rat 488	1:800	Molecular Probes Cat# A-21210 RRID: AB_2535796

Primers

	Target	Forward/Reverse primer (5′ – 3′)
Episomal Plasmids (qPCR)	OCT3/4 Plasmid	CATTCAAACTGAGGTAAGGG/ TAGCGTAAAAGGAGCAACATAG
Endogenous (qPCR)	OCT3/4 Endogenous (CDS)	CCCCAGGGCCCCATTTTGGTACC/ ACCTCAGTTTGAATGCATGGGAGAGC
Episomal Plasmids (qPCR)	KLF4 Plasmid	CCACCTCGCCTTACACATGAAGA/ TAGCGTAAAAGGAGCAACATAG
Endogenous (qPCR)	KLF4 Endogenous (CDS)	ACCCATCCTTCCTGCCCGATCAGA/ TTGGTAATGGAGCGGCGGGACTTG
Episomal Plasmids (qPCR)	SOX2 Plasmid	TTCACATGTCCCAGCACTACCAGA/ TTTGTTTGACAGGAGCGACAAT
Endogenous (qPCR)	SOX2 Endogenous (CDS)	TTCACATGTCCCAGCACTACCAGA/ TCACATGTGTGAGAGGGGCAGTGTGC
Episomal Plasmids (qPCR)	L-MYC Plasmid	GGCTGAGAAGAGGATGGCTAC/ TTTGTTTGACAGGAGCGACAAT
Endogenous (qPCR)	L-MYC Endogenous (CDS)	GCGAACCCAAGACCCAGGCCTGCTCC/ CAGGGGGTCTGCTCGCACCGTGATG
Episomal Plasmids (qPCR)	LIN28 Plasmid	AGCCATATGGTAGCCTCATGTCCGC/ TAGCGTAAAAGGAGCAACATAG
Endogenous (qPCR)	LIN28 Endogenous (CDS)	AGCCATATGGTAGCCTCATGTCCGC/ TCAATTCTGTGCCTCCGGGAGCAGGGTAGG
House-Keeping Gene (qPCR)	GAPDH (1)	ACCACAGTCCATGCCATCAC/ TCCACCACCCTGTTGCTGTA
BBS5 pathogenic variants (Sanger Seq.)	BBS5 ex 4	ACCCACTGCTTACTGGCTTATCAGGAGACAGAATTGACCCTCT/ GAGGGGCAAACAACAGATGGCGCTTCAGTTTGGCCTCGTAA

Taqman probes

	Target	Assay ID
Pluripotency marker (qRT-PCR)	POU5F1/OCT4	Thermo Fisher Scientific Hs04260367_g1
Pluripotency marker (qRT-PCR)	NANOG	Thermo Fisher Scientific Hs04260366_g1
Pluripotency marker (qRT-PCR)	SOX2	Thermo Fisher Scientific Hs01053049_s1
Pluripotency marker (qRT-PCR)	TDGF1	Thermo Fisher Scientific Hs02339497_g1
Pluripotency marker (qRT-PCR)	DNMT3B	Thermo Fisher Scientific Hs00171876_m1
Pluripotency marker (qRT-PCR)	GARB3	Thermo Fisher Scientific Hs00241459_m1
Pluripotency marker (qRT-PCR)	GDF3	Thermo Fisher Scientific Hs00220998_m1
House-Keeping Gene (qRT-PCR)	GAPDH	Thermo Fisher Scientific Hs99999905_m1

Declaration of Competing Interest

The authors declare that there is no conflict of interest regarding the publication of this article

Acknowledgments

We thank Eva Pihl, Pia Hougaard and Pia Skovgaard for technical support and Jette Bune Rasmussen for assistance with generating the figures. The study was supported by grants from Rigshospitalet (R76-A2852) and Velux foundation (VELUX32700).

Supplementary materials

Supplementary material associated with this article can be found, in the online version, at doi:10.1016/j.scr.2019.101594.

References

Forsythe, E., Beales, P.L., 2013. Bardet–Biedl syndrome. Eur. J. Hum. Genet. 21, 8–13. https://doi.org/10.1038/ejhg.2012.115.

Hjortshøj, T.D., Grønskov, K., Philp, A.R., Nishimura, D.Y., Riise, R., Sheffield, V.C., Rosenberg, T., Brøndum-Nielsen, K., 2010. Bardet-Biedl syndrome in Denmark-report of 13 novel sequence variations in six genes. Hum. Mutat. 31, 429–436. https://doi.org/10.1002/humu.21204.

Mourão, A., Christensen, S.T., Lorentzen, E., 2016. The intraflagellar transport machinery in ciliary signaling. Curr. Opin. Struct. Biol. 41, 98–108. https://doi.org/10.1016/j.sbi.2016.06.009.

Nachury, M.V., Loktev, A.V., Zhang, Q., Westlake, C.J., Peränen, J., Merdes, A., Slusarski, D.C., Scheller, R.H., Bazan, J.F., Sheffield, V.C., Jackson, P.K., 2007. A core complex of BBS proteins cooperates with the GTPase Rab8 to promote ciliary membrane biogenesis. Cell 129, 1201–1213. https://doi.org/10.1016/j.cell.2007.03.053.

Okita, K., Matsumura, Y., Sato, Y., Okada, A., Morizane, A., Okamoto, S., Hong, H., Nakagawa, M., Tanabe, K., Tezuka, K., Shibata, T., Kunisada, T., Takahashi, M., Takahashi, J., Saji, H., Yamanaka, S., 2011. A more efficient method to generate integration-free human iPS cells. Nat. Methods 8, 409–412. https://doi.org/10.1038/nmeth.1591.

Manuscript I

A Missense Mutation in *RAB28* in a Family with Cone-Rod Dystrophy and Postaxial Polydactyly Prevents Localization of *RAB28* to the Primary Cilium

Genetics

A Missense Mutation in *RAB28* in a Family with Cone-Rod Dystrophy and Postaxial Polydactyly Prevents Localization of *RAB28* to the Primary Cilium

Cathrine Jespersgaard,[1] Amalie Brunbjerg Hey,[1] Tomas Ilginis,[2] Tina Duelund Hjortshøj,[1] Mingyan Fang,[3] Mette Bertelsen,[1] Niels Bech,[2] Hanne Jensen,[2] Lasse Jonsgaard Larsen,[1] Zeynep Tümer,[1,4] Thomas Rosenberg,[2] Karen Brøndum-Nielsen,[1] Lisbeth Birk Møller,[1] and Karen Grønskov[1]

[1]Department of Clinical Genetics, Kennedy Center, Rigshospitalet, University of Copenhagen, Glostrup, Denmark
[2]Department of Ophthalmology, Rigshospitalet-Glostrup, University of Copenhagen, Glostrup, Denmark
[3]BGI Group, Shenzhen, China
[4]Department of Clinical Medicine, Faculty of Health and Medical Sciences, University of Copenhagen, Copenhagen, Denmark

Correspondence: Karen Grønskov, Department of Clinical Genetics, Kennedy Center, Rigshospitalet, University of Copenhagen, Gl. Landevej 7, DK-2600 Glostrup, Denmark; karen.groenskov@regionh.dk.

CJ and ABH contributed equally to the work presented here and should therefore be regarded as equivalent authors.

Received: July 20, 2019
Accepted: December 2, 2019
Published: February 21, 2020

Citation: Jespersgaard C, Hey AB, Ilginis T, et al. A missense mutation in *RAB28* in a family with cone-rod dystrophy and postaxial polydactyly prevents localization of *RAB28* to the primary cilium. *Invest Ophthalmol Vis Sci.* 2020;61(2):29. https://doi.org/10.1167/iovs.61.2.29

Purpose. Cone-rod dystrophy (CRD) is a rare hereditary eye disorder that causes progressive degeneration of cone and rod photoreceptors. More than 30 genes, including *RAB28*, have been associated with CRD; however, only a few *RAB28* variants have been reported to be associated with CRD. In this study, we describe two brothers with CRD and a homozygous missense variant, c.55G>A (p.Gly19Arg), in *RAB28*.

Methods. The missense variant was identified as part of a study investigating underlying genetic defects in a large patient cohort (n = 667) using targeted next-generation sequencing of 125 genes associated with retinal dystrophy. Cellular localization of *RAB28* and ciliogenesis in patient fibroblasts were investigated by immunofluorescence microscopy. The effect of the missense variant on *RAB28* expression level was investigated by quantitative real-time PCR.

Results. Two brothers of a consanguineous couple presented with CRD, postaxial polydactyly (PAP), and myopia. Both brothers had a homozygous missense *RAB28* variant located in the G1 box of the guanosine triphosphate/guanosine diphosphate binding domain of *RAB28*. This missense variant caused a considerable reduction of *RAB28* localized to the cilia, whereas ciliogenesis seemed unaffected.

Conclusions. The missense variant in *RAB28* is classified as likely pathogenic with functional effect on protein localization. The combination of retinal dystrophy and PAP are well known from ciliopathies; however, more data are needed to finally conclude that the *RAB28* variant described here is the cause of PAP in these brothers.

Keywords: cone-rod dystrophy, *RAB28*, primary clilium, localization, molecular genetics

Inherited retinal diseases (IRDs) are a major cause of visual impairment and affect approximately 1 in 3500.[1] It is a clinically and genetically heterogeneous group of disorders with around 200 associated genes. A common feature is the malfunction of the photoreceptors in the retina. In some cases the cones are predominantly affected; in others, the rods. Both stationary and progressive forms exist, and clinical symptoms and age of onset may vary from severe congenital visual impairment to onset of symptoms in adulthood. IRDs can be isolated or part of a systemic disorder. All modes of Mendelian inheritance as well as mitochondrial inheritance have been observed. Rare cases of digenic inheritance have also been reported.[2]

Genes associated with IRDs are expressed either in the photoreceptors (rods or cones, or both) or in the supporting retinal pigment epithelium (RPE) cells. The most frequent form of IRD is retinitis pigmentosa (RP), presenting with night blindness and peripheral concentric visual field loss, caused by progressive degeneration of the rod photoreceptors and subsequent degeneration of the cones leading to blindness. Cone-rod dystrophy (CRD) is characterized by an initial loss of cones and symptoms of central vision loss, photophobia, progressive visual field loss, and color vision deficiency. In later stages, the rods also degenerate, typically leading to night blindness. Clinical distinction between RP and CRD can be difficult, especially in the late stages. Several

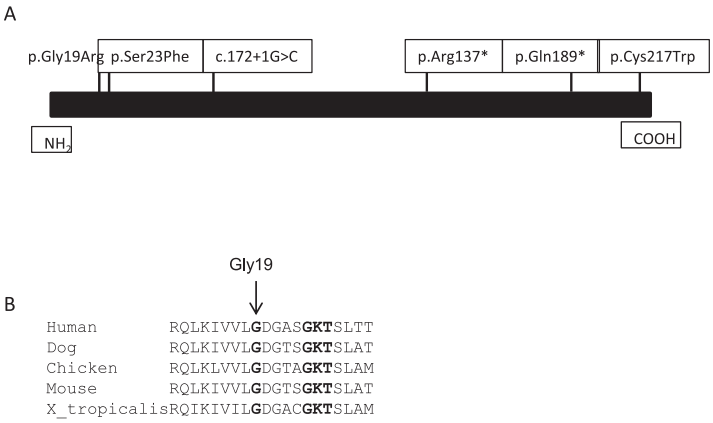

Figure 1. (A) Localization of sequence variants in RAB28 thought to cause CRD. (B) Gly19 is a conserved amino acid through evolution, as are surrounding amino acids.

treatment strategies for IRDs are under development; among these, gene therapy has given promising results.

RAB28 (MIM 612994) belongs to the RAB subfamily of the RAS oncogene family of Ras-related small GTPases. RAB GTPases function as molecular switches to control vesicle transport, vesicle budding, and membrane fission, and they regulate vesicle trafficking between organelles. In *Caenorhabditis elegans* (*C. elegans*), *rab-28* has been linked to an intraflagellar transport (IFT) cargo through the Bardet–Biedl syndrome (BBS) cargo-adaptor protein complex (BBSome).[3]

RAB28 localizes to 4p15.33 and has two pseudogenes, located on chromosome 9 and X chromosome, respectively. The gene consists of nine exons, and alternative splicing gives rise to three isoforms differing in C-terminus.[4] Two of the isoforms contain a C-terminal CAAX farnesylation motif.[4,5] *RAB28* tissue expression patterns differ among the isoforms, but they are all expressed in the retina.[6] In *C. elegans*, *rab-28* is expressed only in ciliated sensory neurons.[3] In 2013, sequence changes in *RAB28* were identified for the first time as the genetic cause of CORD18.[6] To date, only five *RAB28* variants are reported in the Human Gene Mutation Database (Fig. 1A).[7]

We report a family with two affected brothers of a consanguineous couple with a homozygous sequence variant, c.55G>A (p.Gly19Arg), located in the conserved guanosine triphosphate (GTP)/guanosine diphosphate (GDP) binding domain of *RAB28* (Fig. 1B). Previously reported *RAB28* variants have been associated with isolated CRD. Whether the postaxial polydactyly (PAP) observed in the affected brothers is also caused by the *RAB28* variant requires more investigation. We provide a thorough ophthalmological description of the affected brothers as well as retrospective data from their medical history.

Methods

The project was performed according to the Declaration of Helsinki and approved by the Regional Ethics Committee. Written informed consent was obtained before the molecular genetic testing.

Clinical Examinations

Retrospective data from the 1970s from the National Eye Clinic for the Visually Impaired in Copenhagen, Denmark (NEC) archive were reviewed. Both brothers (IV-1 and IV-3) were re-examined in 2018 by spectral domain optical coherence tomography (OCT) and by ultra-wide-field pseudocolor and autofluorescence fundus imaging (Optos, Dunfermline, UK). International Society for Clinical Electrophysiology of Vision standard electroretinography (ERG) and Goldmann (III4e) kinetic visual fields were performed on the younger sibling (IV-3) with better preserved visual function. The brothers, IV-1 and IV-3, informed us of other clinical issues in this family.

Molecular Genetic Analysis

Genomic DNA was extracted from peripheral blood using standard protocols. Targeted next-generation sequencing was performed as described previously.[8] Briefly, 125 genes, including *RAB28*, were sequenced using the custom NimbleGen SeqCap Target Enrichment KIT (NimbleGen, Madison, WI, USA) with capture and enrichment of all coding exons, 5′ and 3′ untranslated regions, and 20-bp flanking intronic regions. The enriched DNA libraries were sequenced using the Illumina HiSeq 2000 platform (Illumina, Inc., San Diego, CA, USA). Interpretation and classification of variants was performed according to the American College of Medical Genetics and Genomics (ACMG) guidelines.[9] In silico analysis of missense variants was performed using Align GVGD,[10,11] SIFT,[12] MutationTaster,[13] PolyPhen-2,[14] and CADD software.[15]

Cell Studies

Fibroblasts from the patients and one control were obtained by skin biopsy. The cells were cultured in Dulbecco's modified Eagle's medium (DMEM)/F-12 + Gibco GlutaMAX(#31331-028; Thermo Fisher Scientific, Waltham, MA, USA) supplemented with Gibco 10% fetal bovine serum (FBS) (#10270-106) and Gibco 1% penicillin/streptomycin

(p/s) (#15140-122). Two different cultures from each patient were established. Cilia were induced by culturing the cells in reduced-serum medium containing 0.5% FBS and 1% p/s for 48 hours unless otherwise specified.

Treatment with siRNA against *RAB28* (#SI03024686 and #SI00061705; Qiagen, Hilden, Germany) and with AllStars Negative Control scramble siRNA (#SI03650318; Qiagen) was performed using the DharmaFECTsystem (#T-2001-03; Dharmacon, Lafayette, CO, USA). Twenty-four hours after siRNA transfection, the cells were cultured in reduced-serum medium for 48 hours followed by fixation for immunofluorescence microscopy, or they were used for RNA extraction. For immunofluorescence microscopy, the cells were grown on glass slides.

Total RNA was extracted using the GeneJET RNA Purification Kit (#K0732; Thermo Fisher Scientific), and cDNA was synthesized using the High Capacity cDNA Reverse Transcription Kit (#4368814; Applied Biosystems, Foster City, CA, USA). Real-time quantitative PCR (qRT-PCR) was performed using TaqMan probes against *RAB28* (#Hs01017480_m1; Applied Biosystems) and *GAPDH* (#Hs99999905_m1; Applied Biosystems). The 7500 Fast Real-Time PCR System (Applied Biosystems) was used for qRT-PCR amplification, and the relative standard curve method was used for calculation. *RAB28* mRNA expression levels were normalized to *GAPDH* mRNA.

For immunofluorescence microscopy, the cells were fixed using 4% paraformaldehyde (1000.1000; Hounisen, Skanderborg, Denmark) for 15 minutes at room temperature, permeabilized using 0.2% TritonX-100 (Sigma Aldrich, St. Louis, MO, USA) in PBS for 15 minutes and blocked for 30 minutes in 3% bovine serum albumin. The fixed cells were incubated with the primary antibodies against RAB28 (#PA5-68303; Thermo Fisher Scientific) diluted 1:1000 and Arl13B (#ab136648; Abcam, Cambridge, UK) or anti-acetylated alfa-tubulin antibody (Ac-TUB) (T6793; Sigma-Aldrich) diluted 1:1000, for either 2 hours at room temperature or 16 hours at 4°C. Incubation with secondary antibodies Alexa Flour Goat Anti-Rabbit 488 (#A11008; Life Technologies, Carlsbad, CA, USA) and Alexa Flour Donkey Anti-Mouse 546 (#A10036, Life Technologies) was carried out in the dark for 45 minutes at room temperature. DAPI (#D9542; Sigma-Aldrich) was used to stain the nucleus. For each cell line, at least 100 primary cilia were analyzed per treatment.

Statistical analysis was performed using *t*-tests or χ^2 tests as indicated. Levels of significance were classified as $^{*}P < 0.05$, $^{**}P < 0.005$, and $^{***}P < 0.0005$.

Results

Clinical features are listed in Table 1, and the family pedigree is shown in Figure 2. Brothers IV-1 and IV-3 had their first visit at NEC in 1971. They both initially presented with high myopia in early childhood. In their teens, both were diagnosed with progressive CRD, and the diagnosis was later confirmed with ERGs revealing undetectable cone responses and moderate to severe reduced rod responses. In adulthood, both developed glaucoma and cataract. At the most recent clinical examination in 2018, IV-1 presented with only light perception, but IV-3 still had useful navigation vision and was able to hold a part-time office job. Both presented with photophobia, absent color vision, and constricted visual fields but only minimal night blindness. The ocular fundus phenotypes in 2018 are shown in Figure 3. Furthermore, both IV-1 and IV-3 had PAP with an extra finger. Only IV-1 and IV-3 had the symptoms of CRD and PAP. Due to the combination of retinal dystrophy and PAP, they were suspected of BBS, and molecular genetic analysis of the BBS genes (*BBS1–BBS17*) was performed for IV-3; however, the BBS diagnosis could not be confirmed.

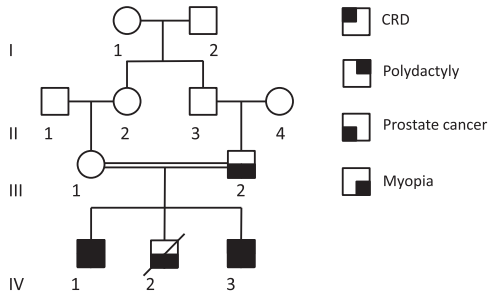

Figure 2. Pedigree of the family. For simplicity not all family members mentioned in the text are shown in the figure. Open circles and squares are unaffected females and males, respectively. Filled squares indicate a symptom depending on location in the square.

Several other clinical findings were described in the family. Deuteranomaly (green) was found in IV-2 and in the brother of III-1 (not shown on the pedigree). Furthermore, a dominant form of myopia was observed in III-2, IV-1, IV-2, and IV-3 and in the daughter of IV-2 (not shown on the pedigree). For IV-1 and IV-3, it could not be determined whether their myopia was related to the retinal dystrophy or if they inherited the apparently dominant myopia segregating in the family, or both. Some of the family members also had prostate cancer (III-2, IV-1, IV-2, and IV-3).

Genetic Studies

Both brothers were homozygous for c.55G>A (p.Gly19Arg). Gly19 is a conserved amino acid located in the G1 box of the G domain of RAB28 (Fig. 1B). Five in silico prediction programs predict p.Gly19Arg to be pathogenic. The variant is reported in 2 out of 257.380 alleles in the gnomAD database.[16] p.Gly19Arg segregates with disease in this family in an autosomal recessive inheritance pattern; however, the family is small, and brother IV-2 was not available for analysis because he died from prostate cancer. This study shows that p.Gly19Arg alters the function of RAB28. Consequently, following the ACMG guidelines for interpretation of variants,[9] c.55G>A is classified as likely pathogenic.

Cell Studies

Previous studies have found *rab-28* to be localized in neurocilia in *C. elegans*[3] and in the RPE cells and outer segments of photoreceptors in mice.[17] Jensen et al.[3] also linked *rab-28* as an IFT cargo through the BBSome. To validate the pathogenicity of the human p.Gly19Arg *RAB28* variant, the expression level of *RAB28* mRNA and the cellular localization of the RAB28 protein were investigated in fibroblast cells obtained from the two affected brothers and control cells for comparison.

Briefly, cells from IV-1, IV-3, and a control individual were grown under standard growth conditions, or under reduced-

Investigative Ophthalmology & Visual Science

Table 1. Clinical Features

Individual	Age at Diagnosis (y)	Age at Last Visit (y)	Refractive Error at Diagnosis	Visual Acuity at Diagnosis	Visual Acuity at Final Visit	Color Vision at Presentation	ERG	Goldmann Visual Field IV4e	Other
IV:1	20	67	–12D BE	RE, 3/60 LE, 6/60	RE, LP – P LE, LP + P	Red-green color vision deficit	Age 20: severely reduced scotopic responses; photopic responses undetectable	Age 20: normal peripheral visual field	Polydactyly Age 26: glaucoma Age 40: bilateral cataract surgery Age 60: prostate cancer
IV:3	14	61	–11D BE	RE, 6/18 LE, 6/24	RE, 6/60 LE, 6/75	Protan-type color vision deficit	Age 29: moderately reduced scotopic responses; absent light-adapted single flash and flicker cone responses, Age 61: recordable but severely reduced scotopic ERG; unrecordable photopic responses	Age 14: mild concentric constriction of peripheral visual field Age 61: eccentric fixation; two paracentral islands of preserved visual field of 20° and 10° diameter, respectively	Polydactyly Age 39: bilateral cataract surgery Age 41: glaucoma Age 54: prostate cancer Age 59: skin melanoma

RE, right eye, LE, left eye, BE, both eyes; LP + P and LP – P, light perception visual acuity with or without projection, respectively.

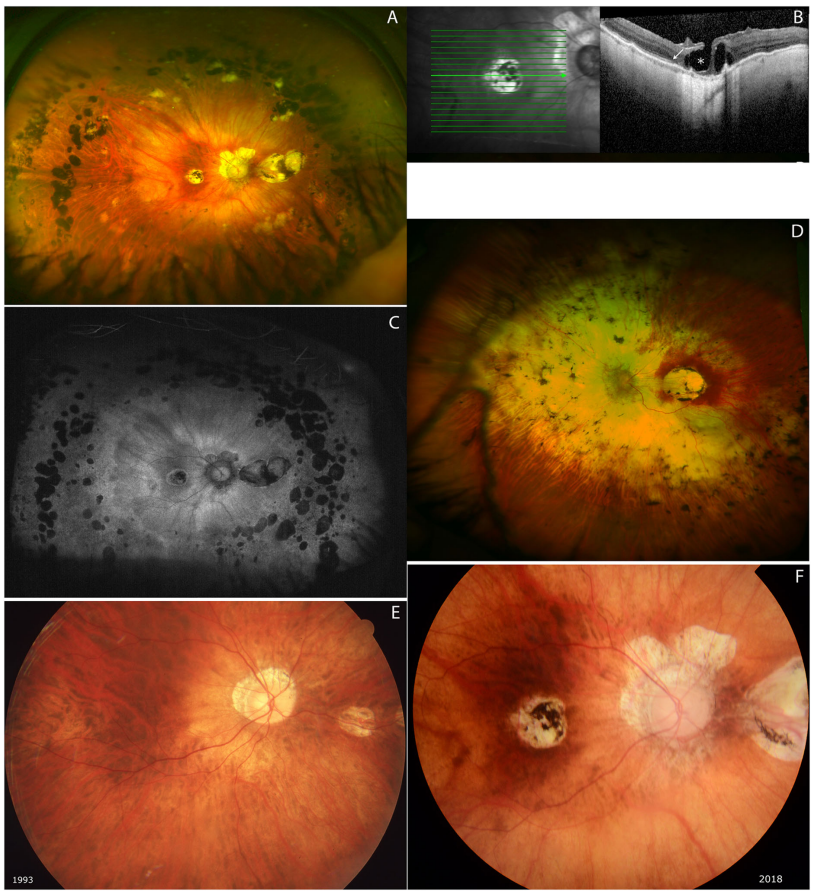

Figure 3. Ultra-wide-field fundus image (A) and blue-light autofluorescence (C) image of IV-3 shows peripapillary atrophy and well-circumscribed chorioretinal atrophy in the macula; furthermore, two to three rows of multiple nummular atrophic and heavily pigmented chorioretinal areas are noted. Severely attenuated retinal vessels, especially arteries, are observed. (B) OCT shows an ellipsoid zone and outer limiting membrane preserved temporal to fovea (white arrow) and intraretinal cysts and lamellar retinal hole formation in the fovea (asterisk). (D) Ultra-wide-field fundus image of IV-1 demonstrates extensive atrophy of the retina and the choroid around the disk and nasal midperiphery and well-demarcated retina and choroid atrophy in the macula. As for IV-3, severely attenuated retinal vessels, especially arteries, are observed. The far-peripheral retina is relatively spared in IV-1. (E, F) Progression of retinal degeneration over time. Right-eye color fundus photographs of younger sibling in 1993 (E) and in 2018 (F). Central chorioretinal atrophy with hyperpigmentation has developed in the macula. Peripapillary and nasal midperipheral atrophy has significantly progressed. Images were taken with different cameras and different angle lenses; therefore, direct comparison of vascular changes was complicated. However, vessels seem to have straightened slightly over time.

serum conditions to induce formation of the primary cilium (referred to as cilium hereafter).

Investigation of the *RAB28* expression level by qRT-PCR revealed that *RAB28* mRNA was expressed in both control and patient cells, indicating that the variant did not affect the expression level; furthermore, the expression level was significantly increased under reduced-serum conditions (Fig. 4A). Investigation of the cellular localization of the RAB28 protein in control cells by immunofluorescence microscopy showed that 73% of the cilia stained positive for RAB28 (Table 2), consistent with ciliary localization of RAB28 in human cells (Fig. 4B). Interesting, the patient cell lines showed a significant reduction in the number of RAB28-positive cilia (36% RAB28-positive cilia each) (Table 2).

To verify the specificity of the RAB28 antibody we performed siRNA-mediated knock down of *RAB28* in the control fibroblasts. Treatment with siRNA against *RAB28* reduced the number of RAB28-positive cilia significantly (from 73% to 28% RAB28-positive cilia), whereas treatment with a negative control siRNA (siScramble) did not, confirming the specificity of the RAB28 antibody (Table 2).

We subsequently investigated whether ciliogenesis was affected by the *RAB28* variant by assessing the percentage

Investigative Ophthalmology & Visual Science

Table 2. Investigation of Cilia in Patient Versus Control Fibroblasts

		Number of Cells	Number of Cilia	RAB28-Positive Cilia (%)
1	Control cells	156	124	91 (73%)
2	Patient IV-1 cells	165	142	51 (36%)**
3	Patient IV-3 cells	223	179	65 (36%)***
4	Control cells + siScramble	166	128	94 (73%)
5	Control cells + siRAB28	155	104	33 (28%)***

Rows 1–3: The numbers represent the sum of the five cultures investigated in two independent experiments. Cilia were labeled with antibody against Arl13B or acetylated alfa-tubulin and the RAB28 protein was labeled with specific RAB28 antibody. Nuclei were visualized with DAPI staining. The ciliary localization of RAB28 was significantly reduced in both patients' cell lines compared to the control (patient IV-1/control, $^{**}P = 0.000746$; patient IV-3/control, $^{***}P = 0.000408$), whereas no significant difference was observed in the number of cilia (ciliogenesis: patient IV-1/control, $P = 0.630227$; patient IV-3/control, $P = 0.950036$). Statistical analysis was performed using the χ^2 test. Rows 4 and 5: Control cell cultures were treated with siRNA against *RAB28* or with a negative control siRNA (siScramble). The numbers represent the sum from two independent experiments. Cilia were labeled with anti-Arl13B or anti-acetylated alpha-tubulin antibody and the RAB28 protein was labeled with specific RAB28 antibody; all cells were grown under serum-restricted conditions. Nuclei were visualized with DAPI staining. The ciliary localization of RAB28 was significantly reduced in the control cells treated with siRNA against *RAB28* compared with cells treated with siScramble (siRAB28/siScramble, $^{***}P = 0.000429$). No significant difference was observed in the number of cilia (ciliogenesis: siRAB28/siScramble, $P = 0.377439$). Statistical analysis was performed using the χ^2 test.

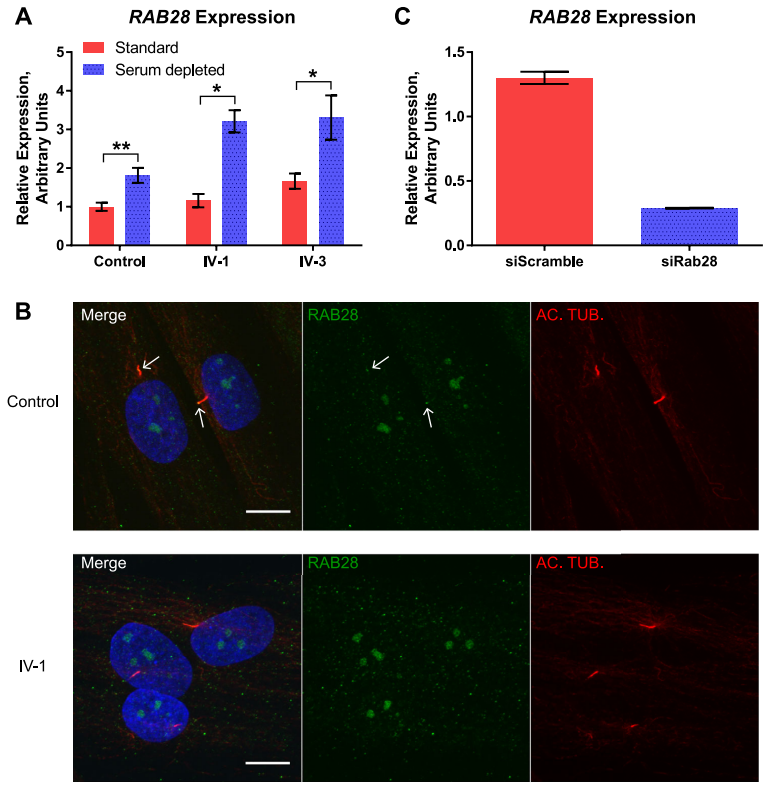

Figure 4. (A) Serum reduction leads to increased expression of *RAB28*. Expression profiles of *RAB28* mRNA were normalized to the amount of endogenous GADPH mRNA. A significant increase in the level of *RAB28* was observed for all samples under reduced-serum conditions compared to standard growth conditions ($^{**}P = 0.001815$ for control; $^{*}P = 0.007181$ for IV-1; $^{**}P = 0.003329$ for IV-3). Three independent experiments were performed with similar results. Statistical analysis was performed using *t*-tests. (B) Ciliary localization of RAB28 is significantly reduced in patient cell lines. IFM analysis of control and patient cells grown under reduced-serum conditions. Cilia were labeled with anti-acetylated alfa-tubulin (AC-TUB) antibody (red). RAB28 protein (green) can be observed in the cilia in the two control cells (white arrows), whereas none of the three displayed patient cells (IV-1) shows ciliary localization of RAB28. Nuclei were visualized with DAPI staining (blue). The ciliary localization of RAB28 was significantly reduced in both patient cell lines compared to control (see Table 2). Scale bar, 10 µm. (C) siRNA-mediated knock down of RAB28 leads to a reduction of ciliary RAB28. Normalized expression profile of RAB28 mRNA expression in control cells treated with siRNA is compared with RAB28 (siRAB28) and a negative control (siScramble) grown under serum reduced conditions. Expression profiles of RAB28 were normalized to the amount of endogenous GAPDH mRNA. The expression level in control cells grown under standard conditions treated with siScramble is set to 1. Treatment with siRab28 decreases RAB28 expression by 75.76 ± 2% under reduced-serum conditions (see Table 2). GADPH, glyceraldehyde 3-phosphate dehydrogenase; AC-TUB, anti-acetylated alfa-tubulin; IFM, immunofluorescence microscopy.

of ciliated cells. Cilia were identified on 79% (124/156) of the control cells grown under reduced-serum conditions (Table 2). Cells from IV-1 had 80% ciliated cells (142/165), whereas cells from IV-3 had 86% ciliated cells (179/223). Also, control cells treated with siRNA against *RAB28* mRNA had a percentage of ciliated cells similar to that found for control cells treated with siScramble: 77% (128/166) versus 69% (104/155) (Table 2). Thus, no significant difference in ciliogenesis was observed.

Investigation of the expression level of *RAB28* mRNA in siRNA-treated cells confirms the specificity of siRNA against *RAB28*. The treatment leads to a significant reduction (75.76 ± 2%) in *RAB28* expression, although it did not completely ablate it (Fig. 4C).

In conclusion, these data underline the pathogenicity of the *RAB28* variant by showing reduced ciliary localization of RAB28 protein. In contrast, the RAB28 variant did not affect ciliogenesis.

Discussion

We have described a family with several clinical features including CRD, PAP, high myopia, at least two forms of dyschromatopsia, and prostate cancer. Brothers IV-1 and IV-3 had all of the above-mentioned clinical features, and the third brother (IV-2) had myopia, deuteranomaly (green), and prostate cancer. Because the father (III-2) also suffered from prostate cancer and myopia, we consider these symptoms

Investigative Ophthalmology & Visual Science

Table 3. Sequence Variants in *RAB28*

Exon/Intron	cDNA (NM_004249.3)	Predicted Protein Change	Domain/Putative Functional Consequence	Status (ho/he)	Phenotype	rs Number/MAF gnomAD	ACMG Classification	Ref.
1	c.55G>A	p.Gly19Arg	G1 domain G domain GXXXXGKS/T	Ho	CRD, polydactyly	0,00000771 only heterozygous alleles (1)	LP (PM1, PM2, PP3, PS3)	This study
1	c.68C>T	p.Ser23Phe	G1 domain G domain GXXXXGKS/T	Ho	CRD	rs769199865 gnomAD 0,00003193 only heterozygous alleles (7)	VUS (PM2, PP3)	Lee et al. (2017)[20]
Intron 2	c.172+1G>C	p.? splicing defect	Skipping of exon 2	Ho	CRD	rs875989778, NP	LP (PVS1, PM2)	Riveiro-Álvarez et al. (2015)[21]
5	c.409C>T	p.Arg137*	—	Ho	CRD	rs398123044 0.000008148 only heterozygous alleles (2)	LP (PVS1, PM2)	Roosing et al. (2013)[6]
6	c.565C>T	p.Gln189*	—	Ho	CRD	rs786200944, NP	LP (PVS1, PM2)	Roosing et al. (2013)[6]
8	c.651T>G	p.Cys217Trp	—	Ho	CRD	rs751163782 0.000004076 only heterozygous alleles (1)	VUS (PM2, PP3)	Riveiro-Álvarez et al. (2015)[21]

Sequence variations reported in *RAB28*. PM1, PM2, PP1, PP3, and PVS1 refer to ACMG classification according to Richards et al.[9] Ho, homozygous; He, heterozygous; VUS, variant of unknown significance; NP, not present; LP, likely pathogenic.

to be inherited independent of the CRD. Apart from IV-2, a maternal uncle also had deuteranomaly (green), suggesting the presence of an X-linked form of deuteranomaly in these two individuals. The finding of a homozygous missense variant in *RAB28* affecting one of the invariable amino acids in the G motif makes this a plausible explanation for the CRD.

PAP has not previously been reported as a clinical symptom in individuals with *RAB28* variants. We speculate that the *RAB28* variant is the cause of PAP in the brothers presented here because RAB28 locates to the cilia like many products of genes associated with PAP, another small GTPase (*Rab34*) has been shown to be associated with PAP in mice,[18] and, finally, *IFT27* (which belongs to the RAB family of genes) is associated with BBS presenting with PAP.[19] We cannot, however, rule out that another recessive gene is causing the PAP, especially as the parents are consanguineous.

Five other disease-causing *RAB28* variants have been reported previously: two missense variants, p.Ser23Phe in a female of Korean descent[20] and p.Cys217Trp in a female of Spanish descent[21]; two nonsense variants: p.Glu189* and p.Arg137* in a German and a Moroccan Jewish family, respectively[6]; and, finally, a splice variant c.172+1G>C in a Spanish family[21] (Table 3). Classification according to the ACMG guidelines[9] renders the two missense variants as variants of unknown significance, and the two nonsense variants and the splice site variant are classified as likely pathogenic. The ophthalmological findings are very similar with early onset of macula dystrophy, dyschromatopsia, progressive visual loss, (high) myopia, and lack of night blindness in all affected individuals. Thus, it seems that different types of *RAB28* variants (missense, nonsense, and splice) are a cause of CRD in different ethnic groups.

As mentioned above, the *RAB28* missense variant found in this study, p.Gly19Arg, reduced the amount of RAB28 localized to the cilium but did not seem to alter ciliogenesis in human dermal fibroblasts. The observed increase in *RAB28* mRNA expression in the human fibroblasts after serum starvation is consistent with localization of RAB28 in the cilium. Our observations are in agreement with the results from Jensen et al.,[3] who showed that *rab-28* in *C. elegans* is not a core component of the BBSome or the IFT pathway. Rather, it could be speculated that RAB28 associates with the BBSome and the IFT in order to be transported into the cilia, where it exerts its function. The BBSome is a highly conserved protein complex essential for IFT in both humans and mice.[22–24] In mice, RAB28 functions in the cilia and is required for phagocytosis of the discs in the outer segments of the photoreceptors.[17] The same mechanism may be present in humans.

As the variant described in this study does not affect the ability of a cell to form a cilium, further experiments are necessary to verify whether the ultrastructure of the cilium is normal in the patient cell lines.

In conclusion, *RAB28* variants are a rare cause of CRD in various ethnic groups. These variants cause a comparable ophthalmological phenotype and furthermore could also be a cause of PAP.

Acknowledgments

We thank the families who participated in this study. We thank Pia Skovgaard, Bodil Olsen, Judy Rasmussen, and Anne Obling Madsen for technical assistance and Jette Bune Rasmussen for help preparing the figures.

Supported by Velux Foundation Grant 32700.

Disclosure: **C. Jespersgaard**, None; **A.B. Hey**, None; **T. Ilginis**, None; **T.D. Hjortshøj**, None; **M. Fang**, None; **M. Bertelsen**, None; **N. Bech**, None; **H. Jensen**, None; **L.J. Larsen**, None; **Z. Tümer**, None; **T. Rosenberg**, None; **K. Brøndum-Nielsen**, None; **L.B. Møller**, None; **K. Grønskov**, None

References

1. Bertelsen M, Jensen H, Bregnhoj JF, Rosenberg T. Prevalence of generalized retinal dystrophy in Denmark. *Ophthalmic Epidemiol*. 2014;21:217–223.
2. Kajiwara K, Berson EL, Dryja TP. Digenic retinitis pigmentosa due to mutations at the unlinked peripherin/RDS and ROM1 loci. *Science*. 1994;264:1604–1608.
3. Jensen VL, Carter S, Sanders AA, et al. Whole-organism developmental expression profiling identifies RAB-28 as a novel ciliary GTPase associated with the BBSome and intraflagellar transport. *PLoS Genet*. 2016;12:e1006469.
4. Brauers A, Schurmann A, Massmann S, et al. Alternative mRNA splicing of the novel GTPase Rab28 generates isoforms with different C-termini. *Eur J Biochem*. 1996;237:833–840.
5. Lee SH, Baek K, Dominguez R. Large nucleotide-dependent conformational change in Rab28. *FEBS Lett*. 2008;582:4107–4111.
6. Roosing S, Rohrschneider K, Beryozkin A, et al. Mutations in RAB28, encoding a farnesylated small GTPase, are associated with autosomal-recessive cone-rod dystrophy. *Am J Hum Genet*. 2013;93:110–117.
7. Stenson PD, Ball E, Howells K, Phillips A, Mort M, Cooper DN. Human Gene Mutation Database: towards a comprehensive central mutation database. *J Med Genet*. 2008;45:124–126.
8. Jespersgaard C, Fang M, Bertelsen M, et al. Molecular genetic analysis using targeted NGS analysis of 677 individuals with retinal dystrophy. *Sci Rep*. 2019;9:1219.
9. Richards S, Aziz N, Bale S, et al. Standards and guidelines for the interpretation of sequence variants: a joint consensus recommendation of the American College of Medical Genetics and Genomics and the Association for Molecular Pathology. *Genet Med*. 2015;17:405–424.
10. Mathe E, Olivier M, Kato S, Ishioka C, Hainaut P, Tavtigian SV. Computational approaches for predicting the biological effect of p53 missense mutations: a comparison of three sequence analysis based methods. *Nucleic Acids Res*. 2006;34:1317–1325.
11. Tavtigian SV, Deffenbaugh AM, Yin L, et al. Comprehensive statistical study of 452 BRCA1 missense substitutions with classification of eight recurrent substitutions as neutral. *J Med Genet*. 2006;43:295–305.
12. Vaser R, Adusumalli S, Leng SN, Sikic M, Ng PC. SIFT missense predictions for genomes. *Nat Protoc*. 2016;11:1–9.
13. Schwarz JM, Rodelsperger C, Schuelke M, Seelow D. MutationTaster evaluates disease-causing potential of sequence alterations. *Nat Methods*. 2010;7:575–576.
14. Adzhubei IA, Schmidt S, Peshkin L, et al. A method and server for predicting damaging missense mutations. *Nat Methods*. 2010;7:248–249.
15. Rentzsch P, Witten D, Cooper GM, Shendure J, Kircher M. CADD: predicting the deleteriousness of variants throughout the human genome. *Nucleic Acids Res*. 2019;47:D886–D894.
16. Karczewski KJ, Weisburd B, Thomas B, et al. The ExAC browser: displaying reference data information from over 60 000 exomes. *Nucleic Acids Res*. 2017;45:D840–D845.

17. Ying G, Boldt K, Ueffing M, Gerstner CD, Frederick JM, Baehr W. The small GTPase RAB28 is required for phagocytosis of cone outer segments by the murine retinal pigmented epithelium. *J Biol Chem*. 2018;293:17546–17558.
18. Dickinson ME, Flenniken AM, Ji X, et al. High-throughput discovery of novel developmental phenotypes. *Nature*. 2016;537:508–514.
19. Schaefer E, Delvallee C, Mary L, et al. Identification and characterization of known biallelic mutations in the IFT27 (BBS19) gene in a novel family with Bardet-Biedl syndrome. *Front Genet*. 2019;10:21.
20. Lee GI, Lee C, Subramanian S, et al. A novel likely pathogenic variant in the RAB28 gene in a Korean patient with cone-rod dystrophy. *Ophthalmic Genet*. 2017;38:587–589.
21. Riveiro-Alvarez R, Xie YA, Lopez-Martinez MA, et al. New mutations in the RAB28 gene in 2 Spanish families with cone-rod dystrophy. *JAMA Ophthalmol*. 2015;133:133–139.
22. Mourao A, Nager AR, Nachury MV, Lorentzen E. Structural basis for membrane targeting of the BBSome by ARL6. *Nat Struct Mol Biol*. 2014;21:1035–1041.
23. Nakayama K, Katoh Y. Ciliary protein trafficking mediated by IFT and BBSome complexes with the aid of kinesin-2 and dynein-2 motors. *J Biochem*. 2018;163:155–164.
24. Wei Q, Zhang Y, Li Y, Zhang Q, Ling K, Hu J. The BBSome controls IFT assembly and turnaround in cilia. *Nat Cell Biol*. 2012;14:950–957.

Investigative Ophthalmology & Visual Science

Draft I

BBS1, BBS5 and BBS10 patient cells show signaling defects and dysregulated ciliary length

BBS1, BBS5 and BBS10 patient cells show signaling defects and dysregulated ciliary length

Abstract:

Bardet-Biedl syndrome (BBS) is a rare disease characterized by retinal dystrophy, renal cysts, obesity and polydactyly. 23 genes are associated with BBS and they function in the primary cilium, an organelle present on cells in growth arrest that regulates signaling and tissue homeostasis. Here we investigated implications of three BBS genes; *BBS1*, *BBS5* and *BBS10* on regulation of Hedgehog (Hh) signaling and effects in ciliary morphology. Fibroblast cells from 5 individuals with BBS did not induce Hh signaling after purmorphamine stimulation when *GLI1* mRNA expression was investigated under serum depleted conditions. All five BBS cell lines showed reduced *GLI1* expression. Knock-down of *BBS1*, *BBS5* and *BBS10* in hTERT-RPE1 cells gave a similar result. Only BBS1 and the control had significantly increased *GLI1* expression after Hh activation by purmorphamine stimulation. The receptor Smoothened (SMO) was accumulated in cilia in all cell lines when Hh signaling was activated. However, we also saw SMO accumulation in the five BBS cell lines without purmorphamine stimulation. Length and number of cells with cilia was investigated in the five BBS cell lines. No change in number of ciliated cells was seen compared to control cells but ciliary length in the BBS cells is different compared to control cells. Together, these data established the importance of *BBS1*, *BBS5* and *BBS10* for proper Hh signaling function and hint that these proteins may also be important in length regulation of the cilium.

Introduction:

Bardet-Biedl syndrome (BBS) is a rare autosomal recessive ciliopathy with an estimate prevalence of 1:59 000 in Denmark (Hjortshøj *et al.*, 2010). It is characterized by retinitis pigmentosa progressing to blindness before the age of 20, polydactyly, renal malformations, learning disabilities and early onset obesity (Forsythe and Beales, 2013). 23 genes have been associated with BBS to date, all of which play a role in the primary cilium – a membrane protrusion present in a single copy on cells in quiescence important for cellular signaling processes and tissue homeostasis (Forsythe and Beales, 2013; Heon *et al.*, 2016; Schaefer *et al.*, 2016; Anvarian *et al.*, 2019; Shamseldin *et al.*, 2020). Primary cilia are immotile but share structural features with motile cilia. Both types are composed of 9 doublet microtubules in the shape of a ring forming the axoneme. Motile cilia also have a singlet pair of microtubules in the center of the axoneme giving a "9+2" configuration whereas primary cilia have "9+0" structure reflecting the lack of the central pair. The cilia themselves cannot synthesize proteins so their composition relies on transport processes both to build the cilium and to maintain ciliary function (Anvarian *et al.*, 2019).

Primary cilia are considered as separate organelles as their membrane composition differ from that of the cell they protrude from. Due to the structure of the cilium and ciliary base, active transport is needed for most proteins to enter the cilium. Two protein complexes, IFTA and IFTB consisting of two sub-complexes; IFTB1 and IFTB2, in combination with the motor proteins kinesin II and cytoplasmic dynein II carry out anterograde (towards the tip) and retrograde (towards the base) transport (Fu *et al.*, 2016; Taschner *et al.*, 2016; Prevo, Scholey and Peterman, 2017).

The BBSome complex, consisting of BBS1, BBS2, BBS4, BBS5, BBS7, BBS8, BBS9, BBS17 and BBS18, also play a role in IFT serving as an adaptor between cargo and the transport complex. The role of the BBSome was suggested to be an adaptor for G-protein coupled receptors in the process of ciliary delivery but now studies suggest that the BBSome is mainly involved in retrograde transport and exit from the cilium (Ou *et al.*, 2005; Nachury *et al.*, 2007; Lechtreck *et al.*, 2009; Jin *et al.*, 2010; Seo *et al.*, 2011; Nachury and Mick, 2019). Another BBS protein complex is necessary for IFT; the chaperonin-complex consisting of BBS6, BBS10 and BBS12. This protein complex assembles the BBSome (Seo *et al.*, 2010).

Many signaling receptors are concentrated in the primary cilium coupling these pathways to the cilium; Wnt, TGF-beta, NOTCH and Hh to mention a few. Hedgehog (Hh) is important during embryonic development to determine cell fate, tissue patterning and for tissue homeostasis. Defects in this signaling pathway has been associated with polydactyly – one of the symptoms of BBS (Tayeh *et al.*, 2008; Wheway, Nazlamova and Hancock, 2018; Anvarian *et al.*, 2019).

Hh signaling is one of the most studied signaling pathways connected to the cilium having two important receptors that rely on transport into and out of the cilium for activation of the pathway. When the pathway is inactive, the receptor Patched1 (PTCH1) is localized in the cilium blocking the other receptor Smoothened (SMO) from entering the cilium. Other receptors and proteins keep the pathway inactive by targeting GLI transcription factors for cleavage to repressor form or restraining them to the cytoplasm preventing transcription of target genes (Mukhopadhyay and Rohatgi, 2014). Upon binding of one of the Hh ligands to PTCH1, the repression on SMO is relieved; PTCH1 leaves the cilium and SMO can enter and accumulate in the cilium (Corbit *et al.*, 2005; Rohatgi, Milenkovic and Scott, 2007) shifting the processing of the GLI transcription factors to the active forms turning on canonical Hh signaling (Niewiadomski *et al.*, 2014).

In this work purmorphamine was used to activate Hh signaling (Sinha and Chen, 2006). Hh signaling was compared for the five patient cell lines harboring variants in *BBS1*, *BBS5* and *BBS10.* Percentage of ciliated cells and ciliary length was also investigated. The observed Hh phenotype was replicated with siRNA mediated knockdown of *BBS1*, *BBS5* and *BBS10* in immortalized human retinal pigment epithelium (RPE) cell line hTERT-RPE1 to rule out cell type differences.

Results:

Cells from 5 individuals suffering from BBS were obtained who had expected pathogenic variants in three BBS genes; *BBS1*, *BBS5* and *BBS10* (see Table 1).

As one of the frequent features of BBS is polydactyly and previous studies have linked skeletal anomalies to Hh signaling which is deeply dependent on BBS mediated IFT (Tayeh *et al.*, 2008; Seo *et al.*, 2011; Zhang *et al.*, 2012; Airik *et al.*, 2016), Hh signaling was tested in the five patient cell lines. To induce ciliogenesis, the cells were grown at serum depleted conditions. Reducing the amount of serum in the growth medium cause the cells to go into growth arrest and start forming primary cilia. Serum can also contain growth factors that inhibit ciliogenesis (Santos and Reiter, 2008). We investigated Hh signaling by looking at the expression of *GLI1* mRNA under standard and serum reduced conditions with and without purmorphamine stimulation. The experiment was run in biological triplicate (Fig. 1A). The control (Ctrl) showed a significant increase in *GLI1* expression after purmorphamine stimulation (pur) both under standard and under serum depleted (dpl.) conditions whereas only BBS1 of the five BBS cell lines showed a significant increase in *GLI1* expression with purmorphamine stimulation under standard growth conditions and none of the BBS cell

lines under serum depleted conditions. For all five BBS cell lines, the overall *GLI1* expression was severely downregulated compared to the control regardless of treatment. Even though BBS1 showed a significant increase in *GLI1* expression after pur stimulation it failed to do so under serum depleted growth conditions in contrast to the control.

We next examined the sub-cellular localization of the Hh receptor SMO using immunofluorescence microscopy of serum depleted cells with and without purmorphamine stimulation and antibodies against SMO and acetylated tubulin (AC. TUB) to label the cilia (Fig.1 B). SMO accumulation in cilia is usually seen after Hh stimulation (Anvarian *et al.*, 2019). For both control cell lines, the percentage of SMO positive cilia increased significantly after purmorphamine stimulation (Fig. 1C). With the exception of BBS10A and BBS10B, all tested BBS cell lines showed almost equal levels of SMO positive cilia with and without purmorphamine stimulation. Only BBS10A had a significant increase in ciliary SMO after purmorphamine stimulation however both cell lines as well as the three other BBS cell lines had a high basal level of SMO. The analyzed cilia are pooled from three separate experiments.

To validate the findings above, and to make sure the results obtained were not due to genetic differences between the cell lines that are not caused by the *BBS* variants, Hh signaling was also tested in an immortalized RPE cell line, derived from a one year old female; hTERT-RPE1 (RPE1). The RPE1 cells were treated with siRNA to knock down gene-expression of *BBS1*, *BBS5* and *BBS10* under serum depleted conditions with and without purmorphamine stimulation, as with the fibroblast cells. A negative control siRNA (siSCR) was included. The experiment was run in triplicate. Knock-down efficiency is shown in supplementary fig. 1. The siSCR treated cells showed normal induction of Hh signaling with a significant increase in *GLI1* expression after purmorphamine stimulation in serum depleted cells (Fig. 1D), comparable to the control in Fig. 1A. Knock-down of *BBS1* gave a significant response somewhat smaller than siSCR whereas *BBS5* and *BBS10* showed a slight, but non-significant increase in *GLI1* expression after purmorphamine stimulation.

These data, together with the decreased Hh response and SMO accumulation in primary cilia in patient fibroblast cells, underlined the signaling defects in these cells and indicated that it was not cell type specific.

We next examined how the cilia of the patient fibroblast cells were affected by looking at ciliary length and the percentage of cells with cilia. Fibroblasts were grown in serum reduced media for 48 hours before they were fixed and stained with antibodies targeting ARL13B and acetylated α-tubulin, both ciliary markers. Nuclei were visualized using DAPI (see Fig. 2A). The experiment was run in biological triplicate with three control cell lines and the five BBS cell lines. There was no significant difference in ciliary length between the three controls; control A, control C and control E. Compared to control A, investigation of ciliary length showed that BBS1 cells had significantly shorter cilia whereas BBS5A, BBS5B and BBS10A all had significantly longer cilia (see Fig. 2B).

A tendency for a wider ciliary length distribution was observed for BBS5A+B and BBS10A+B cells compared to control and BBS1 cells when ciliary length was visualized as a boxplot (Fig.2 C, not quantified). This should be investigated further to determine if a significant difference in length variation between BBS cells and control cells exist.

The percentage of ciliated cells was also analyzed (Fig. 2D). The control cells had a mean percentage of ciliated cells of 95.75±0.75% (ctrl. A), 89.18±1.30% (ctrl. D) and 93.82±0.32% (ctrl. E) respectively. BBS1 cells had a similar ciliation percent with a mean ciliation of 94.98±2.37%. BBS5A cells a percentage similar to control cells; 92,77±1.58% but BBS5B had fewer ciliated cells having 79.55±3.6% ciliated cells. BBS10A and BBS10B cells both have fewer cilia showing 89.16±4.14% and 85.78±0.35% ciliated cells respectively. None of the ciliary percentages were significantly different from control cells. Together these data imply that ciliogenesis was not grossly affected by the three *BBS* gene variants, but that ciliary length was different. The specific mechanism underlying this phenotype needs further investigation.

In summary for the five BBS cell lines, we saw that Hh signaling was severely downregulated, SMO accumulated in primary cilia without activating the pathway and there was a tendency for ciliary length regulation disruption in cells with gene variants in *BBS1*, *BBS5* or *BBS10*.

Discussion and Conclusion:

In the present study, we showed that *BBS1*, *BBS5* and *BBS10* are important for proper Hh signaling and that the length of the cilium was different for the patient cells compared to control. The role of cilia in Hh signaling transduction has been widely investigated, and the BBSome complex has been linked to the ciliary export of SMO through studies in mutant mice harboring variants in *BBS1, BBS2, BBS4* and *BBS7* (Nachury *et al.*, 2007; Jin *et al.*, 2010; Seo *et al.*, 2011; Ye, Nager and Nachury, 2018). Although the BBS proteins are highly conserved throughout evolution, the mutant mice investigated did not have polydactyly or any other skeletal anomalies, showing a potential difference between this model system and the human disease mechanisms (Xu *et al.*, 2015). As we observed the same signaling defects in both patient fibroblast cells and RPE1 BBS-knock down cells, the observed Hh defects can be attained to the *BBS* genes and the human cell system as well.

We demonstrated that SMO accumulated in cilia of unstimulated cells from individuals with BBS, without activating the pathway. In BBS10A the increase in SMO after pur stimulation was significant, in similarity to the control cells, but this did not correspond with an increase in *GLI1* expression. This is in agreement, with a previously investigation, proving that ciliary localization of SMO is not to sufficient for Hh pathway activation, SMO needs to be activated as well (Rohatgi *et al.*, 2009). All BBS cell lines had a high basal level of ciliary SMO which can be linked to the role in ciliary export the BBS proteins carry out (Lechtreck *et al.*, 2009, 2013; Liu and Lechtreck, 2018).

Length regulation of cilia has been reported to be linked to BBS proteins; BBS4 and BBS6 deficient cells showed fewer and shorter cilia with poor cell migration, hinting that BBS proteins may play a role in regulation of the cytoskeleton. Furthermore, the BBSome is important for IFT that transport tubulin in the cilium. Thus, disturbing the BBSome may lead to abnormal trafficking of tubulin and altered ciliary length homeostasis (Hernandez-Hernandez *et al.*, 2013; Anvarian *et al.*, 2019). Patnaik *et al.* find BBS proteins to protect ciliary length through interaction with INVERSIN which is a regulator of Aurora A kinase that activates histone deacetylase 6 (HDAC6) which in turn destabilizes ciliary axonemal microtubules in RPE cells leading to disassembly of the cilium. They find *BBS6* and *BBS8* knock-out mice to have RPE cells with fewer ciliated cells and cilia that are shorter than the untreated control (Patnaik *et al.*, 2019).

Comparing our obtained results from BBS1 and BBS5 cells, that are part of the BBSome, with BBS10, that is part of the chaperonin complex, did not show any major differences in ciliary length. This indicates that the

effect is the same whether it is the BBSome or the chaperonin-complex that is disturbed. However, BBS1 and BBS5 patient cells had opposite effects on ciliary length showing that proteins in the same complex can have different functions. In contrast to the study by Patnaik et al., fibroblast cells with *BBS* gene variants did not have fewer cilia. As it seems BBS1 have the opposite effect on ciliary length than BBS5 and BBS10 it is worth investigating if HDAC6 mediated ciliary disassembly is disturbed. It would also be interesting to see if this mechanism is as pronounced in human fibroblast cells as it is in mouse RPE cells.

In conclusion, variants in *BBS1*, *BBS5* and *BBS10* all cause Hh signaling defects apparent by decreased *GLI1* expression in stimulated cells and SMO accumulation in cilia without Hh stimulation. Furthermore, the length of the primary cilium was also affected in the BBS patient cells where BBS1 had shorter cilia and BBS5 and BBS10 cells had slightly longer compared to control cells. The variation in cilia length appeared larger in general for the BBS cells but the number of ciliated cells was not affected by the BBS variants.

Materials and methods:

Cell culture:

Fibroblast cells from five BBS patients were obtained through skin biopsy and cells from 3 healthy control individuals were included for comparison (Control A, Control D, Control E). RPE1 (hTERT-RPE1) cells were a kind gift from Lotte Bang Pedersen (University of Copenhagen, Department of Biology, Section for Cell Biology and Physiology), originally obtained from ATCC (hTERT RPE-1 ATCC ® CRL-4000™). All cells were grown in either standard growth conditions; DMEM-F12 + GlutaMAX (Gibco), 10% fetal bovine serum (FBS) (Gibco) and 1% penicillin-streptomycin (Gibco) or serum depleted growth conditions with FBS reduced to 0.5%.

Gene knockdown with siRNA:

Cells were incubated with 25nM negative control siRNA (siSCR), siBBS1 (SI03191622, Qiagen), siBBS5 (SI04339020, Qiagen), siBBS10 (SI04270371, Qiagen) overnight using DharmaFECT 1 (Dharmacon) as per manufacturer's instructions. Next morning medium was changed to serum reduced (0.5% FCS) and 24 hours after serum reduction, cells were stimulated with 5µM purmorphamine in serum reduced media for an additional 24 hours. Knock-down efficiency was assessed using qPCR.

Gene expression (qPCR):

RNA was purified using GeneJET RNA purification kit (thermo fisher scientific) and cDNA was synthesized using high capacity cDNA kit (thermo fisher scientific). Taqman probes against endogenous *GAPDH* (thermo fisher scientific, Hs99999905_m1) and *GLI1* (thermo fisher scientific, Hs01110766_m1) were used in combination with TaqMan™ Universal PCR Master Mix (thermo fisher scientific) on the 7500-fast system (Applied Biosystems). Three technical replicates were tested per sample. The relative standard curve method was used, and samples were normalized to GAPDH and a control sample.

Immunofluorescence microscopy:

Cells were fixed with 4% paraformaldehyde (Hounisen) for 15 minutes, permeabilized with 0.2% TritonX-10 in PBS and blocked with 3% bovine serum albumin (BSA) in permeabilization buffer. Incubation with primary antibodies diluted in 3% BSA was done for 45 minutes at room temperature or overnight at 4°C. Secondary antibody incubation was carried out for 1 hour at room temperature before mounting. Nuclei were visualized using DAPI. All images were obtained using an Olympus Fluoview 1000 confocal microscope and images were analyzed using ImageJ. The following antibodies were used: Anti-α-Acetylated tubulin (Sigma-Aldrich #T6793), Anti-Smoothened (Abcam #ab38686) and Anti-ARL13B (Proteintech #1711-1-AP).

Statistical methods

Students t-test or the χ^2-test were used as indicated. The t-test was calculated as un-paired two-tailed test. For both methods, significance level at 0.05 was chosen. Significance starts are in the following categories: *$p \leq 0.05$, **$p \leq 0.005$, ***$p \leq 0.0005$. Only data from three separate biological experiments were used for statistical analysis.

References:

Airik, R. *et al.* (2016) 'SDCCAG8 Interacts with RAB Effector Proteins RABEP2 and ERC1 and Is Required for Hedgehog Signaling', *PLOS ONE*. Edited by Y. Komarova, 11(5), p. e0156081. doi: 10.1371/journal.pone.0156081.

Anvarian, Z. *et al.* (2019) 'Cellular signalling by primary cilia in development, organ function and disease', *Nature Reviews Nephrology*, 15(4), pp. 199–219. doi: 10.1038/s41581-019-0116-9.

Corbit, K. C. *et al.* (2005) 'Vertebrate Smoothened functions at the primary cilium', *Nature*, 437(7061), pp. 1018–1021. doi: 10.1038/nature04117.

Forsythe, E. and Beales, P. L. (2013) 'Bardet-Biedl syndrome', *European Journal of Human Genetics*, 21(1), pp. 8–13. doi: 10.1038/ejhg.2012.115.

Fu, W. *et al.* (2016) 'Role for the IFT-A Complex in Selective Transport to the Primary Cilium', *Cell Reports*, 17(6), pp. 1505–1517. doi: 10.1016/j.celrep.2016.10.018.

Heon, E. *et al.* (2016) 'Mutations in C8ORF37 cause Bardet Biedl syndrome (BBS21)', 25(11), pp. 2283–2294. doi: 10.1093/hmg/ddw096.

Hernandez-Hernandez, V. *et al.* (2013) 'Bardet–Biedl syndrome proteins control the cilia length through regulation of actin polymerization', *Human Molecular Genetics*, 22(19), pp. 3858–3868. doi: 10.1093/hmg/ddt241.

Hjortshøj, T. D. *et al.* (2010) 'Bardet-Biedl syndrome in Denmark-report of 13 novel sequence variations in six genes', *Human Mutation*, 31(4), pp. 429–436. doi: 10.1002/humu.21204.

Jin, H. *et al.* (2010) 'The conserved bardet-biedl syndrome proteins assemble a coat that traffics membrane proteins to Cilia', *Cell*. Elsevier Ltd, 141(7), pp. 1208–1219. doi: 10.1016/j.cell.2010.05.015.

Lechtreck, K. F. *et al.* (2009) 'The Chlamydomonas reinhardtii BBSome is an IFT cargo required for export of specific signaling proteins from flagella', *Journal of Cell Biology*, 187(7), pp. 1117–1132. doi:

10.1083/jcb.200909183.

Lechtreck, K. F. *et al.* (2013) 'Cycling of the signaling protein phospholipase D through cilia requires the BBSome only for the export phase', *Journal of Cell Biology*, 201(2), pp. 249–261. doi: 10.1083/jcb.201207139.

Liu, P. and Lechtreck, K. F. (2018) 'The Bardet–Biedl syndrome protein complex is an adapter expanding the cargo range of intraflagellar transport trains for ciliary export', *Proceedings of the National Academy of Sciences*, 115(5), pp. E934–E943. doi: 10.1073/pnas.1713226115.

Mukhopadhyay, S. and Rohatgi, R. (2014) 'G-protein-coupled receptors, Hedgehog signaling and primary cilia', *Seminars in Cell & Developmental Biology*. Elsevier Ltd, 33, pp. 63–72. doi: 10.1016/j.semcdb.2014.05.002.

Nachury, M. V. *et al.* (2007) 'A Core Complex of BBS Proteins Cooperates with the GTPase Rab8 to Promote Ciliary Membrane Biogenesis', *Cell*, 129(6), pp. 1201–1213. doi: 10.1016/j.cell.2007.03.053.

Nachury, M. V. and Mick, D. U. (2019) 'Establishing and regulating the composition of cilia for signal transduction', *Nature Reviews Molecular Cell Biology*. Springer US, 20(7), pp. 389–405. doi: 10.1038/s41580-019-0116-4.

Niewiadomski, P. *et al.* (2014) 'Gli Protein Activity Is Controlled by Multisite Phosphorylation in Vertebrate Hedgehog Signaling', *Cell Reports*. The Authors, 6(1), pp. 168–181. doi: 10.1016/j.celrep.2013.12.003.

Ou, G. *et al.* (2005) 'Functional coordination of intraflagellar transport motors', *Nature*, 436(7050), pp. 583–587. doi: 10.1038/nature03818.

Patnaik, S. R. *et al.* (2019) 'Bardet–Biedl Syndrome proteins regulate cilia disassembly during tissue maturation', *Cellular and Molecular Life Sciences*. Springer International Publishing, 76(4), pp. 757–775. doi: 10.1007/s00018-018-2966-x.

Prevo, B., Scholey, J. M. and Peterman, E. J. G. (2017) 'Intraflagellar transport: mechanisms of motor action, cooperation, and cargo delivery', *FEBS Journal*, 284(18), pp. 2905–2931. doi: 10.1111/febs.14068.

Rohatgi, R. *et al.* (2009) 'Hedgehog signal transduction by Smoothened: Pharmacologic evidence for a 2-step activation process', *Proceedings of the National Academy of Sciences*, 106(9), pp. 3196–3201. doi: 10.1073/pnas.0813373106.

Rohatgi, R., Milenkovic, L. and Scott, M. P. (2007) 'Patched1 Regulates Hedgehog Signaling at the Primary Cilium', *Science*, 317(5836), pp. 372–376. doi: 10.1126/science.1139740.

Santos, N. and Reiter, J. F. (2008) 'Building it up and taking it down: The regulation of vertebrate ciliogenesis', *Developmental Dynamics*, 237(8), pp. 1972–1981. doi: 10.1002/dvdy.21540.

Schaefer, E. *et al.* (2016) 'Identification of a novel mutation confirms the implication of IFT172 (BBS20) in Bardet–Biedl syndrome', *Journal of Human Genetics*, 61(5), pp. 447–450. doi: 10.1038/jhg.2015.162.

Seo, S. *et al.* (2010) 'BBS6, BBS10, and BBS12 form a complex with CCT/TRiC family chaperonins and mediate BBSome assembly', *Proceedings of the National Academy of Sciences*, 107(4), pp. 1488–1493. doi: 10.1073/pnas.0910268107.

Seo, S. *et al.* (2011) 'A novel protein LZTFL1 regulates ciliary trafficking of the BBSome and smoothened', *PLoS Genetics*, 7(11). doi: 10.1371/journal.pgen.1002358.

Shamseldin, H. E. *et al.* (2020) 'The morbid genome of ciliopathies: an update', *Genetics in Medicine*. Springer US, 0(0), pp. 1–10. doi: 10.1038/s41436-020-0761-1.

Sinha, S. and Chen, J. K. (2006) 'Purmorphamine activates the Hedgehog pathway by targeting Smoothened', *Nature Chemical Biology*, 2(1), pp. 29–30. doi: 10.1038/nchembio753.

Taschner, M. *et al.* (2016) 'IFT-B 2 complex', *The EMBO journal*, 35(7), pp. 1–18.

Tayeh, M. K. *et al.* (2008) 'Genetic interaction between Bardet-Biedl syndrome genes and implications for limb patterning', *Human Molecular Genetics*, 17(13), pp. 1956–1967. doi: 10.1093/hmg/ddn093.

Wheway, G., Nazlamova, L. and Hancock, J. T. (2018) 'Signaling through the Primary Cilium', *Frontiers in Cell and Developmental Biology*, 6(February), pp. 1–13. doi: 10.3389/fcell.2018.00008.

Xu, Q. *et al.* (2015) 'BBS4 and BBS5 show functional redundancy in the BBSome to regulate the degradative sorting of ciliary sensory receptors', *Scientific Reports*. Nature Publishing Group, 5(December 2014), pp. 1–16. doi: 10.1038/srep11855.

Ye, F., Nager, A. R. and Nachury, M. V. (2018) 'BBSome trains remove activated GPCRs from cilia by enabling passage through the transition zone', *The Journal of Cell Biology*, 217(5), pp. 1847–1868. doi: 10.1083/jcb.201709041.

Zhang, Q. *et al.* (2012) 'BBS proteins interact genetically with the IFT pathway to influence SHH-related phenotypes', *Human Molecular Genetics*, 21(9), pp. 1945–1953. doi: 10.1093/hmg/dds004.

Figures and Tables:

TABLE 1

Patient number (abbreviation)	***Variant***
Patient 1 (BBS1)	Compound heterozygous; *BBS1* c.1169T>G, p. (Met390Arg)/c.1135G>C, p.(Gly370Arg)
Patient 2 (BBS5A)	Homozygous; *BBS5* c.214G>A, p.(Gly72Ser)
Patient 3 (BBS5B)	Homozygous; *BBS5* c.214G>A, p.(Gly72Ser)
Patient 4 (BBS10A)	Homozygous; *BBS10* c.271insT (p. Cys91fs*95)
Patient 5 (BBS10B)	Homozygous; *BBS10* c.271insT (p. Cys91fs*95)

Figure 1: Investigation of Hh signaling in fibroblast control and BBS cells. **A:** mRNA expression of *GLI1* was investigated under standard and serum depleted conditions with and without purmorphamine (pur) stimulation. Under standard growth conditions, pur stimulation gives a significant rise in *GLI1* mRNA expression for the control and BBS1 but not the other BBS cells (Ctrl. ***p=0.0005, BBS1 *p=0.013, BBS5A p=0.166, BBS5B p=0.291, BBS10A p=0.0535, BBS10B p=0.471, n=3 for all, students t-test with p<0.05 significance level). Under serum depleted growth conditions, a significant rise in *GLI1* expression for the control was observed but not in any of the BBS cells (ctrl. ***p=0.0002, BBS1 p=0.077, BBS5A p=0.246, BBS5B p=0.379, BBS10A p=0.054, BBS10B p=0.153, n=3 for all, students t-test with p<0.05 significance level). Error bars represent the standard deviation. **B:** Subcellular localization of SMO was investigated with immunofluorescence microscopy. Control cells did not have SMO in the cilium without pur stimulation, but all five BBS cell lines had SMO in the cilium without pur stimulation. SMO was present in the cilium of control and BBS cells after pur treatment (not shown). Arrows indicate ciliary localization. **C:** quantitation of B. Both control cell lines had a significant increase in ciliary SMO localization after pur stimulation (ctrl. A ***p<0.0001 n=224, ctrl. D ***p<0.0001 n=270). BBS cells showed a high basal level of ciliary SMO that only increased significantly in BBS10A after pur stimulation (BBS1 p=0.960 n=222, BBS5A p=0.371 n=228, BBS5B p=0.802 n=242, BBS10A *p=0.045, n=333, BBS10B p=0.219 n=202). All included cilia were pooled from three independent experiments and χ^2-tests performed with significance level p<0.05 determined significance). Error bars represent the standard deviation. **D:** *GLI1* mRNA expression was investigated in RPE1 cells treated with siRNA against *BBS1*, *BBS5*, *BBS10* and a negative control siRNA (siSCR) in serum reduced growth conditions with and without pur stimulation. Cells treated with siSCR showed a significant increase in *GLI1* expression after pur stimulation. Cells treated with siBBS1 also gave a significant rise in *GLI1* expression after pur stimulation somewhat smaller than for siSCR treated cells (siSCR **p=0.001, siBBS1 *p=0.022, siBBS5 p=0.573, siBBS10 p=0.051, n=3 for all, students t-test with p<0.05 significance level). Error bars represent the standard deviation.

Figure 2: Investigation of the primary cilium in fibroblast cells. **A:** Immunofluorescence microscopy of the ciliary membrane protein ARL13B, images with representative cilia for each cell line are shown. **B:** Quantitation of A. Mean ciliary length was compared between three control cell lines with no significant difference (ctrl A n=224, ctrl D n=270, ctrl. E n=243. Ctrl. A vs. ctrl. D p=0.0918, ctrl. A vs. ctrl. E p=0.675, ctrl. D vs. ctrl. E p=0.207). Ctrl. A was used for comparison with the 5 BBS cell lines. BBS1 had significantly

shorter cilia (***p<0.0001, n=222), BBS5A, BBS5B and BBS10A all had significantly longer cilia (BBS5A ***p<0.0001, n=228, ***BBS5B p<0.0001, n=242, ***BBS10A p<0.0001, n=333). BBS10B had longer cilia but not significantly (p=0.153, n=202). P values and significance was determined using students t-test, n values consist of pooled data from three separate experiments. Error bars represent the standard deviation. **C:** Quantitation of A showing the length variation for all cell lines. Compared to control cell lines BBS5A, BBS5B and BBS10A had a wide length variation. Non-significant data. **D:** Calculated percent of cells with cilia. There was no significant difference in percent ciliated cells between the cell lines and ctrl. A. Ctrl. A 97.73±0.75% n=234, ctrl D 89.18±1.3% p=0.572 n=305, ctrl. E 93.82±0.32% p=0.875 n=259, BBS1 94.98±2.37% p=0.953 n=239, BBS5A 92.77±1.58% p=0.810 n=249, BBS5B 79.55±3.6% 0.144 n=308, BBS10A 89.16±4.14% p=0.555 n=369, BBS10B 85.78±0.35% p=0.418 n=225. χ^2-tests performed with significance level p<0.05. Error bars represent the standard deviation.

Suppl. Fig. 1: Knock-down efficiency of the used siRNA targeting *BBS1*, *BBS5* and *BBS10* in RPE1 cells was assessed through qPCR. N=3 biological replicates. Colors represent target of taqman probe (*BBS1*, *BBS5* and *BBS10*), error bars the standard deviation. Data was calculated used the delta CT method with normalization to *GAPDH* and siSCR.

Figure 1

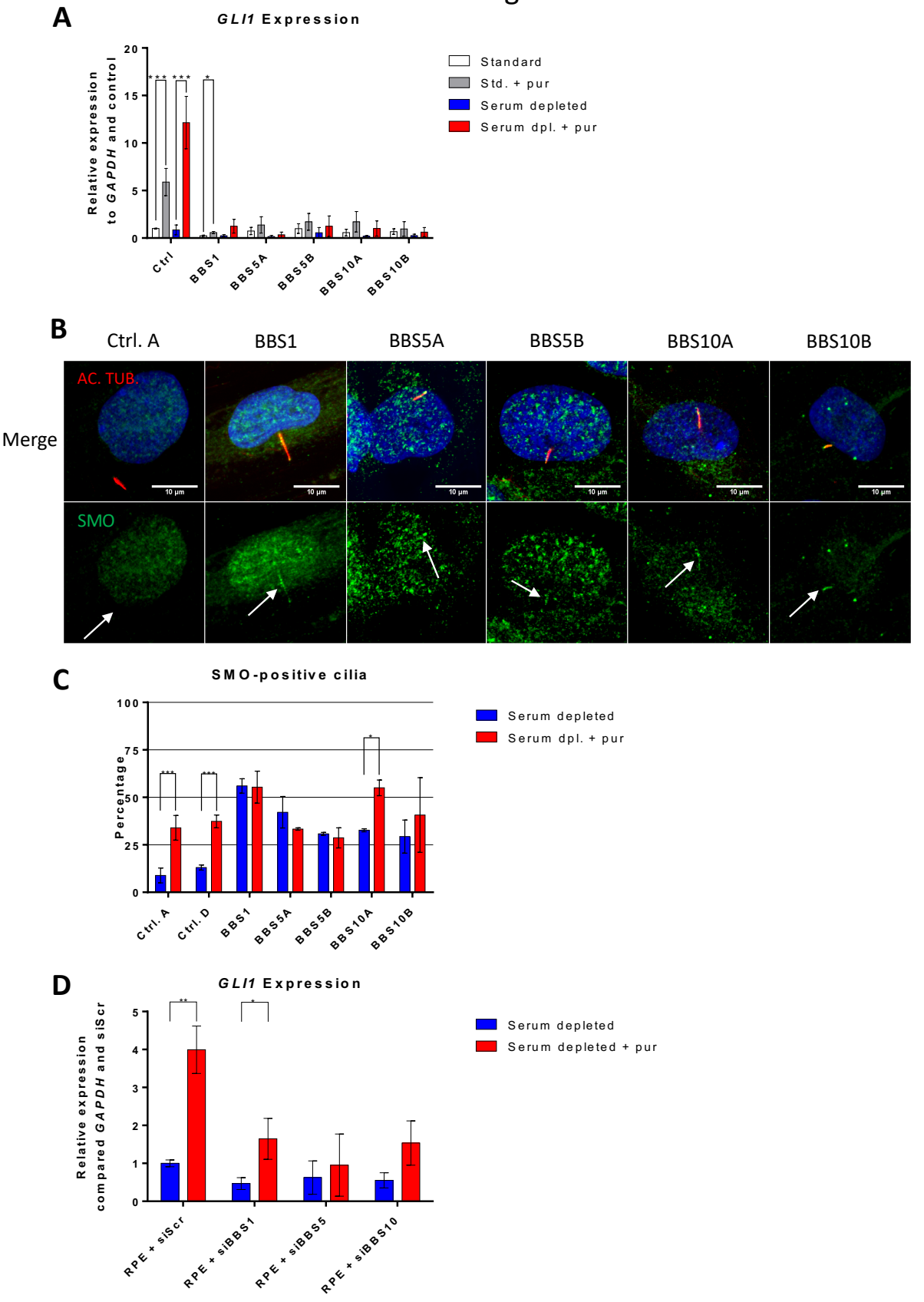
A
GLI1 Expression
Relative expression to GAPDH and control
Standard
Std. + pur
Serum depleted
Serum dpl. + pur
Ctrl
BBS1
BBS5A
BBS5B
BBS10A
BBS10B
B
Ctrl. A
BBS1
BBS5A
BBS5B
BBS10A
BBS10B
Merge
AC. TUB.
SMO
C
SMO-positive cilia
Percentage
Serum depleted
Serum dpl. + pur
Ctrl. A
Ctrl. D
BBS1
BBS5A
BBS5B
BBS10A
BBS10B
D
GLI1 Expression
Relative expression compared GAPDH and siScr
Serum depleted
Serum depleted + pur
RPE + siScr
RPE + siBBS1
RPE + siBBS5
RPE + siBBS10

Figure 2

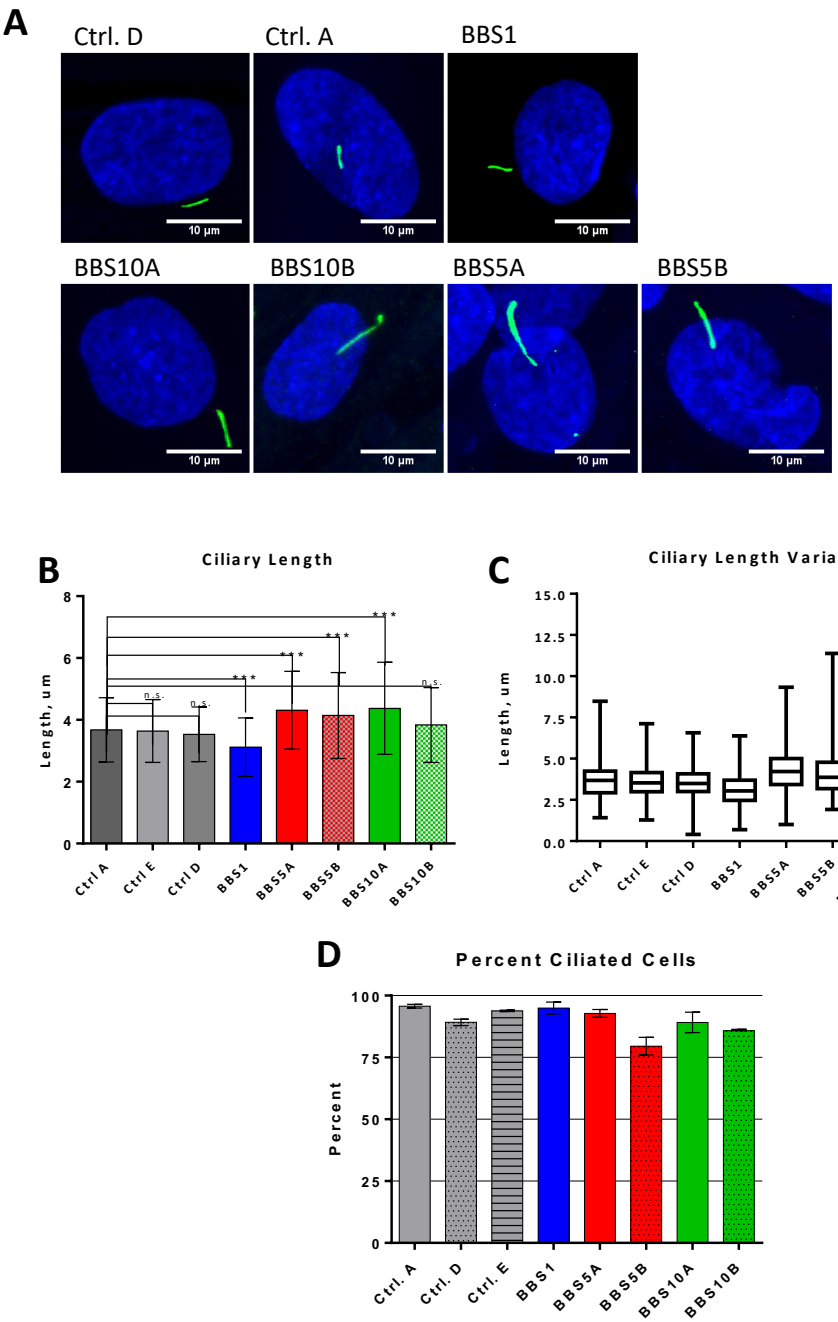
A
Ctrl. D
Ctrl. A
BBS1
BBS10A
BBS10B
BBS5A
BBS5B
10 µm
B
Ciliary Length
Length, um
Ctrl A
Ctrl E
Ctrl D
BBS1
BBS5A
BBS5B
BBS10A
BBS10B
C
Ciliary Length Variation
Length, um
D
Percent Ciliated Cells
Percent
Ctrl. A
Ctrl. D
Ctrl. E
BBS1
BBS5A
BBS5B
BBS10A
BBS10B

Supplementary figure 1

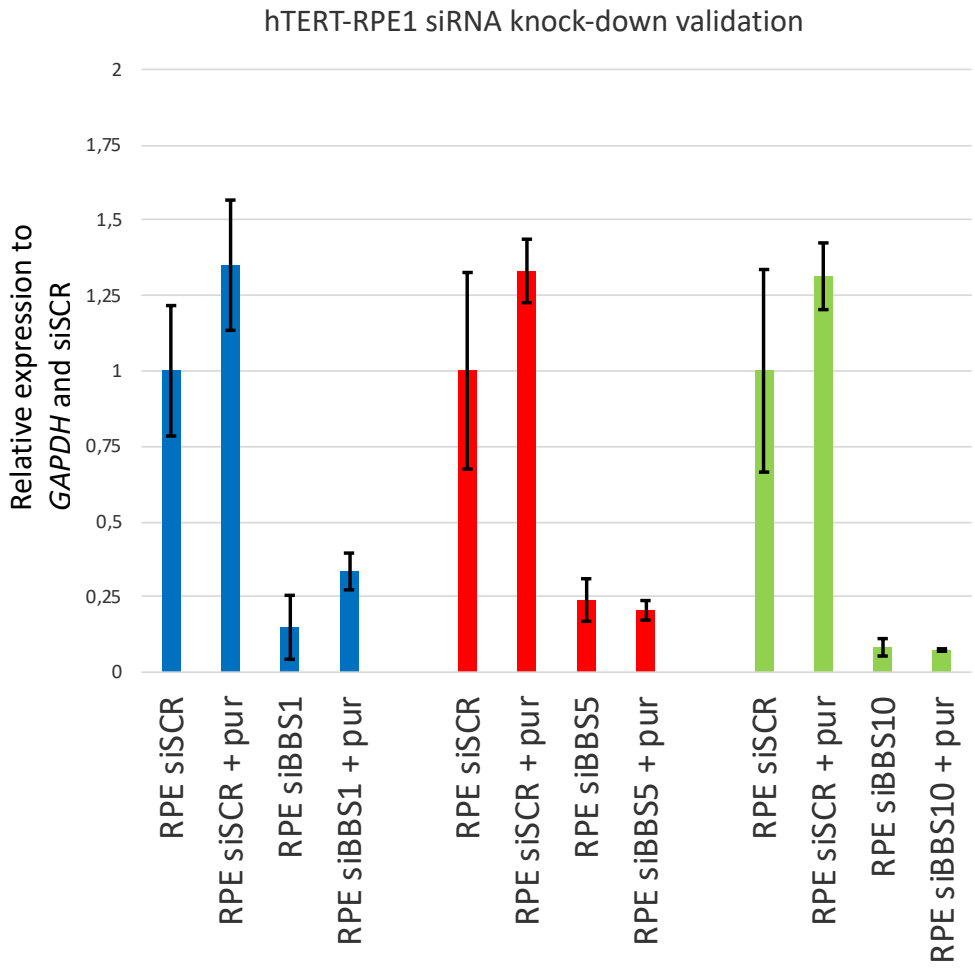

Blue: Taqman targeting *BBS1*
Red: Taqman targeting *BBS5*
Green: Taqman targeting *BBS10*

Draft II

The BBS proteins are required for RPE cell maturation

The BBS proteins are required for RPE cell maturation

Abstract:

Bardet-Biedl syndrome (BBS) affects the primary cilium and leads to obesity, polydactyly, renal cysts and progressive loss of vison before the age of 20. Vision loss has been linked to the death of photoreceptor cells in the retina, but another important cell type has recently been proposed involved as well. The retinal pigment epithelium (RPE) cells have primary cilia and form a monolayer with protrusions that cover the photoreceptor outer segments. They recycle proteins that are important for function of the photoreceptors cells through phagocytosis of shed outer segments. To investigate the role of BBS1 and BBS10 proteins in RPE cell function, induced pluripotent stem cells (iPSC) from individuals with BBS and gene variants in either *BBS1* or *BBS10* were differentiated into RPE cells and investigated. The BBS cell were not able to form mature RPE cells as seen by morphology, lack of pigmentation and tight junctions, poor phagocytic capability and no expression of genes associated with mature RPE cells. Furthermore, these cells had long primary cilia, showed signs of mitochondrial stress seen as a thickened mitochondrial membrane and increased expression of *RHOT1* and *COXIV* and lastly, both Hedgehog (Hh) signaling and Wnt signaling was disturbed in these cells. Prolonged culture in the presence of agonists and antagonists targeting Hh and Wnt did not improve maturation in the BBS-RPE cells but Wnt inhibition did benefit maturation of RPE cells derived from a control iPSC line. Altogether, these data underline the importance of *BBS1* and *BBS10* for RPE cell differentiation and maturation.

Introduction:

Bardet-Biedl syndrome (BBS) is a rare autosomal recessive multisystemic ciliopathy with a prevalence of 1:59 000 in Denmark (Hjortshøj *et al.*, 2010). The most frequent symptoms are retinal dystrophy, polydactyly, cystic kidneys, learning disabilities, anosmia and obesity (Forsythe and Beales, 2013). BBS affects the primary cilium and 23 BBS proteins have been associated with the disease (Forsythe *et al.*, 2018; Shamseldin *et al.*, 2020) all with functions connected to primary cilia function, a cellular organelle important in signaling and tissue homeostasis. The proteins BBS1, BBS2, BBS4, BBS5, BBS7, BBS8, BBS9 and the BBIP10 form a complex termed the BBSome that function in ciliary intra flagellar transport (IFT) processes (Nachury *et al.*, 2007; Jin *et al.*, 2010). BBS6, BBS10 and BBS12 form a protein complex with chaperonin-functions that aid in assembly of the BBSome (Seo *et al.*, 2010). The cilium is important in cellular signaling pathways such as Hedgehog (Hh) and Wnt signaling (Mukhopadhyay and Rohatgi, 2014; Anvarian *et al.*, 2019).

Both Hh signaling and Wnt signaling has been reported disturbed in BBS. Hedgehog signaling defects most likely underlay the development of post-axial polydactyly during embryonic development for BBS-affected individuals (Gerdes *et al.*, 2007; Airik *et al.*, 2016; Patnaik *et al.*, 2019).

Hh signaling relies on the transport of receptors PATCHED1 (PTCH1), GPR161 and Smoothened (SMO) in and out of the cilium. During basal repression, PTCH1 and GPR161 are both localized in the cilium and promote the formation of GLI repressor (GLIR) through protein kinase A (PKA) preventing the transcription of target genes. When a ligand, e.g. sonic Hh, bind to PTCH1, this leads to the removal of PTCH1 and GPR161 from the cilium allowing SMO to enter and accumulate in the ciliary membrane. This promotes the

dissociation of GLI with suppressor of Fused (SUFU) and subsequent processing of GLI to its activator form (GLIA) that translocate to the nucleus turning on transcription of target genes, e.g. *GLI1* (Anvarian *et al.*, 2019). SMO activation after transport into the cilium is required before the pathway is activated (Rohatgi *et al.*, 2009). The agonist purmorphamine activates the pathway by targeting SMO and the Hh antagonist cyclopamine induces SMO accumulation in the cilium but inhibits activation of the pathway (Sinha and Chen, 2006; Rohatgi *et al.*, 2009).

Two branches of Wnt signaling have been described; planar cell polarity/non-canonical Wnt and canonical Wnt. Non-canonical Wnt signaling is involved in cell migration and does not depend on the cilium whereas several components of canonical Wnt have been found localized in the cilium. The exact role of the cilium in Wnt signaling has not been determined yet (Corbit *et al.*, 2008; He, 2008; Ocbina, Tuson and Anderson, 2009; Gerhardt *et al.*, 2016). But several BBS proteins have been suggested linked to Wnt signaling (Gerdes *et al.*, 2007; Wiens *et al.*, 2010).

The focus here is on canonical Wnt. This branch of Wnt signaling depends on β-catenin. During basal repression, a destruction complex consisting of adenomatous polypsis coli (APC), glycogen synthase kinase-3β (GSK3β) and casein kinase 1α (CK1α) and Axin targets β-catenin for degradation through the E3 ubiquitin-proteasome pathway. This leads to a decreased concentration of β-catenin in the cytoplasm. Upon ligand binding to the receptor Frizzled (FRZ), a complex of FRZ and lipoprotein-receptor-related protein (LRP) 5/6 is formed at the plasma membrane activating Disheveled (DVL) that recruits CK1, GSK3β and AXIN from the destruction complex. This leads to β-catenin stabilization and transport to the nucleus where target gene transcription is activated (Foulquier *et al.*, 2018). In this study, the canonical Wnt activator CHIR99021 is used. It works by inhibiting GSK3β and consequently the destruction complex cannot form (Bennett *et al.*, 2002). The canonical Wnt inhibitor IWR-1 is also used and it works by stabilizing AXIN in the destruction complex ultimately leading to degradation of β-catenin (Chen *et al.*, 2009).

Most quiescent cells in our bodies have primary cilia – this is also the reason why the symptom spectrum of BBS is so broad. Treatment of BBS is symptomatic, but so far nothing can be done regarding vision loss. The main affected retinal cell type in BBS is the photoreceptors (Forsythe and Beales, 2013; Datta *et al.*, 2015). Photoreceptors have a modified primary cilium connecting the inner segment, where all protein synthesis take place, with the outer segment where the light transduction cascade take place making IFT fundamental for proper photoreceptor function (Datta *et al.*, 2015; May-Simera, Nagel-Wolfrum and Wolfrum, 2017). Although it is mainly the photoreceptors that are affected in BBS, the retinal pigment epithelial (RPE) cells have gained interest through the last years. These cells have primary cilia and they carry out processes that are important for the function for the photoreceptor cells (Strauss, 2005). The RPE cells could very well be affected in BBS as well (Strauss, 2005; May-Simera, Nagel-Wolfrum and Wolfrum, 2017; May-Simera *et al.*, 2018; Patnaik *et al.*, 2019).

The RPE cells form a pigmented monolayer of cells at the back of the retina between the photoreceptors and Bruchs membrane. They form a polarized epithelium sheet with tight junctions and carry out several processes that support the function of the photoreceptor cells. They exchange nutrients, ions and metabolic waste between the photoreceptors and the blood stream – the tight junctions are essential for this to function properly. The RPE cells are able to absorb scattered light due to their pigmentation and they phagocytose shed out segments from the photoreceptor cells and recycle important proteins, such as retinal used in light transduction (Strauss, 2005).

Stem cells present an opportunity to create any cell type or cell system of interest and after the ground-breaking discovery that somatic cells can be reversed to a pluripotent state, the interest in stem cell

research has boomed (Takahashi and Yamanaka, 2006; Takahashi *et al.*, 2007; Yamanaka, 2007). Induced pluripotent stem cells (iPSC) have been used to study RPE cells, photoreceptor cells and retinal organoids (Foltz and Clegg, 2018; Hallam *et al.*, 2018). Several protocols for differentiation of stem cells into retinal RPE cells have been described. The protocol developed by David Buchholz and Dennis Clegg was chosen for its simplicity having cells in continuous adherent culture (Buchholz *et al.*, 2013). Modulation of Wnt signaling has been shown to promote RPE differentiation and the addition of canonical Wnt pathway activator CHIR99021 in the 14 day protocol increased efficiency generating up to 97.7% PMEL positive cells after the initial 14 days of directed differentiation. Another benefit from this is that a homogenous layer of RPE cells is formed so there is no need for manual dissection enrichment and high quality RPE cells can be acquired after allowing the cells to mature for three passages (P0, P1, P2) (Buchholz *et al.*, 2013; Leach *et al.*, 2015; Foltz and Clegg, 2017).

In this study, RPE cells were generated from iPSC derived from individuals suffering from BBS that have a gene variant in *BBS1* or in *BBS10*. The maturation and function of these cells were assessed, and it was investigated if prolonged modulation of Hh or Wnt signaling had any beneficial effects on RPE cell maturation and function.

Results:

Induced pluripotent stem cells (iPSC) were generated from 2 individuals suffering from Bardet-Biedl syndrome (BBS) using electroporation and non-integrating episomal plasmids. They were characterized to validate their pluripotent state and to make sure the reprogramming factors had not been integrated into the genome. Karyotype was normal. The iPSCs were assessed for expression of pluripotency related genes through immunofluorescence microscopy and analyzing expression level on harvested mRNA and found to express levels similar to control iPSC. A spontaneous differentiation assay validated the ability of the iPSC to form cells of all three germ layers proving that we created high quality iPSC that have a gene variant in either *BBS1* or *BBS10* (Hey *et al.*, 2018a, 2018b).

RPE cells were generated from these two iPSC lines and control iPSC. To assess the maturation of the generated RPE cells, morphology, pigmentation, expression of RPE-specific markers and phagocytotic capabilities was investigated at day 14 and at the end of each of the three subsequent passages, P0, P1, and P2. BBS1-RPE refer to the RPE cells derived from the patient with a *BBS1* variant, and BBS10-RPE from the patient with a *BBS10* variant. Part 1 investigates the maturation of the generated RPE cells and part 2 elucidates other phenotypes observed in the BBS-RPE cells.

Please note *– due to many technical issues, the results presented here are derived from one experiment, and should thus be regarded with caution and as very preliminary results. This is also the reason statistical analysis has not been performed yet and hence why no final conclusions are drawn in this draft, only tendencies are discussed. The implications of this will be discussed further later on. The experiment is being replicated as this draft is being written.*

PART1

Morphology:

The BBS1 and BBS10 iPSC were differentiated into RPE cells together with a healthy control iPSC line. Morphological changes were observed during the differentiation process. Fig. 1 show the development in morphology for the control (left panels), the BBS1-RPE cells (middle panels) and BBS10-RPE cells (right

panels). At day 14, the control had densely packed cells whereas both the BBS1- and BBS10-RPE cells were larger, more stretched out and spikey. During the following three passages, the control continued to be densely packed and the characteristic cobble stone morphology started to appear during P1. The morphology of both BBS-RPE was more mixed with some cells showing a long, stretched out morphology and others a more tightly packed pattern. However, the size of the cells still appeared bigger than the control cells. The BBS10-RPE had poor survival at the end of P1 and was not included at P2 due to very low cell density and survival for the rest of the experiment.

Junctions:

The formation of tight junctions is essential for the polarized structure of mature RPE cells. Investigation of the localization protein ZO-1 revealed that both control-RPE and BBS1-RPE form cell-cell junctions however their patterns looked very different. For the control-RPE, there was a strong ZO-1 expression at day 14 while the cells still looked a little disorganized. The appearance of a very structured mesh of cobblestone-like junctions was already apparent from P0 and persisted for the duration of the experiment in P1 and P2 (Fig. 2 A top panels). The BBS1-RPE did express a somewhat organized pattern of ZO-1 from day 14 and in P0, however the cells were lager and during P0, P1 and P2 the edges became less defined with a zig-zag pattern developing instead (Fig. 2 A bottom panels). This led us to believe that the BBS1-RPE might not have formed tight junctions. To investigate the type of junction these cells had formed, we performed electron microscopy and RNA expression studies of genes encoding proteins involved in different types of junctions; ZO-1, Claudin2 and N-Cadherin (encoded by the *CDH2* gene). Electron microscopy pictures of the control-RPE revealed a tight, zipper-like junction whereas the BBS1-RPE had a much looser cell-cell connection resembling a desmosome (Fig. 2 B, un-edited pictures in supplementary figure 1 A and B). The expression of the genes encoding the junctional protein ZO-1 supported the immunofluorescence images showing expression of the protein in control-RPE, BBS1-RPE and BBS10-RPE (Fig. 2 C). *CLAUDIN2* is a late marker of tight-junctions (Rizzolo, 2007) and the expression of the gene in control-RPE increased during the differentiation protocol from a very low level in the original iPSC used to P2 where it reached the highest expression level. For both BBS1-RPE and BBS10-RPE there was a slight increase in expression of *CLAUDIN2* at day 14 but then the expression was low during the rest of the experiment (Fig. 2 D). These results indicate that control-RPE formed tight junctions but the BBS-derived RPE did not. The expression of *CDH2* decreased in the control-RPE during the differentiation but in both the BBS1-RPE and the BBS10-RPE the expression increased, indicating that a different type of junction was forming in these cells as N-cadherin is found in adherent junctions and desmosomes (Green *et al.*, 2010) (Fig. 2 E).

Pigmentation:

A second hallmark of RPE cells is pigmentation, so they are able to absorb scattered light (Strauss, 2005). We investigated the expression of the genes encoding proteins PMEL, DCT and MART1 all of which are involved in producing pigment granules and thus are markers of melanosomes at different stages of maturation (Raposo and Marks, 2007; Yamaguchi and Hearing, 2014). Their overall expression pattern looked very similar, with a high expression that increased over time in the control-RPE and a low/close to zero expression in BBS1-RPE and BBS10-RPE (Fig. 3 A and B). Electron microscopy images at P1 revealed melanosomal structures in the control-RPE (Fig. 3 C left panel). These structures were not present in BBS1-RPE that had an abundance of dense membranous structures (Fig. 3 C right panel) varying in size. These two observations and the fact that melanosomes and lysosomes are both derived from early endosomes (Orlow, 1995; Raposo and Marks, 2007) led us to investigate if the BBS cells had a higher level of early stage melanosomes, endosomes and lysosomes than the control cells. *MART1* expression was investigated, as the MART1 protein is required for PMEL maturation and is present in late endosomes and early melanosomes.

Only control cells showed expression of *MART1* (fig. 3 D) and it had the highest expression level at P0, perhaps indicating that this is an early marker of melanosomes in this case. The GPR143 protein is present at early stage melanosomes lysosomes (Bassi *et al.*, 1996; Cortese *et al.*, 2005). We observed robust expression of the gene in the control-RPE and a somewhat lower expression in the BBS1-RPE and very low in BBS10-RPE (fig. 3 E). This made us investigate the expression of the gene encoding LAMP1 (lysosome associated membrane protein 1), which is present in lysosomes and late endosomes (Humphries, Szymanski and Payne, 2011; Cheng *et al.*, 2018; Sjödin *et al.*, 2019), to see if the BBS-RPE cells had lysosomes or late endosomes. Both BBS1-RPE and BBS10-RPE showed a high expression of *LAMP1*, compared to the control-RPE, that appear to increase during the time course of the differentiation (fig. 3 F). Since *MART1* expression was low in the BBS-RPE we speculated if an earlier marker of endosomes might be present. The gene encoding marker of early endosomes, EEA1 (early endosomal antigen 1) (Lakadamyali, Rust and Zhuang, 2006; Cheng *et al.*, 2018), showed an expression pattern similar to expression of *LAMP1*, where the control-RPE had a decreasing expression of these genes and BBS1- and BBS10-RPE had an increasing expression during the differentiation time course (fig. 3 G). Thus, in this experiment, only the control-RPE cells expressed genes important for melanosomes whereas the BBS-RPE cells had a higher expression level of genes involved in formation of lysosomes and early endosomes.

In figure 4, the pigmentation process can be followed for control-RPE (left panels), BBS1-RPE (middle panels) and BBS10-RPE (right panels). From P0 and onwards, bright field images were included. Pigmentation can be observed as early as P0 in all three cells types, with the BBS-RPE seeming to have a darker appearance than the control-RPE. However, the pigmentation was much less pronounced at P1 for the BBS-RPE cells whereas it increased for the control RPE-cells and was present in a more homogenous layer. At P2 the pigmentation of BBS1-RPE almost seemed gone when it was compared to the control cells that had formed a sheet of darkly pigmented cells.

Maturation

Expression of *RPE65* was monitored throughout the differentiation with immunofluorescence microscopy and qPCR. In control-RPE anti-RPE65 antibody increased in intensity over time (Fig. 5 A top panels). Supplementary figure 2 shows the images with a higher magnification. BBS1-RPE did not show any RPE65 signal (Fig. 5 A lower panels). RNA expression levels confirmed this finding; some expression in P0 and P1 was visible for the control RPE and high expression in P2 where BBS1-RPE had zero expression of *RPE65* (Fig. 5 B). *BEST1* expression was also investigated, and the BBS1-RPE cells did not have any expression of this gene either. The control-RPE showed high expression of *BEST1* at P1 and P2 (Fig. 5 C). Expression of *MITF*, encoding a marker of the optic vesicle and RPE cells, was investigated to see if the BBS-RPE cells had expression of any eye-field proteins. There was a low expression level of *MITF* in BBS1-RPE and BBS10-RPE but control-RPE had a much higher expression (Fig. 5 D). As a final check, expression of the stem cell-associated gene *DNMT3B* was investigated. Only stem cells from control, BBS1 and BBS10 showed expression of *DNMT3B* (Fig. 5 E).

Phagocytosis:

Phagocytic capabilities of the RPE were tested at P2 in control-RPE and in BBS1-RPE using bioparticles that emit red fluorescence when engulfed into acidic phagosomes. Only control-RPE showed phagocytosis shown in Fig. 6 as red dots surrounding the nuclei. There was a small fraction of red dots in BBS1-RPE, but the signal was very low compared to control-RPE.

Altogether for this experiment, these data indicate that only the control-RPE matured to obtain pigmentation, tight junctions, phagocytic activity and expression of RPE-specific markers whereas BBS1-

and BBS10-RPE only seemed to lose expression of stem cell-related gene *DNMT3B* and showed an increase in proteins associated with lysosomes and endosomes. The cells that harbor a *BBS1* or *BBS10* variant failed to produce mature RPE cells under these experimental conditions. The overall results from part 1 indicated that *BBS1* and *BBS10* may be important for RPE cell differentiation and maturation.

PART 2

Cilia:

As BBS affects the primary cilium, these organelles were investigated. IF pictures showed increased ciliary length in BBS1-RPE cells compared to control-RPE (Fig. 7 A). This was especially clear at P2. To validate this finding, expression of the gene encoding the ciliary membrane protein ARL13B was measured through qPCR. The control-RPE cells showed a slight increase in *ARL13B* expression from the stem cell state to day 14 and P0, but at P1 and P2 the expression was approximately half than at day 14. For both BBS-RPE cells, *ARL13B* expression was higher than the control-RPE at P0, P1 and P2 (Fig. 7 B). This underlined the observed long cilia with IF where the BBS1-RPE cells at P2 had exceptionally long cilia compared to the control-RPE. Whether this had anything to do with the IFT machinery was investigated by analyzing expression of the genes encoding IFT88, which is part of the IFTB complex, and IFT 140, which is part of the IFTA complex (Nakayama and Katoh, 2018). Both IFT genes seemed to have a higher expression level in the BBS-RPE cells compared to control where especially *IFT140* expression drops at P1 and P2 (Fig. 7 C and D). This could indicate an increased IFT activity in BBS-RPE cells.

Mitochondria:

When the iPSC-derived RPE cells were analyzed by electron microscopy to visualize junctions, pigmentation and microvilli, abnormal mitochondria were observed in BBS1-RPE (FIG8 A). The control iPSC-RPE had normal mitochondria with clearly visible membrane folds and cristae. In BBS1-RPE, the membrane was much denser indicating that these cells may be stressed. As we only analyzed cells from P1 for electron microscopy, we wanted to see if there was an effect during the time course of RPE differentiation on the BBS-RPE cells. qPCR using taqman probes for the genes encoding the mitochondria proteins COXIV and RHOT1 were analyzed at day 14, P0, P1 and P2. The expression pattern for both genes looked very similar, with a high expression at P0 for control-RPE, BBS1-RPE and BBS10-RPE. At P1 and P2 the expression dropped in the control-RPE whereas it increased in BBS1-RPE and BBS10-RPE who both had higher expression level of both *COXIV* and *RHOT1* than control-RPE cells (Fig. 8 B and C).

Wnt:

BBS cells have several signaling disruptions and the literature states that BBS cells have increased Wnt signaling (Gerdes *et al.*, 2007). This led us to speculate if the addition of pathway agonists or antagonists of Hh or Wnt signaling pathways at a low concentration for a prolonged time during P1 and P2 would promote RPE maturation in both control-RPE and BBS-RPE cells. To modify Hh and Wnt signaling, the agonist CHIR99021 (1.5 µM) and antagonist Endo-IWR-1 (10 µM) and 0.5 µM purmorphamine (Hh agonist) and 10 µM cyclopamine (Hh antagonist) was added during P1 and P2 three days post splitting and for the duration of the passage.

We investigated the sub-cellular localization of β-catenin in control-RPE and BBS1-RPE at P1 and P2 (Fig. 9 A). Control-RPE showed a combination of nuclear and membrane localization of β-catenin in both P1 and P2 under untreated, +CHIR99021, +purmorphamine and +cyclopamine. There was a strong nuclear

localization of β-catenin when IWR-1 was added. This was surprising and puzzling as nuclear localization is associated with Wnt pathway activation. The BBS1-RPE had a strong nuclear localization of β-catenin at both passages and under all conditions indicating active Wnt signaling that was not affected by the added pathway modulators.

Fig. 9B show *AXIN* expression, a Wnt target gene, in control-RPE, BBS1-RPE and BBS10-RPE in unstimulated cells. Both BBS1-RPE and BBS10-RPE had higher expression levels of *AXIN* compared to control-RPE indicating that these cells had a higher level of Wnt signaling.

Looking deeper into the effects of Wnt signaling modulation, mRNA expression of markers associated with maturation, junctions, cilia, Wnt activation and mitochondria was investigated. In Fig. 10 a "+" indicate addition of CHIR99021 and thus Wnt activation and a "–" indicate addition of IWR-1 and Wnt inhibition. Hh signaling modulation was not included as no change was visible (data not shown).

When Wnt signaling was inhibited, there was an increase in *RPE65*, *BEST1* and a slight increase in *MITF* expression in control-RPE whereas Wnt stimulation led to a decrease of all three (Fig. 10 A, B and C). This effect was not observed for the BBS-RPE cells, where only *MITF* expression showed a very slight increase with Wnt inhibition. The expression pattern of *RPE65* and *BEST1* did not change and remained very low/close to zero. Expression of the stem cell marker *DNMT3B* did not change for any of the cell types or treatments (Fig. 10 D). As mentioned above, expression of *ZO-1* was higher in the BBS-RPE cells. This difference became more pronounced when Wnt was inhibited (Fig. 10 E) but when Wnt was activated, the expression decreased to levels comparable to the control cells. This pattern was not obvious for *CLAUDIN2*, where only the control had increased expression with Wnt inhibition and the BBS-RPE both remained very low (Fig. 10 F). Wnt modulation did not seem to induce formation of tight junctions in BBS-RPE. Addition of CHIR99021 seemed to rescue ciliary length, as seen by a decrease in expression of *ARL13B*, in BBS1-RPE and BBS10-RPE. There was little effect on control-RPE (Fig. 10 G). *AXIN* expression was higher in the BBS1-RPE and BBS10-RPE and was not changed by Wnt modulation. A small effect was seen in control-RPE at P1, slight increase in expression of *AXIN* with CHIR99021, but not at P2 (Fig. 10 H). Interestingly, Wnt modulation seemed to have an effect on expression of the mitochondrial markers *COXIV* and *RHOT1*. Wnt activation lowered their expression to levels comparable to control-RPE whereas Wnt inhibition led to an increase in both *COXIV* and *RHOT1* (Fig. 10 I-J).

All together these data show a tendency that Wnt signaling does influence RPE cell maturation. Inhibition of Wnt using endo-IWR1 lead to an increase in mature RPE gene expression (*RPE65*, *BEST1*, and slightly *MITF* expression) and increased *CLAUDIN2* expression in control-RPE. However, modulation of Wnt did not help the BBS-RPE to become more mature when used at these timepoints. Different timepoints of Wnt and Hh modulation should be tested further. More experiments are necessary to determine the exact WNT-defect observed in the BBS-RPE cells.

Hh:

Localization of Hh receptor SMO was also investigated under Hh and Wnt modulation in control-RPE and BBS1-RPE (see Fig. 11). In control-RPE SMO localized to the membrane under all treatments and also localized to cilia when purmorphamine or cyclopamine was added. This is in accordance with the mode of action of these two pathway modulators. In BBS1-RPE SMO localized to both membrane and cilia under all tested conditions.

In conclusion for part 2, the BBS-RPE had long cilia, they had more mitochondria and in addition, Hh and Wnt signaling seemed disturbed. Modulation of Wnt and Hh signaling did not have an effect on BBS-RPE cell maturation under the tested conditions.

In summary, data from part 1 and part 2 show the importance of the BBS proteins BBS1 and BBS10 in RPE cell development, maturation and function.

Discussion and Perspectives:

Even though these data are derived from one experiment, there are several things that can be discussed – and several things to consider when the experiment is replicated. In the following sections, the findings from this experiment will be discussed followed by a discussion of how the experiment can be optimized and what should be included in the future before publication. No conclusions can be drawn from this data alone, but a discussion will shed light on potential links to existing knowledge from other experiments and inspire more things to test in the future.

In this experiment, the BBS-RPE were not able to form mature RPE cells. The fibroblast cell the BBS-RPE are derived from show defective Hh signaling and ciliary morphological changes (manuscript in prep.) in accordance with literature (Hernandez-Hernandez *et al.*, 2013; Liu *et al.*, 2014). The BBS-RPE also seemed to have signaling deficiencies as shown by SMO and β-catenin localization. Whether these ciliary defects are the reason the RPE differentiation was unsuccessful in these cells needs further investigation, e.g. through CRISPR-Cas9 induction of the patient variant in control iPSC or by correction of the variant in the patient iPSC followed by RPE differentiation and functional assays. If possible, the inclusion of non-affected family members would also be a good control – or age and sex equivalent control iPSC (Foltz and Clegg, 2018). Both Hh and Wnt signaling are important during embryonic development and for the RPE differentiation protocol to be successful. Whether the signaling defects observed in fibroblasts and RPE are also present in the iPSC cells remains to be investigated but one can speculate that the observed Hh signaling deficiency in the original fibroblast cells may be enough to disturb the RPE differentiation process perhaps making it inefficient.

Shimada *et al.* investigated the effects of a *CEP290* gene variant in fibroblast cells and in iPSC-derived 3D organoid photoreceptor cells and found severe phenotype of defective ciliogenesis in the photoreceptor cells but not in the fibroblast cells. This highlights the importance of using stem cell model systems to investigate other cell types that are known or suspected to be affected by the gene variant (Shimada *et al.*, 2017).

BBS-RPE cells did not gain proper pigmentation and showed formation of membranous structures when investigated by electron microscopy. We speculate if these vesicles might be malformed melanosomes (Gidanian *et al.*, 2008). RNA studies showed increased expression of endosomal and lysosomal proteins in BBS-RPE cells and not melanosomal proteins.

The BBS1-RPE had mitochondria with dense membranes, supported by increased expression of mitochondrial markers in the RNA studies, this could indicate mitochondrial stress in these cells. This needs to be further investigated, to see if this is also the case in BBS10-RPE and at P2. Mitochondrial stress may add to the observed abnormal phenotype of the BBS-RPE cells. The morphology of the mitochondria in BBS1-RPE cells look abnormal but whether this is due to the BBS1 variant or other factors should be investigated further. The cilium has been linked to mitochondrial function through regulation of mTOR and autophagy (Walz, 2017). Abnormal ciliary function and mitochondrial defects have been observed in

heterotaxy congenital heart disease (Chaudhry and Henderson, 2019). A study of the effects of BBS on mitochondria could add levels of complexity to this disease.

Wnt modulation did not show an effect on BBS-RPE cell maturation, but control-RPE benefitted from Wnt inhibition. This is in accordance with the finding that Wnt needs to be suppressed for RPE cells to mature properly (May-Simera *et al.*, 2018). The fact that Wnt cannot be suppressed in the BBS-RPE may explain why these cells are not able to form mature RPE cells.

BBS-RPE cells in this experiment had long cilia. This is in contrast to previous findings by Patnaik *et al.* who found short cilia in the RPE cells of *BBS6* and *BBS8* knock-out mice (Patnaik *et al.*, 2019). Whether this difference is due to investigation of different BBS proteins remains to be determined.

All of these observations need to be replicated before any conclusion can be drawn as the results seen in this experiment may be due to technical differences and not actual biological differences caused by the *BBS* variants. The RPE differentiation protocol needs to be adapted to the BBS-iPSC cell lines individually e.g. with respect to initial cell seeding density. The inclusion of flow cytometry at several time points would aid in determining if the right cell types are formed during the differentiation process and at the end of the protocol to see if the generated RPE cells are as mature as they can be. The control RPE still had short cilia which could indicate that they may not be fully mature at day 30 in P2. Growing the cells on trans-well membranes could also help the maturation process by allowing the RPE cells form a polarized barrier as they do *in vivo*. Measuring the media composition of the inner and outer chamber in this culture system can also be used to asses maturity. This system was tested but unfortunately these cells had to be discarded due to a mycoplasma infection.

The RPE cells serve important functions in aiding the photoreceptors and protecting our sense of vision. Although there does not seem to be a clinical effect on RPE cells when BBS patients are investigated by doctors, the results presented here together with other studies show that the primary cilium in RPE cells is affected in BBS both in cell cultures and in mouse models. May-Simera *et al.* actually show that the RPE cells are affected before the photoreceptor cells in ciliopathy mice (May-Simera *et al.*, 2018). The main reason for photoreceptor degeneration is most likely due to ciliary transport defects in the photoreceptor cells themselves (Datta *et al.*, 2015) but if the RPE are stressed, or work somewhat poorer, this could potentially speed up the rate at which the photoreceptors die. Further studies are needed to dissect the exact mechanism of the observed effects on RPE cells in BBS but if a delay in vision-loss could be obtained through therapy of the RPE cells, that is something worth investigating further.

Materials and methods:

iPSC generation and culture

All iPSCs were cultured on hESC-qualified Corning® Matrigel® (Corning #354277) in mTeSR™1 (STEMCELL Technologies #85850). Reprogramming of BBS1-iPSC is described in (Hey *et al.*, 2018a) and BBS10-iPSC in (Hey *et al.*, 2018b).

RPE Differentiation

The protocol developed by Dennis Clegg (Buchholz *et al.*, 2013; Leach *et al.*, 2015; Foltz and Clegg, 2017) was applied. Briefly, iPSCs were cultured with different small molecules and growth factors for 14 days and then left to mature for three passages (P0, P1 and P2) of 28-30 days in continuous adherent 2D culture. The combination of growth factors added and small molecules during the initial 14 days are as follows;

- Day 0 and day 1: 10mM NIC, 50ng/mL noggin, 10ng/mL DKK-1, 10ng/ml IGF-1
- day 2: 10mM NIC, 5 ng/µL FGF-basic, 10ng/mL noggin, 10ng/mL DKK-1, 10 ng/mL IGF-1.
- Day 4: 100 ng/mL activin A, 10 ng/mL DKK-1, 10 ng/mL IGF-1.
- Day 6: 100 ng/mL activin A, 10 µM SU 5402
- Day 8, 10, 12: 100ng/mL activin A, 10 µM SU 5402, 3 µM CHIR99021

After the initial 14 days, the iPSC-RPE cells were cultured in X-vivo 10 on growth factor reduced Matrigel-coated surfaces. During the last two passages, a fraction of cells was treated with 1.5 µM CHIR99021, 10 µM IWR-1, 0.5 µM purmorphamine or 10 µM cyclopamine.

At the end of the initial 14 days, and at the end of all three passages P0, P1 and P2, a fraction of the cells was harvested for RNA studies and immunofluorescence microscopy. End of P2 (P2 day 30) is considered the endpoint of the differentiation.

qRT-PCR

RNA was purified using GeneJET RNA purification kit (Thermo Fisher Scientific #K0732) and synthesized using high capacity cDNA kit (Applied Biosystems # 4368814). Taqman reagents and probes were used, a list of applied Taqman probes can be found in table 1. All Taqman probes are from Thermo Fisher Scientific. All calculations were performed as ΔΔCT and values were normalized to GAPDH and the control-RPE at day 14.

Immunofluorescence Microscopy

Cells were grown on Matrigel coated Lab-Tek 8 well chamber slides (Thermo Fisher Scientific #177402). Fixation was done in 4% paraformaldehyde (Hounisen), permeabilization for 15 minutes in 0.2% TritonX-100 in PBS, blocking in 3% BSA in permeabilization buffer for 1 hour, all at room temperature. Incubation with primary antibody was done at room temperature for two hours or at 4°C overnight and secondary antibody for 45 minutes at room temperature. All antibodies were diluted in 3% BSA, details on antibodies and dilutions are found in table 2. DAPI was used to stain the nuclei.

Electron microscopy

Cells were grown on Matrigel coated 13mm Thermanox Plastic coverslips (NUNC #174950) and cultured as described above. Fixation and processing were done as described by Høffding *et al*. Briefly, the cells were fixed with 3% Glutaraldehyde (Merck #1042390250) diluted in 0.1M Na-phosphate buffer for 1 hour at 4°C and stored in 0.1M Na-phosphate buffer until further processing (Høffding and Hyttel, 2015).

Phagocytosis assay

For this assay, cells were cultured on Matrigel coated Lab-Tek 8 well chamber slides (Thermo Fisher Scientific #177402) and incubated with pHrodo *Escherichia coli* BioParticles, red (Life Technologies #P35361) dissociated in Invitrogen™ Molecular Probes™ Live Cell Imaging Solution (Invitrogen™ #A14291DJ) for 2 hours at 37°C without CO_2. Then the cells were washed with PBS to remove un-phagocytosed particles and incubated with Live Cell Imaging Solution for another 4 hours before they were fixed, stained with DAPI and mounted for analysis as described in "*Immunofluorescence Microscopy"*-section (Duong *et al.*, 2018).

References

Airik, R. *et al.* (2016) 'SDCCAG8 Interacts with RAB Effector Proteins RABEP2 and ERC1 and Is Required for Hedgehog Signaling', *PLOS ONE*. Edited by Y. Komarova, 11(5), p. e0156081. doi: 10.1371/journal.pone.0156081.

Anvarian, Z. *et al.* (2019) 'Cellular signalling by primary cilia in development, organ function and disease', *Nature Reviews Nephrology*, 15(4), pp. 199–219. doi: 10.1038/s41581-019-0116-9.

Bassi, M. T. *et al.* (1996) 'Cloning of the murine homolog of the ocular albinism type 1 (OA1) gene: sequence, genomic structure, and expression analysis in pigment cells.', *Genome Research*, 6(9), pp. 880–885. doi: 10.1101/gr.6.9.880.

Bennett, C. N. *et al.* (2002) 'Regulation of Wnt Signaling during Adipogenesis', *Journal of Biological Chemistry*, 277(34), pp. 30998–31004. doi: 10.1074/jbc.M204527200.

Buchholz, D. E. *et al.* (2013) 'Rapid and Efficient Directed Differentiation of Human Pluripotent Stem Cells Into Retinal Pigmented Epithelium', *STEM CELLS Translational Medicine*, 2(5), pp. 384–393. doi: 10.5966/sctm.2012-0163.

Chaudhry, B. and Henderson, D. J. (2019) 'Cilia, mitochondria, and cardiac development', *Journal of Clinical Investigation*. Am Soc Clin Investig, 129(7), pp. 2666–2668. doi: 10.1172/JCI129827.

Chen, B. *et al.* (2009) 'Small molecule–mediated disruption of Wnt-dependent signaling in tissue regeneration and cancer', *Nature Chemical Biology*, 5(2), pp. 100–107. doi: 10.1038/nchembio.137.

Cheng, X.-T. *et al.* (2018) 'Characterization of LAMP1-labeled nondegradative lysosomal and endocytic compartments in neurons', *The Journal of Cell Biology*, 217(9), pp. 3127–3139. doi: 10.1083/jcb.201711083.

Corbit, K. C. *et al.* (2008) 'Kif3a constrains β-catenin-dependent Wnt signalling through dual ciliary and non-ciliary mechanisms', *Nature Cell Biology*, 10(1), pp. 70–76. doi: 10.1038/ncb1670.

Cortese, K. *et al.* (2005) 'The Ocular Albinism Type 1 (OA1) Gene Controls Melanosome Maturation and Size', *Investigative Opthalmology & Visual Science*, 46(12), p. 4358. doi: 10.1167/iovs.05-0834.

Datta, P. *et al.* (2015) 'Accumulation of non-outer segment proteins in the outer segment underlies photoreceptor degeneration in Bardet–Biedl syndrome', *Proceedings of the National Academy of Sciences*, 112(32), pp. E4400–E4409. doi: 10.1073/pnas.1510111112.

Duong, T. T. *et al.* (2018) 'Use of induced pluripotent stem cell models to probe the pathogenesis of Choroideremia and to develop a potential treatment', *Stem Cell Research*. The Authors, 27, pp. 140–150. doi: 10.1016/j.scr.2018.01.009.

Foltz, L. P. and Clegg, D. O. (2017) 'Rapid, Directed Differentiation of Retinal Pigment Epithelial Cells from Human Embryonic or Induced Pluripotent Stem Cells', *Journal of Visualized Experiments*, e56274(128). doi: 10.3791/56274.

Foltz, L. P. and Clegg, D. O. (2018) 'Patient-derived induced pluripotent stem cells for modelling genetic retinal dystrophies', *Progress in Retinal and Eye Research*. Elsevier, (September), pp. 1–13. doi: 10.1016/j.preteyeres.2018.09.002.

Forsythe, E. *et al.* (2018) 'Managing Bardet-Biedl syndrome-now and in the future', *Frontiers in Pediatrics*, 6(February), pp. 1–8. doi: 10.3389/fped.2018.00023.

Forsythe, E. and Beales, P. L. (2013) 'Bardet-Biedl syndrome', *European Journal of Human Genetics*, 21(1), pp. 8–13. doi: 10.1038/ejhg.2012.115.

Foulquier, S. *et al.* (2018) 'WNT Signaling in Cardiac and Vascular Disease', *Pharmacological Reviews*. Edited by M. C. Michel, 70(1), pp. 68–141. doi: 10.1124/pr.117.013896.

Gerdes, J. M. *et al.* (2007) 'Disruption of the basal body compromises proteasomal function and perturbs intracellular Wnt response', *Nature Genetics*, 39(11), pp. 1350–1360. doi: 10.1038/ng.2007.12.

Gerhardt, C. *et al.* (2016) 'The cilia-regulated proteasome and its role in the development of ciliopathies and cancer', *Cilia*. BioMed Central, 5(1), pp. 1–14. doi: 10.1186/s13630-016-0035-3.

Gidanian, S. *et al.* (2008) 'Melanosomal Damage in Normal Human Melanocytes Induced by UVB and Metal Uptake—A Basis for the Pro-oxidant State of Melanoma', *Photochemistry and Photobiology*, 84(3), pp. 556–564. doi: 10.1111/j.1751-1097.2008.00309.x.

Green, K. J. *et al.* (2010) 'Intercellular Junction Assembly, Dynamics, and Homeostasis', *Cold Spring Harbor Perspectives in Biology*, 2(2), pp. a000125–a000125. doi: 10.1101/cshperspect.a000125.

Hallam, D. *et al.* (2018) 'Human-Induced Pluripotent Stem Cells Generate Light Responsive Retinal Organoids with Variable and Nutrient-Dependent Efficiency', *STEM CELLS*, 36(10), pp. 1535–1551. doi: 10.1002/stem.2883.

He, X. (2008) 'Cilia put a brake on Wnt signalling', *Nature Cell Biology*, 10(1), pp. 11–13. doi: 10.1038/ncb0108-11.

Hernandez-Hernandez, V. *et al.* (2013) 'Bardet–Biedl syndrome proteins control the cilia length through regulation of actin polymerization', *Human Molecular Genetics*, 22(19), pp. 3858–3868. doi: 10.1093/hmg/ddt241.

Hey, C. A. B. *et al.* (2018a) 'Generation of induced pluripotent stem cells, KCi001-A derived from a Bardet-Biedl syndrome patient compound heterozygous for the BBS1 variants c.1169T>G/c.1135G>C', *Stem Cell Research*. Elsevier, 31(February), pp. 235–239. doi: 10.1016/j.scr.2018.08.005.

Hey, C. A. B. *et al.* (2018b) 'Generation of induced pluripotent stem cells, KCi002-A derived from a patient with Bardet-Biedl syndrome homozygous for the BBS10 variant c.271insT', *Stem Cell Research*. Elsevier, 33(February), pp. 46–50. doi: 10.1016/j.scr.2018.09.013.

Hjortshøj, T. D. *et al.* (2010) 'Bardet-Biedl syndrome in Denmark-report of 13 novel sequence variations in six genes', *Human Mutation*, 31(4), pp. 429–436. doi: 10.1002/humu.21204.

Høffding, M. K. and Hyttel, P. (2015) 'Ultrastructural visualization of the Mesenchymal-to-Epithelial Transition during reprogramming of human fibroblasts to induced pluripotent stem cells', *Stem Cell Research*, 14(1), pp. 39–53. doi: 10.1016/j.scr.2014.11.003.

Humphries, W. H., Szymanski, C. J. and Payne, C. K. (2011) 'Endo-Lysosomal Vesicles Positive for Rab7 and LAMP1 Are Terminal Vesicles for the Transport of Dextran', *PLoS ONE*. Edited by S. H. Caplan, 6(10), p. e26626. doi: 10.1371/journal.pone.0026626.

Jin, H. *et al.* (2010) 'The conserved bardet-biedl syndrome proteins assemble a coat that traffics membrane proteins to Cilia', *Cell*. Elsevier Ltd, 141(7), pp. 1208–1219. doi: 10.1016/j.cell.2010.05.015.

Lakadamyali, M., Rust, M. J. and Zhuang, X. (2006) 'Ligands for Clathrin-Mediated Endocytosis Are Differentially Sorted into Distinct Populations of Early Endosomes', *Cell*, 124(5), pp. 997–1009. doi: 10.1016/j.cell.2005.12.038.

Leach, L. L. *et al.* (2015) 'Canonical/ -Catenin Wnt Pathway Activation Improves Retinal Pigmented Epithelium Derivation From Human Embryonic Stem Cells', *Investigative Ophthalmology & Visual Science*, 56(2), pp. 1002–1013. doi: 10.1167/iovs.14-15835.

Liu, Y. P. *et al.* (2014) 'Ciliopathy proteins regulate paracrine signaling by modulating proteasomal degradation of mediators', *Journal of Clinical Investigation*, 124(5), pp. 2059–2070. doi: 10.1172/JCI71898.

May-Simera, H. L. *et al.* (2018) 'Primary Cilium Mediated Retinal Pigment Epithelium Maturation is Retarded in Ciliopathy Patient Cells', *Cell Reports*. ElsevierCompany., 22(1), pp. 189–205. doi: 10.1016/j.celrep.2017.12.038.

May-Simera, H. louise, Nagel-Wolfrum, K. and Wolfrum, U. (2017) 'Cilia - The sensory antennae in the eye', *Progress in Retinal and Eye Research*. Elsevier Ltd, 60, pp. 144–180. doi: 10.1016/j.preteyeres.2017.05.001.

Mukhopadhyay, S. and Rohatgi, R. (2014) 'G-protein-coupled receptors, Hedgehog signaling and primary cilia', *Seminars in Cell & Developmental Biology*. Elsevier Ltd, 33, pp. 63–72. doi: 10.1016/j.semcdb.2014.05.002.

Nachury, M. V. *et al.* (2007) 'A Core Complex of BBS Proteins Cooperates with the GTPase Rab8 to Promote Ciliary Membrane Biogenesis', *Cell*, 129(6), pp. 1201–1213. doi: 10.1016/j.cell.2007.03.053.

Nakayama, K. and Katoh, Y. (2018) 'Ciliary protein trafficking mediated by IFT and BBSome complexes with the aid of kinesin-2 and dynein-2 motors', *Journal of Biochemistry*, 163(3), pp. 155–164. doi: 10.1093/jb/mvx087.

Ocbina, P. J. R., Tuson, M. and Anderson, K. V. (2009) 'Primary Cilia Are Not Required for Normal Canonical Wnt Signaling in the Mouse Embryo', *PLoS ONE*. Edited by C.-P. Heisenberg, 4(8), p. e6839. doi: 10.1371/journal.pone.0006839.

Orlow, S. J. (1995) 'Melanosomes Are Specialized Members of the Lysosomal Lineage of Organelles', *Journal of Investigative Dermatology*. Elsevier Masson SAS, 105(1), pp. 3–7. doi: 10.1111/1523-1747.ep12312291.

Patnaik, S. R. *et al.* (2019) 'Bardet–Biedl Syndrome proteins regulate cilia disassembly during tissue maturation', *Cellular and Molecular Life Sciences*. Springer International Publishing, 76(4), pp. 757–775. doi: 10.1007/s00018-018-2966-x.

Raposo, G. and Marks, M. S. (2007) 'Melanosomes — dark organelles enlighten endosomal membrane transport', *Nature Reviews Molecular Cell Biology*, 8(10), pp. 786–797. doi: 10.1038/nrm2258.

Rizzolo, L. J. (2007) 'Development and Role of Tight Junctions in the Retinal Pigment Epithelium', in *International Review of Cytology*, pp. 195–234. doi: 10.1016/S0074-7696(07)58004-6.

Rohatgi, R. *et al.* (2009) 'Hedgehog signal transduction by Smoothened: Pharmacologic evidence for a 2-step activation process', *Proceedings of the National Academy of Sciences*, 106(9), pp. 3196–3201. doi: 10.1073/pnas.0813373106.

Seo, S. *et al.* (2010) 'BBS6, BBS10, and BBS12 form a complex with CCT/TRiC family chaperonins and mediate BBSome assembly', *Proceedings of the National Academy of Sciences*, 107(4), pp. 1488–1493. doi: 10.1073/pnas.0910268107.

Shamseldin, H. E. *et al.* (2020) 'The morbid genome of ciliopathies: an update', *Genetics in Medicine*. Springer US, 0(0), pp. 1–10. doi: 10.1038/s41436-020-0761-1.

Shimada, H. *et al.* (2017) 'In Vitro Modeling Using Ciliopathy-Patient-Derived Cells Reveals Distinct Cilia Dysfunctions Caused by CEP290 Mutations', *Cell Reports*. ElsevierCompany., 20(2), pp. 384–396. doi: 10.1016/j.celrep.2017.06.045.

Sinha, S. and Chen, J. K. (2006) 'Purmorphamine activates the Hedgehog pathway by targeting Smoothened', *Nature Chemical Biology*, 2(1), pp. 29–30. doi: 10.1038/nchembio753.

Sjödin, S. *et al.* (2019) 'Endo-lysosomal proteins and ubiquitin CSF concentrations in Alzheimer's and Parkinson's disease', *Alzheimer's Research & Therapy*. Alzheimer's Research & Therapy, 11(1), p. 82. doi: 10.1186/s13195-019-0533-9.

Strauss, O. (2005) 'The Retinal Pigment Epithelium in Visual Function', *Physiological Reviews*, 85(3), pp. 845–881. doi: 10.1152/physrev.00021.2004.

Takahashi, K. *et al.* (2007) 'Induction of pluripotent stem cells from adult human fibroblasts by defined factors', *cell*. Elsevier, 131(5), pp. 861–872.

Takahashi, K. and Yamanaka, S. (2006) 'Induction of pluripotent stem cells from mouse embryonic and adult fibroblast cultures by defined factors', *cell*. Elsevier, 126(4), pp. 663–676.

Walz, G. (2017) 'Role of primary cilia in non-dividing and post-mitotic cells', *Cell and Tissue Research*. Cell and Tissue Research, 369(1), pp. 11–25. doi: 10.1007/s00441-017-2599-7.

Wiens, C. J. *et al.* (2010) 'Bardet-Biedl Syndrome-associated Small GTPase ARL6 (BBS3) Functions at or near the Ciliary Gate and Modulates Wnt Signaling', *Journal of Biological Chemistry*, 285(21), pp. 16218–16230. doi: 10.1074/jbc.M109.070953.

Yamaguchi, Y. and Hearing, V. J. (2014) 'Melanocytes and Their Diseases', *Cold Spring Harbor Perspectives in Medicine*, 4(5), pp. a017046–a017046. doi: 10.1101/cshperspect.a017046.

Yamanaka, S. (2007) 'Strategies and New Developments in the Generation of Patient-Specific Pluripotent Stem Cells', *Cell Stem Cell*, 1(1), pp. 39–49. doi: 10.1016/j.stem.2007.05.012.

Figure Legends:

Figure 1: Morphological changes of the cells were observed during the course of RPE differentiation. Control-RPE had small tightly packed cells and developed the characteristic cobblestone morphology during P1. BBS1- and BBS10-RPE had a more mixed morphology with larger and more elongated cells. N=1.

Figure 2: The formation of tight junctions was monitored at day 14, P0, P1 and P2. A: Control RPE established an organized junction pattern with a cuboidal shape at P0 and it is maintained at P1 and P2. BBS1-RPE had a more disrupted junction pattern with larger cell boarders that are blurrier. Anti-ZO-1 was used to visualize cell junctions. B: Electron microscopy revealed tight junction structures in control-RPE at P1 whereas BBS1-RPE only had structures resembling desmosomes or adherens junctions. Scalebar 0.25μM in both images. C, D, and E: mRNA expression of *ZO-1*, *CLAUDIN2* and *CDH2* revealed that control RPE had high CLAUDIN2 expression, indicating presence of tight junctions and BBS1- and BBS10-RPE had higher expression of *CDH2* indicating that these cells did not formed tight junctions. N=1.

Figure 3: Development of pigmentation. A and B: mRNA expression of *PMEL* and *DCT* showed increasing expression in control-RPE over time but low expression in BBS-RPE. C: Electron microscopy images show presence of melanin fibrils in control-RPE. BBS1-RPE did not have these structures but had many large, dense, un-organized vacuolar structures. D: mRNA expression of *MART1* was high in control-RPE but very low in BBS-RPE. E, F and G: mRNA expression of *GPR143*, *LAMP1* and *EEA1* show that control-RPE had a high and increasing expression of *GPR143* and low expression of *LAMP1* and *EEA1*. The reverse is seen for the BBS-RPE that had low *GPR143* expression and high *LAMP1* and *EEA1* expression that increased over time. N=1.

Figure 4: Development of pigmentation was observed by phase-contrast and bright field microscopy. At P0 all three cell lines had started to gain pigmentation, however only the control-RPE continued to increase in degree of pigmentation whereas the BBS-RPE cells lost their pigmentation. BF: bright field. N=1.

Figure 5: Investigation of mature RPE cell proteins. A: Control-RPE and BBS1-RPE were investigated for expression of RPE65 protein. Only control-RPE showed expression that increased during the course of RPE differentiation. B, C and D: mRNA expression *RPE65*, *BEST1* and *MITF* likewise showed that only control-RPE expressed these. E: mRNA expression of *DNMT3B* indicated that control-RPE and BBS-RPE lost their pluripotency. N=1.

Figure 6: Phagocytosis assay of bioparticles that emit red fluorescence after phagocytosis showed the ability of control-RPE to perform phagocytosis. The BBS1-RPE had poor phagocytic capabilities. Scalebar 50 μm. N=1.

Figure 7: Investigation of primary cilia. A: Immunofluorescence microscopy of anti-ARL13B and anti-GT335 revealed the presence of cilia in both control-RPE and BBS1-RPE. Cilia in control-RPE were very short whereas BBS1-RPE developed long cilia especially apparent at P2. B: mRNA expression of *ARL13B* confirmed that finding. C and D: mRNA expression of *IFT88* and *IFT140*, part of the IFTA and IFTB complexes respectively, revealed increased expression in BBS-RPE compared to control at P1 and P2. N=1.

Figure 8: Mitochondrial effects. A: Electron microscopy revealed the presence of mitochondria with a thick and dense membrane in BBS1-RPE at P1. B and C: mRNA expression of *COXIV* and *RHOT1* increased in BBS1- and BBS10-RPE demonstrating an increased amount of mitochondria membrane proteins. N=1.

Figure 9: Investigation of Wnt signaling. A: Immunofluorescence microscopy of anti-β-catenin revealed increased nuclear localization in control-RPE treated with IWR-1 at P1 and P2. BBS1-RPE had a high nuclear expression at P1 and P2 that does not change with Wnt or Hh modulation. B: *AXIN2* mRNA expression was higher in BBS-RPE. N=1.

Figure 10: Effects of Wnt modulation. "+" indicate CHIR99021 Wnt activation and "–" indicate IWR-1 Wnt inhibition. A, B, C: Wnt modulation did not change mRNA expression of *RPE65*, *BEST1* and *MITF* for BBS-RPE. Wnt inhibition increased expression of these slightly in control-RPE. D: No change occurred in mRNA expression of stem cell gene *DNMT3B* in control- and BBS-RPE. E and F: mRNA expression of *ZO-1* and *CLAUDIN2*. Wnt inhibition led to increased *ZO-1* expression in BBS-RPE. The expression in control-RPE did not change. *CLAUDIN2* expression increased in control-RPE with Wnt inhibition. No change was seen in BBS1-RPE expression. G: *ARL13B* mRNA expression was unchanged in control-RPE but Wnt stimulation decreased expression in BBS1-RPE. H: *AXIN2* mRNA expression was unchanged in control-RPE and BBS-RPE with Wnt modulation. I and J: mRNA expression of *COXIV* and *RHOT1* did not change with Wnt modulation in control-RPE but decreased with Wnt activation in BBS-RPE. N=1.

Figure 11: SMO localization in control-RPE and BBS1-RPE. Both cell lines had SMO in the cell membrane. Control-cells showed ciliary localization with purmorphamine and cyclopamine treatment but not in untreated cells. BBS1-RPE showed ciliary SMO localization regardless of treatment. Scalebar 20μm. N=1.

Figures and tables

GENE	Assay ID
ARL13	Hs00376583_m1
IFT140	Hs01076403_m1
IFT88	Hs00197926_m1
ZO-1	Hs01551861_m1
CLAUDIN2	Hs01549234_m1
BEST1	Hs04397293_m1
RPE65	Hs01071462_m1
MERTK	Hs01031979_m1
PMEL	Hs00173854_m1
DCT	Hs01098278_m1
DNMT3B	Hs00171876_m1
Axin2	Hs00610344_m1
MITF	Hs01117294_m1
RHOT1	Hs00430256_m1
COXIV	Hs00971639_m1
LAMP1	Hs00931461_m1
EEA1	Hs00929215_m1
GPR143	Hs00173432_m1
MART1	Hs00194133_m1
CDH2	Hs00983056_m1

Table 1 – List of applied Taqman probes.

Antibody	Dilution	Company Cat #
Rabbit anti-ARL13B	1:800	Proteintech #1711-1-AP
Mouse anti-ARL13B	1:500	Abcam #ab136648
Mouse anti-GT335	1:800	Adipogen #AG-20B-0020
Mouse anti-TUBULIN, Acetylated	1:1000	Sigma-Aldrich #T6793
Rabbit anti-SMOOTHENED	1:800	Abcam #ab38686
Rabbit anti-ZO-1	1:250	Thermo Fisher Scientific #40-2200
Mouse anti-RPE65	1:250	Abcam #ab13826
Rabbit anti-SOX2	1:200	Thermo Fisher Scientific #PA1-094
Rabbit anti-PAX6	1:500	Sigma-Aldrich #HPA030775
Rabbit anti-MITF	1:500	Sigma-Aldrich #HPA003259
Mouse anti-BEST1	1:500	Abcam #ab2182
Mouse anti-Beta-catenin	1:100	Sigma-Aldrich #C7738
Alexa Flour Goat Anti-Rabbit 488	1:800	Life Technologies Cat# A11008
Alexa Flour Donkey Anti-Mouse 546	1:800	Life Technologies Cat# A10036

Table 2 – Antibody list.

Figure 1 – Morphology

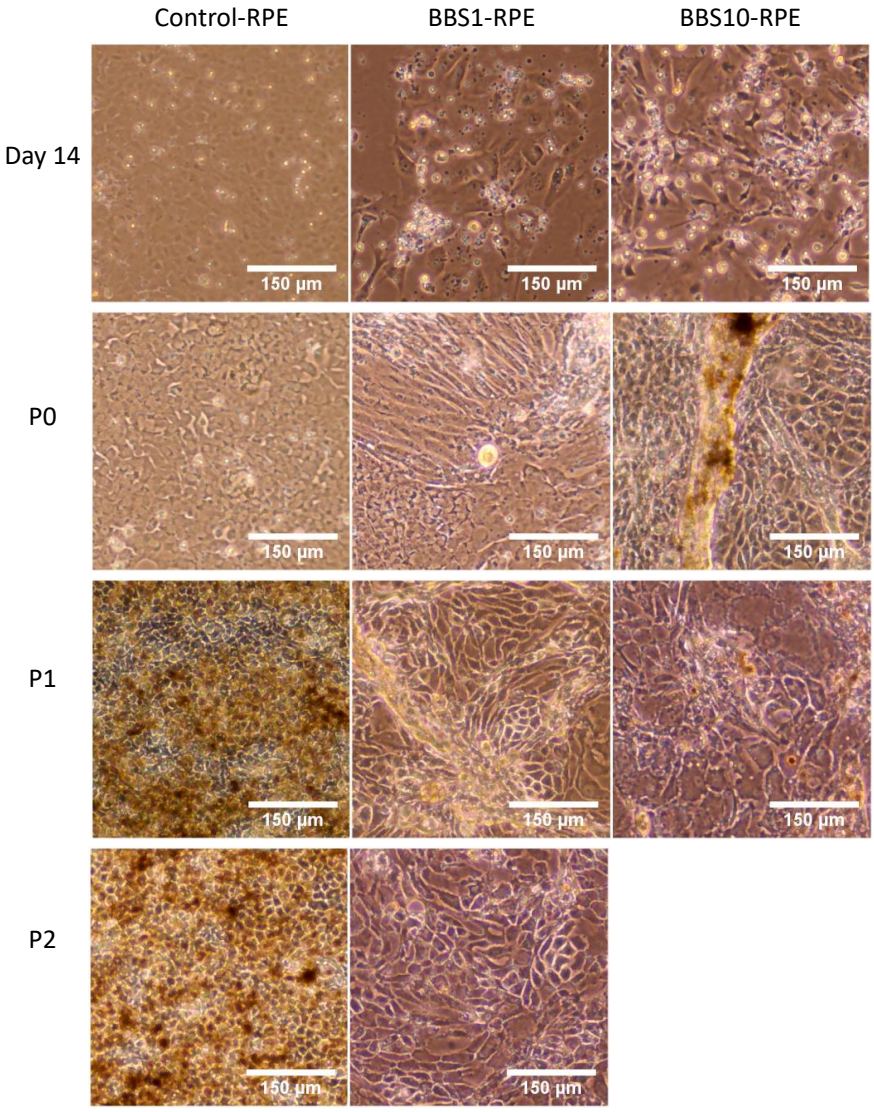

Figure 2: Formation of tight junctions

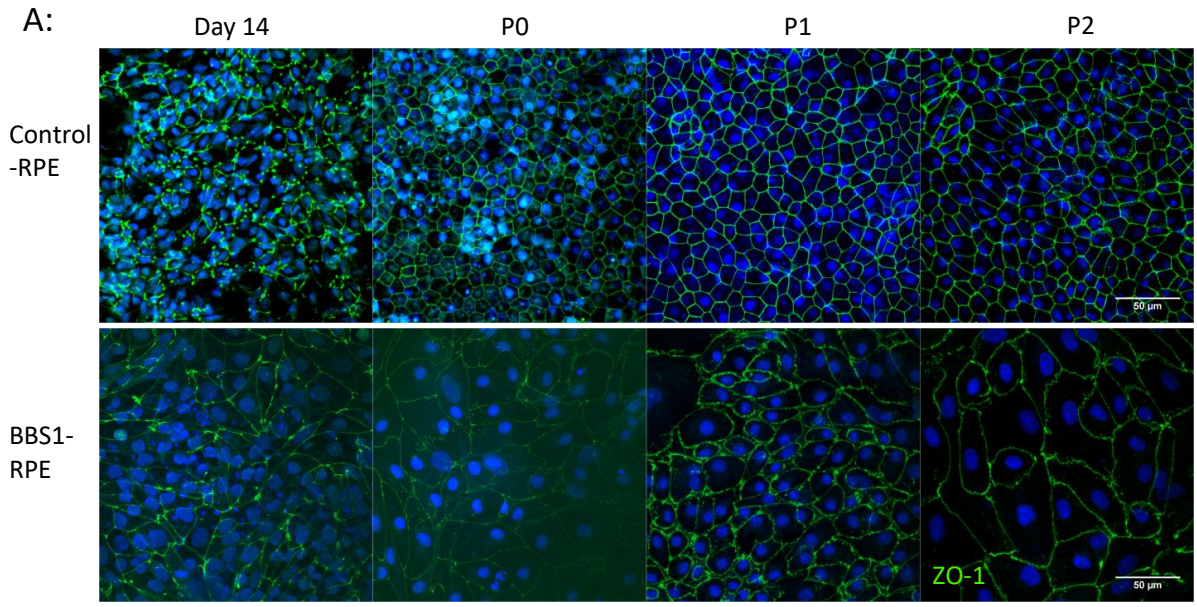

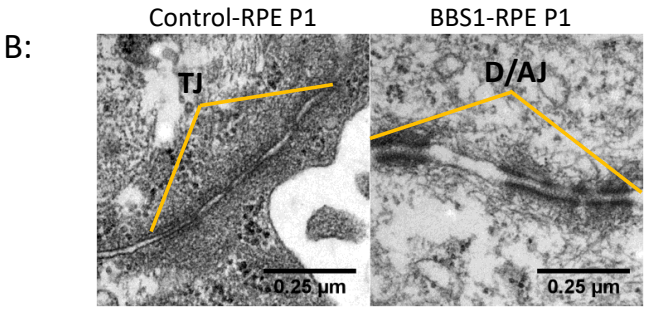

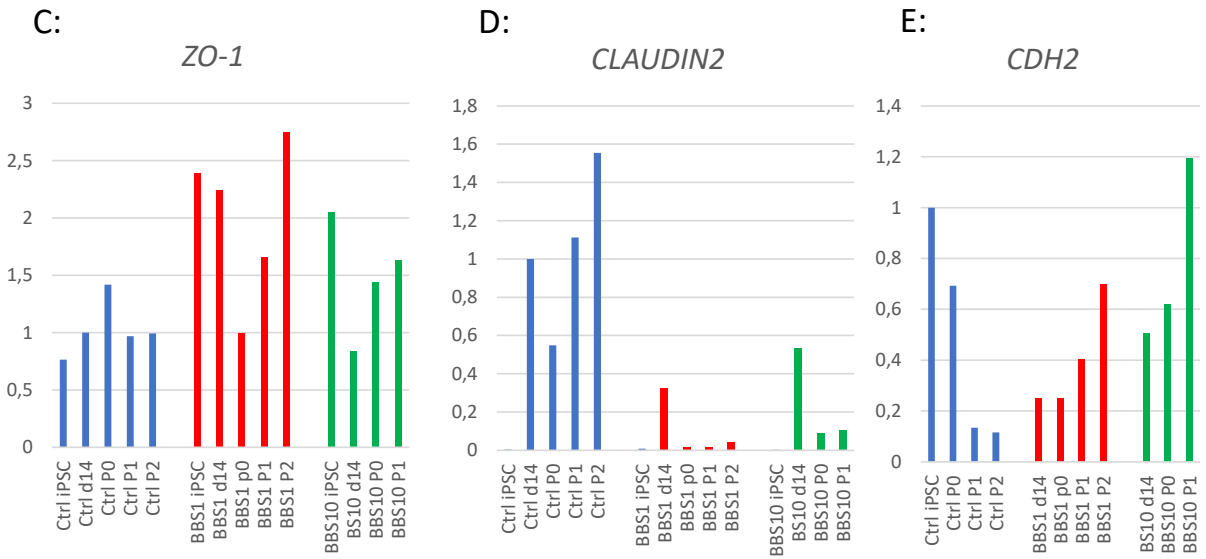

Figure 3: Pigmentation

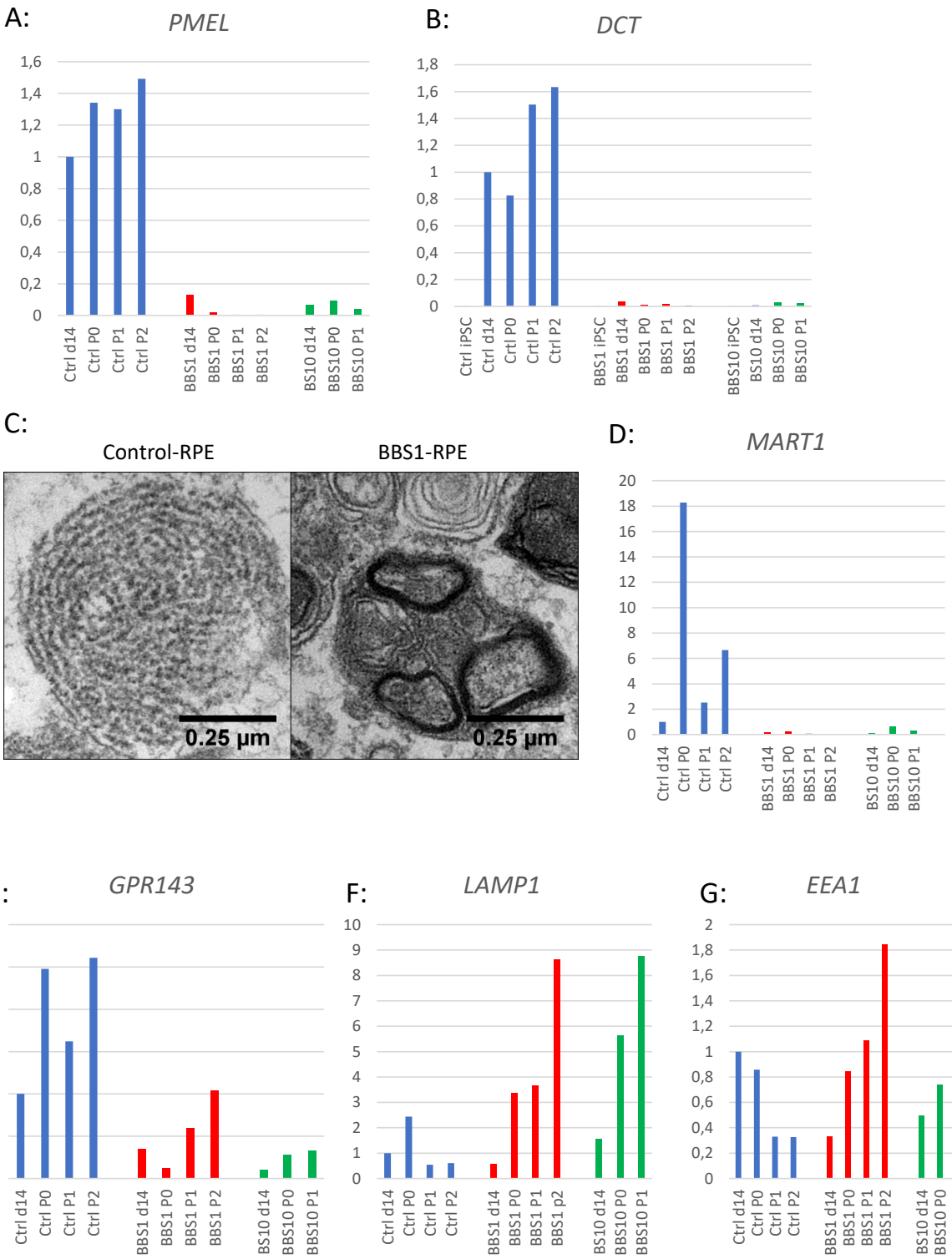

Figure 4:
Pigmentation II

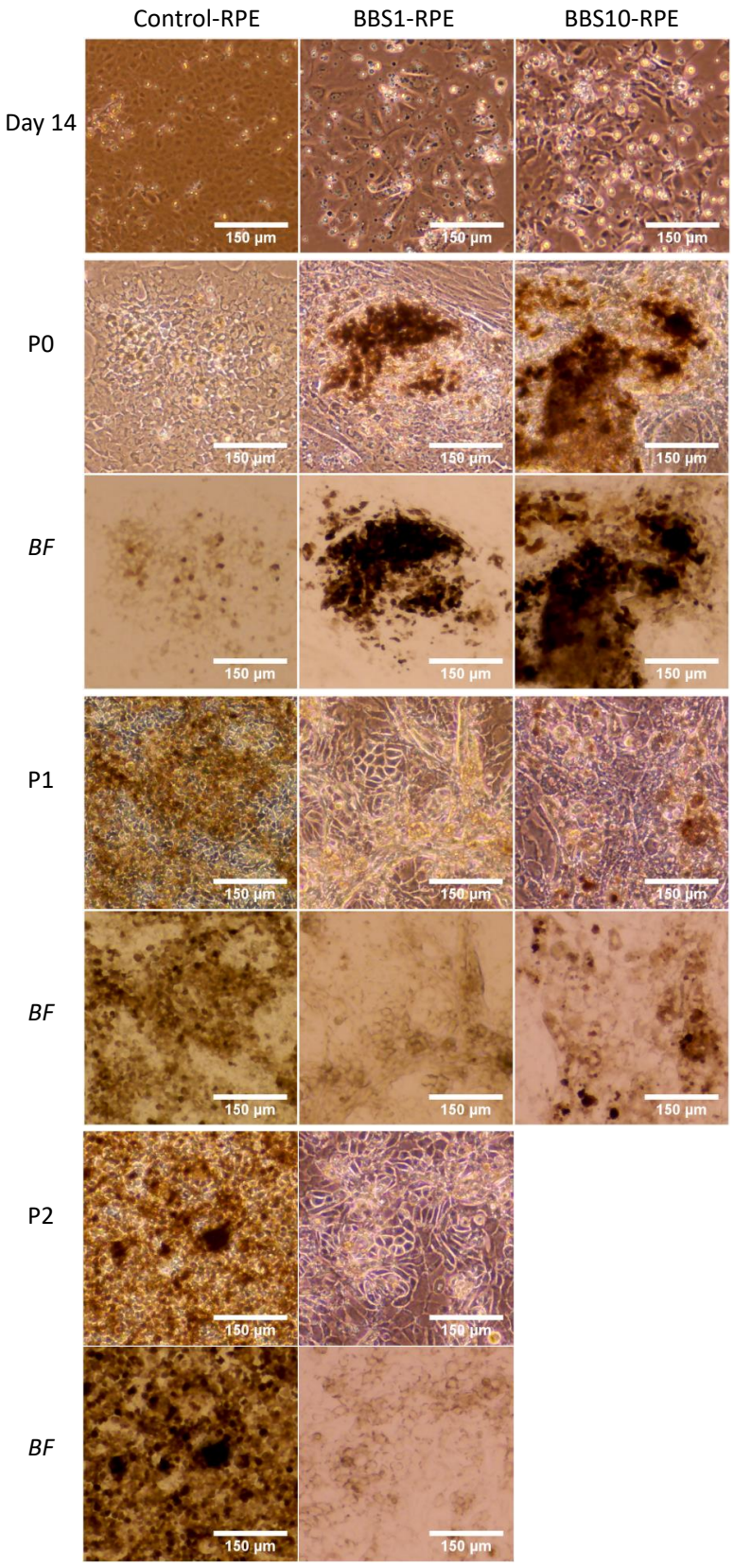

Figure 5: Expression of RPE markers

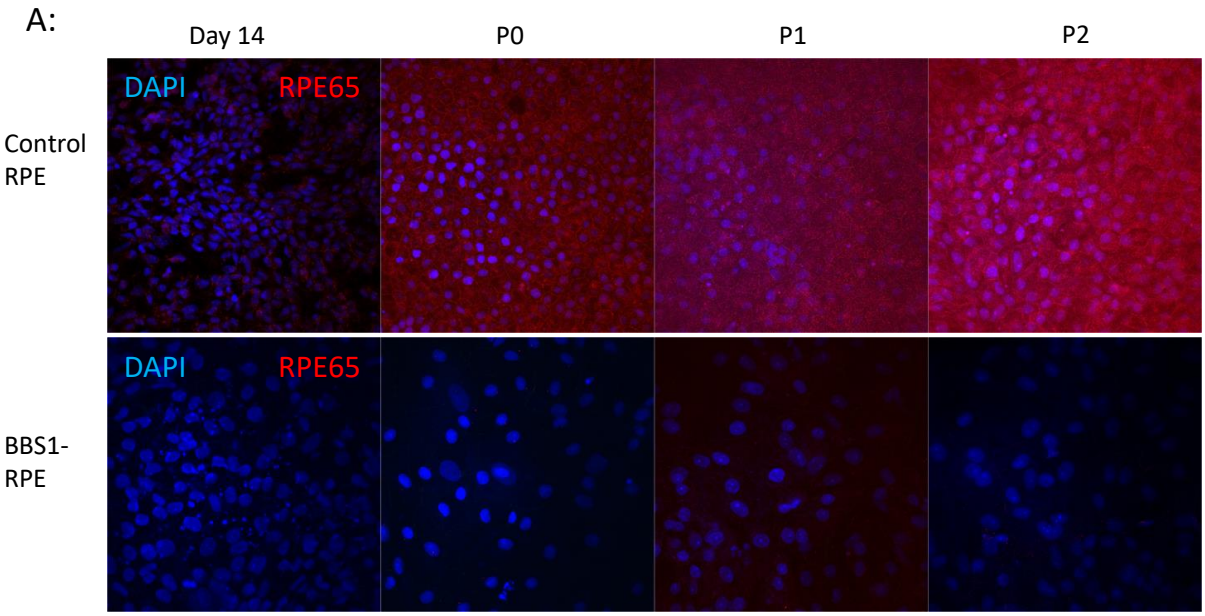

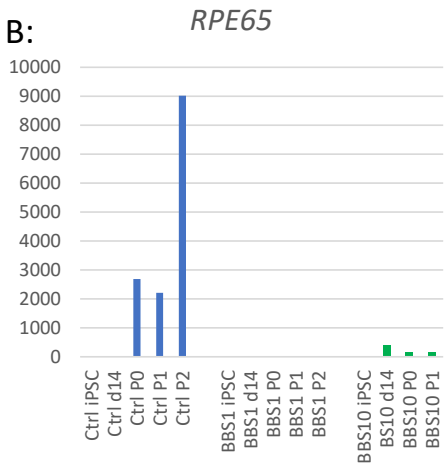

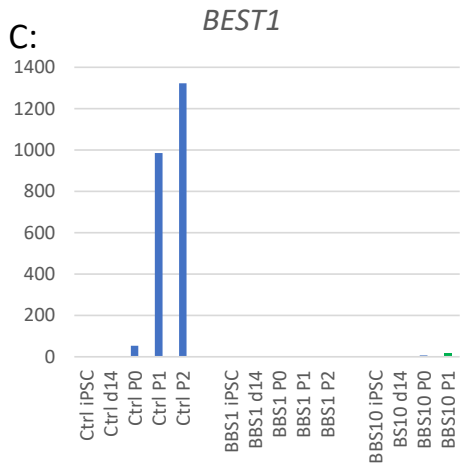

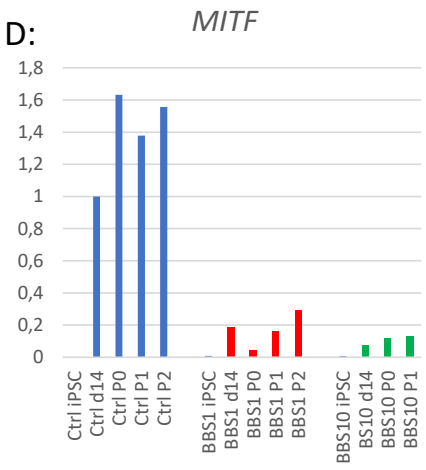

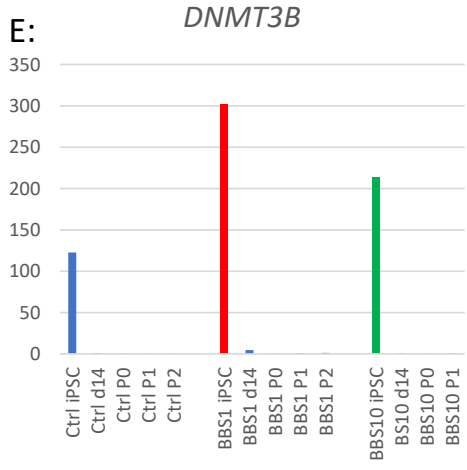

Figure 6: phagocytosis P2

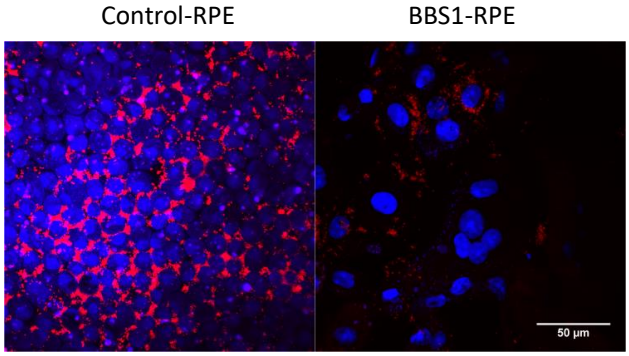

Figure 7: Primary cilia morphology

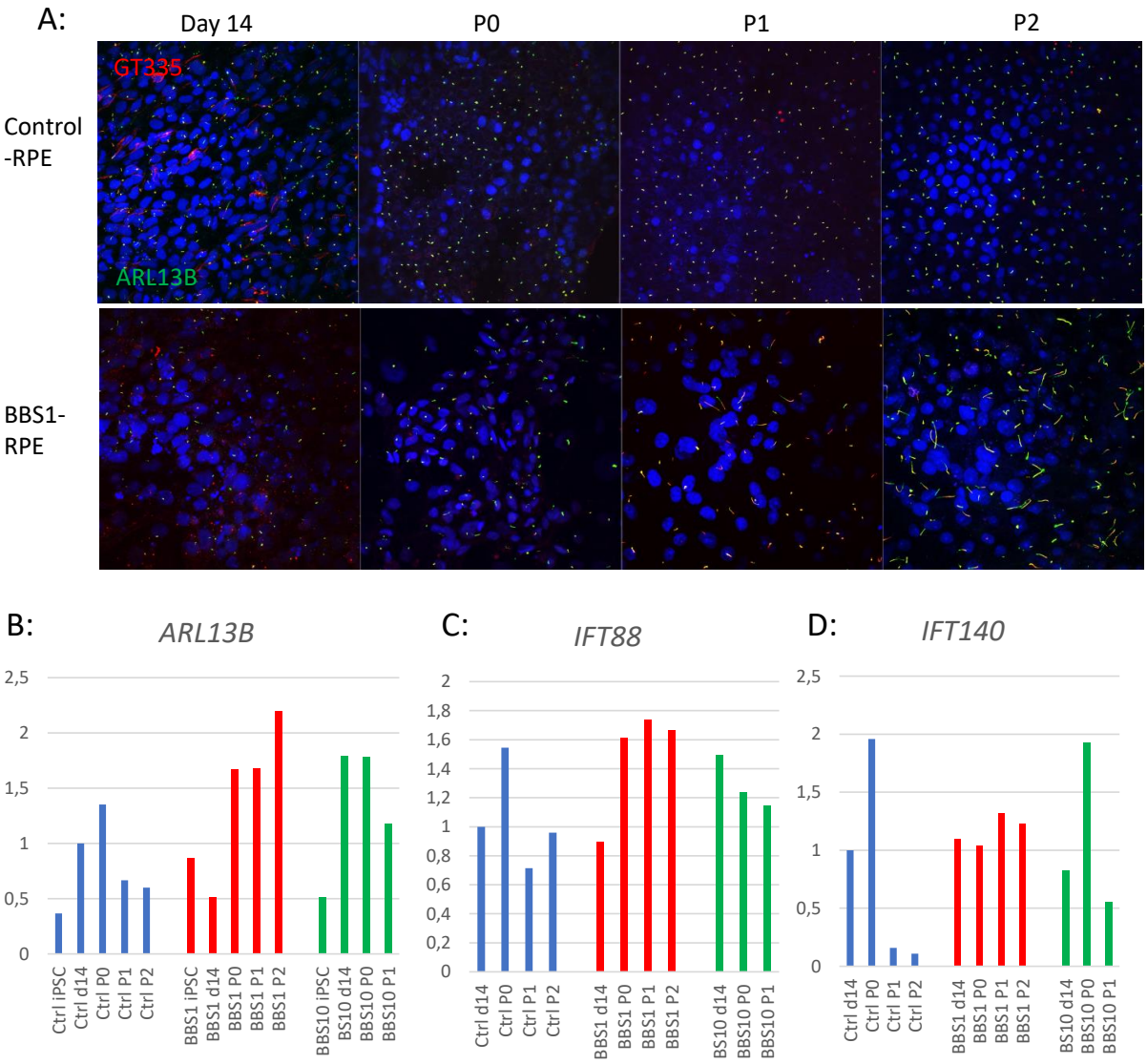

Figure 8: mitochondrial effects

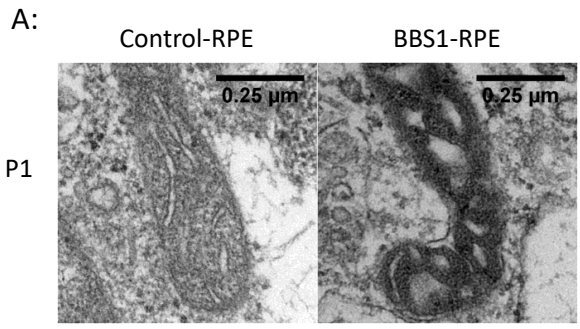

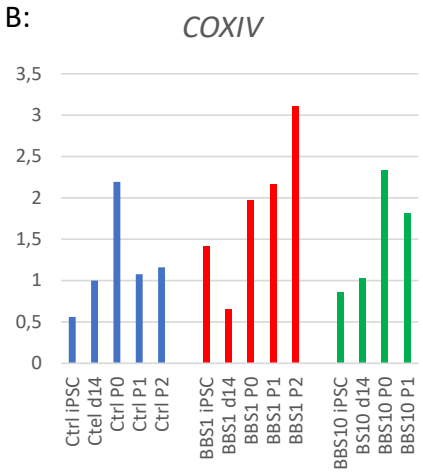

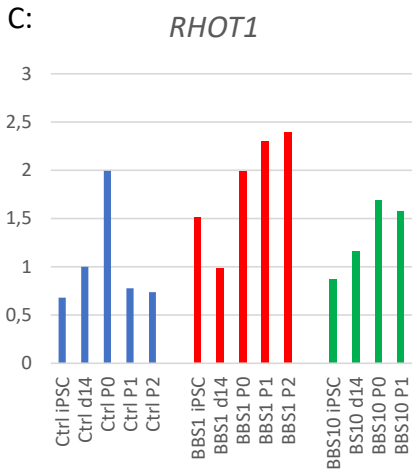

Figure 9: Wnt signaling

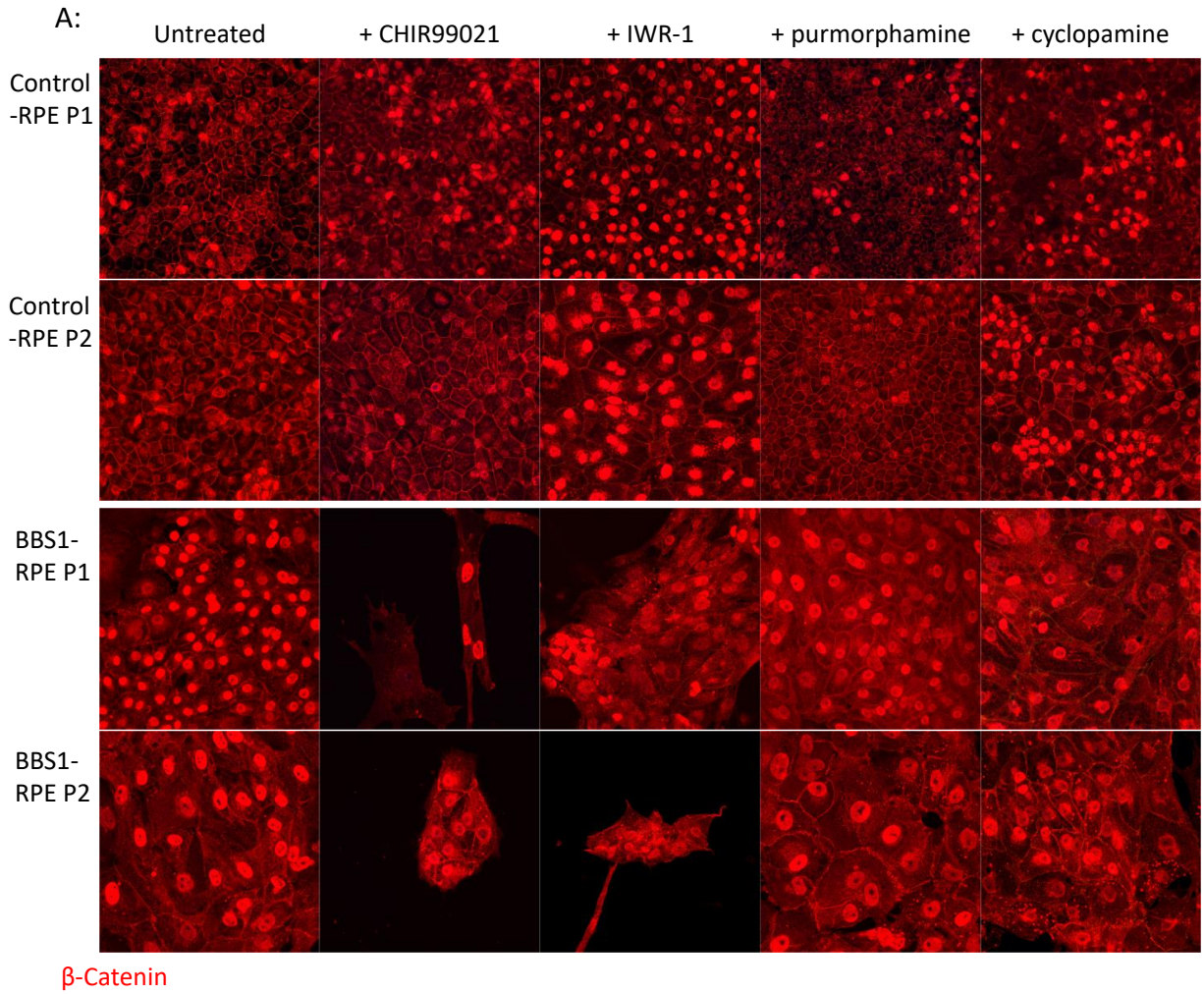

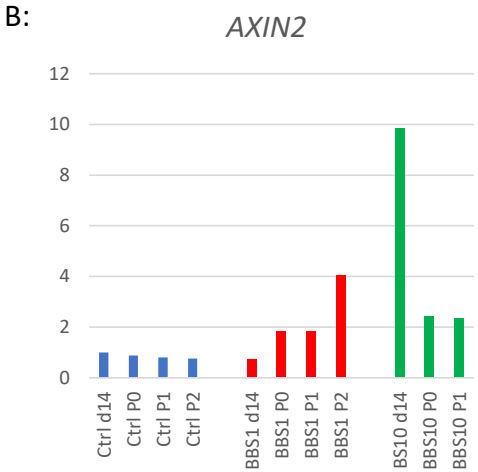

Figure 10: Wnt signaling treatments, RNA studies

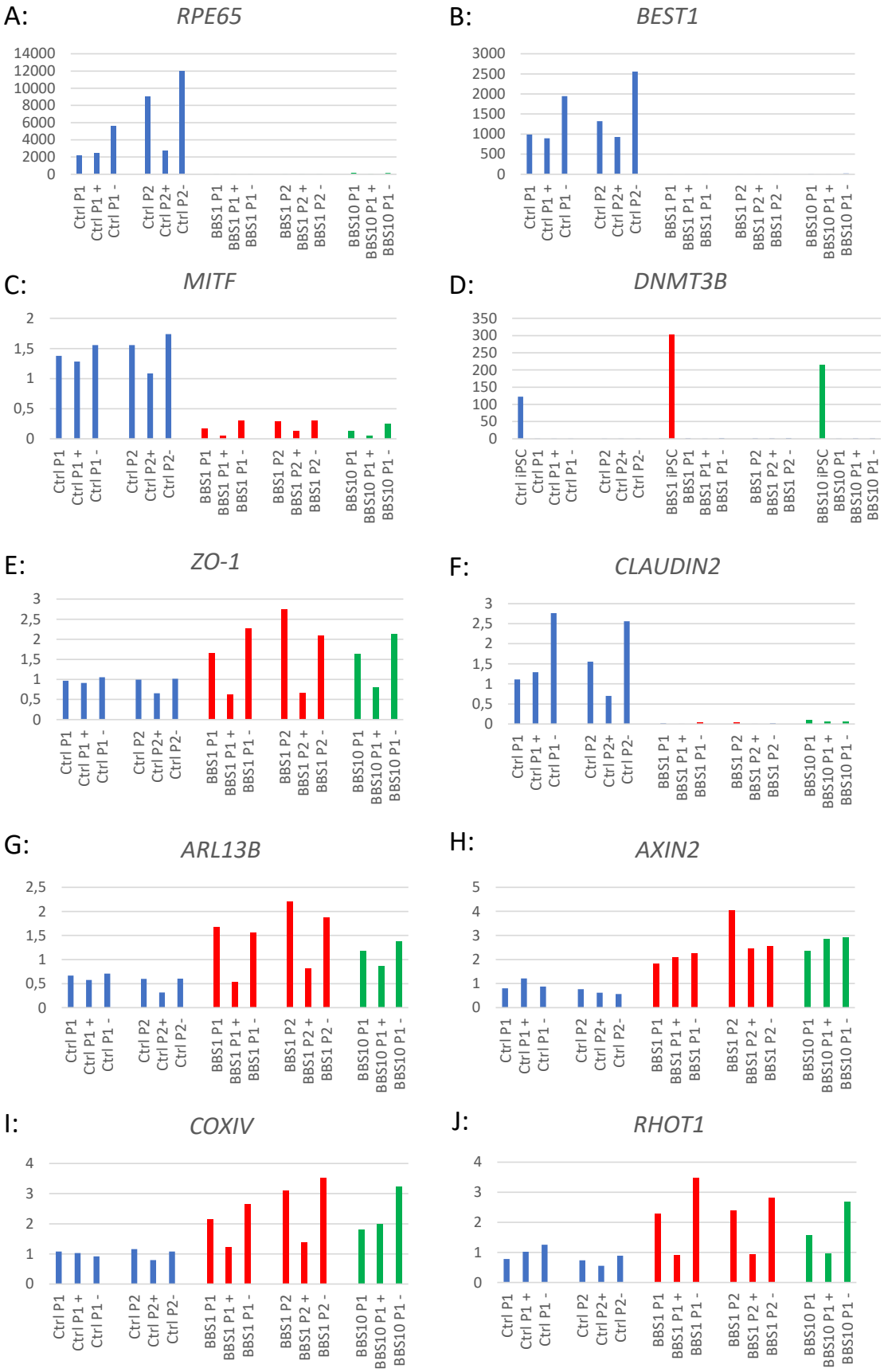

Figure 11: Smoothened localization

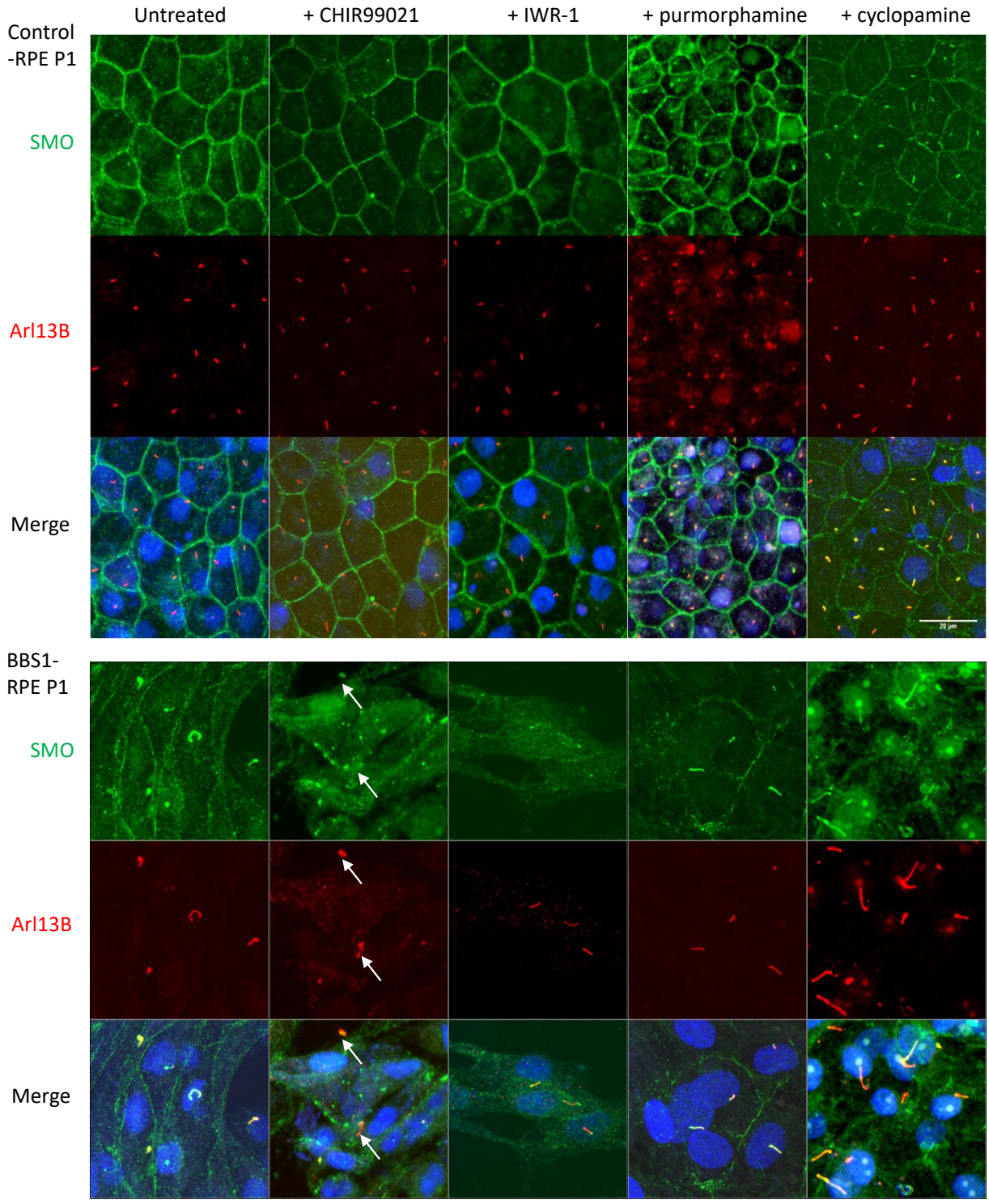

Supplementary figure 1 – Unedited pictures

A: Control RPE

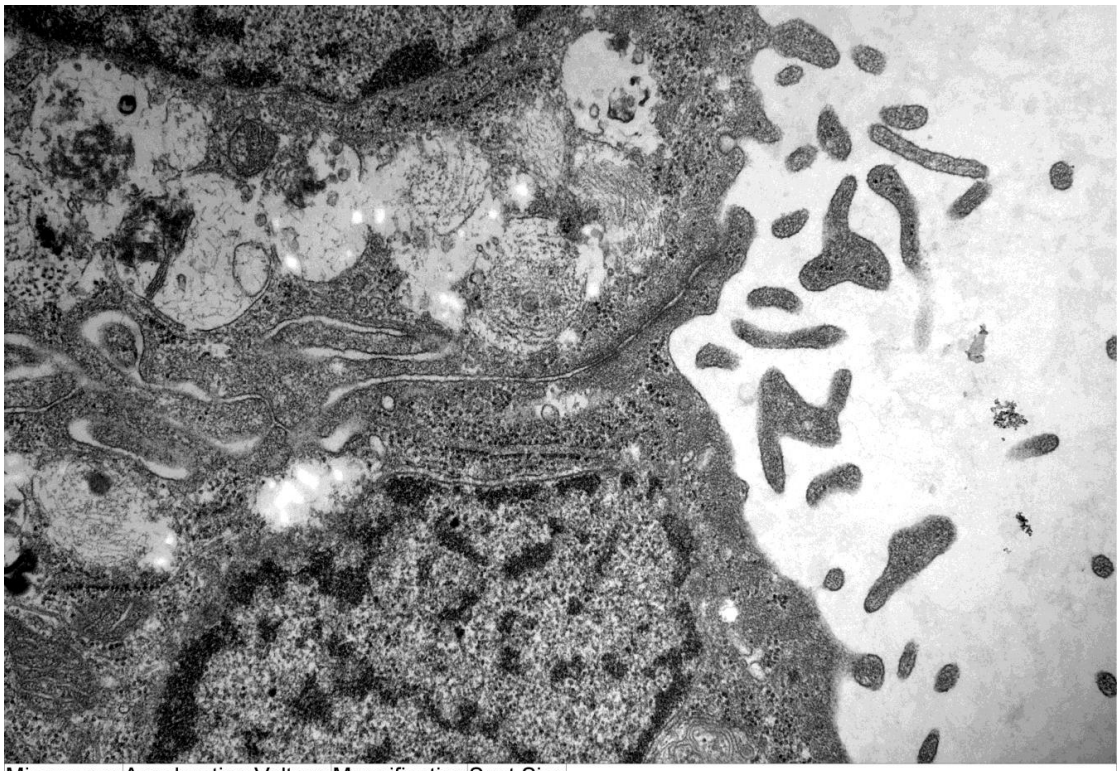

Microscope	Accelerating Voltage	Magnification	Spot Size	-
CM	80 kV	25000 x	5 µm	1 µm

B: BBS1-RPE

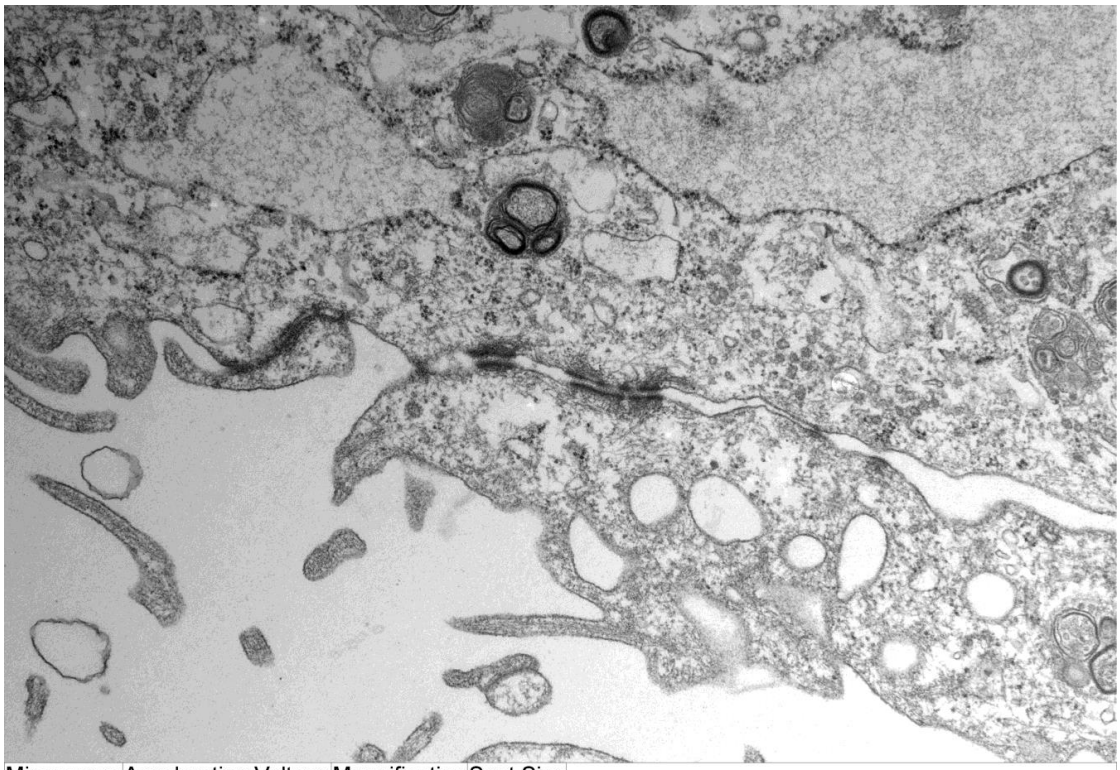

Microscope	Accelerating Voltage	Magnification	Spot Size	-
CM	80 kV	25000 x	5 µm	1 µm

Supplementary figure 2